การศึกษาอันตรกิริยาระหว่างไนเฟดิปีนและพอลิเมอร์ในสารกระจายตัวของแข็ง
โดยใช้รามานสเปกโทรสโกปี

นางสาวสุจินดา กีรติชีวนันท์

วิทยานิพนธ์นี้เป็นส่วนหนึ่งของการศึกษาตามหลักสูตรปริญญาเภสัชศาสตรดุษฎีบัณฑิต
สาขาวิชาเภสัชกรรม ภาควิชาวิทยาการเภสัชกรรมและเภสัชอุตสาหกรรม
คณะเภสัชศาสตร์ จุฬาลงกรณ์มหาวิทยาลัย
ปีการศึกษา 2557

AN INVESTIGATION OF INTERACTIONS BETWEEN NIFEDIPINE AND POLYMER IN SOLID DISPERSION USING RAMAN SPECTROSCOPY

Miss Sujinda Keratichewanun

A Dissertation Submitted in Partial Fulfillment of the Requirements
for the Degree of Doctor of Philosophy Program in Pharmaceutics
Department of Pharmaceutics and Industrial Pharmacy
Faculty of Pharmaceutical Sciences
Chulalongkorn University
Academic Year 2014

Thesis Title	AN INVESTIGATION OF INTERACTIONS BETWEEN NIFEDIPINE AND POLYMER IN SOLID DISPERSION USING RAMAN SPECTROSCOPY
By	Miss Sujinda Keratichewanun
Field of Study	Pharmaceutics
Thesis Advisor	Jittima Chatchawalsaisin, Ph.D.
Thesis Co-Advisor	Professor Katsuhide Terada, Ph.D.
	Narueporn Sutanthavibul, Ph.D.

Accepted by the Faculty of Pharmaceutical Sciences, Chulalongkorn University in Partial Fulfillment of the Requirements for the Doctoral Degree

.....Dean of the Faculty of Pharmaceutical Sciences
(Assistant Professor Rungpetch Sakulbumrungsil, Ph.D.)

THESIS COMMITTEE

.....Chairman
(Associate Professor Parkpoom Tengamnuay, Ph.D.)

.....Thesis Advisor
(Jittima Chatchawalsaisin, Ph.D.)

.....Thesis Co-Advisor
(Professor Katsuhide Terada, Ph.D.)

.....Thesis Co-Advisor
(Narueporn Sutanthavibul, Ph.D.)

.....Examiner
(Assistant Professor Walaisiri Muangsiri, Ph.D.)

.....Examiner
(Associate Professor Pornchai Rojsitthisak, Ph.D.)

.....External Examiner
(Associate Professor Satit Puttipipatkhachorn, Ph.D.)

สุจินดา กีรติชีวนันท์ : การศึกษาอันตรกิริยาระหว่างไนเฟดิปีนและพอลิเมอร์ในสารกระจายตัวของแข็งโดยใช้รามานสเปกโทรสโกปี (AN INVESTIGATION OF INTERACTIONS BETWEEN NIFEDIPINE AND POLYMER IN SOLID DISPERSION USING RAMAN SPECTROSCOPY) อ.ที่ปรึกษาวิทยานิพนธ์หลัก: อ. ภญ. ดร.จิตติมา ชัชวาลย์สายสินธ์, อ.ที่ปรึกษาวิทยานิพนธ์ร่วม: Prof. Katsuhide Terada, Ph.D., อ. ภญ. ดร.นฤพร สุตัณฑวิบูลย์, 115 หน้า.

อันตรกิริยาระหว่างยาและพอลิเมอร์หรือสภาพผสมเข้ากันได้เป็นปัจจัยสำคัญในการยับยั้งการตกผลึกของยาที่กระจายตัวอยู่ในเมทริกซ์พอลิเมอร์ของสารกระจายตัวของแข็ง วัตถุประสงค์ของการศึกษานี้เพื่อแสดงความเป็นไปได้ในการใช้รามานสเปกโทรสโกปีในการตรวจวัดระดับของอันตรกิริยาระหว่างยาและพอลิเมอร์ในสารกระจายตัวของแข็ง และเพื่อตรวจสอบว่าอันตรกิริยาที่เกิดขึ้นสามารถคงสภาพสัณฐานของของแข็งของตัวยา เตรียมสารกระจายตัวของแข็งของไนเฟดิปีนและพอลิเมอร์ร่วมแบบกราฟต์ของพอลิไวนิลคาโปรแลคแทม พอลิไวนิลอะซิเตต และพอลิเอธิลีนไกลคอล (โซลูพลัส) ที่มีปริมาณตัวยาร้อยละ 10, 30, 50, 70, 90 โดยน้ำหนัก ด้วยวิธีการทำแห้งเยือกแข็ง การหลอม และการระเหยตัวทำละลาย ตรวจสอบสภาพผสมเข้ากันได้ของสารกระจายตัวของแข็งโดยใช้วิธีการเลี้ยวเบนรังสีเอกซ์ ดิฟเฟอเรนเชียลสแกนนิงคาลอรีเมตรี อินฟราเรดสเปกโทรสโกปีชนิดฟูเรียร์ทรานสฟอร์ม นิวเคลียร์แมกเนติกเรโซแนนซ์สเปกโทรสโกปีชนิดสำหรับวิเคราะห์ของแข็งและรามานสเปกโทรสโกปี และหาระดับของอันตรกิริยาระหว่างตัวยาและพอลิเมอร์ในตัวอย่างที่แสดงรูปแบบการเลี้ยวเบนรังสีเอกซ์ของสารอสัณฐานโดยการใช้เกาส์เซียนฟังก์ชันในการปรับรามานสเปกตรัม ผลการศึกษาแสดงให้เห็นว่าตัวยาและพอลิเมอร์มีอันตรกิริยาชนิดพันธะไฮโดรเจนซึ่งบ่งชี้โดยใช้อินฟราเรดสเปกโทรสโกปีชนิดฟูเรียร์ทรานสฟอร์ม และนิวเคลียร์แมกเนติกเรโซแนนซ์สเปกโทรสโกปีชนิดสำหรับวิเคราะห์ของแข็ง และมีอันตรกิริยาชนิดไม่ชอบน้ำซึ่งระบุได้ด้วยรามานสเปกโทรสโกปี ระดับของอันตรกิริยาระหว่างตัวยาและพอลิเมอร์รวมถึงระดับสภาพผสมเข้ากันได้ขึ้นกับระดับของปริมาณยามากกว่าวิธีการเตรียม และพบว่าปริมาณยาร้อยละ 30 โดยน้ำหนักเป็นความเข้มข้นอิ่มตัวของไนเฟดิปีนที่จะผสมเข้ากันได้กับพอลิเมอร์ การตกผลึกและการแยกเฟสอสัณฐานสามารถชะลอในของผสมที่เข้ากันได้ เมื่อปริมาณยาต่ำกว่าความเข้มข้นอิ่มตัวมาก ความแข็งแรงของอันตรกิริยาระหว่างยาและพอลิเมอร์เพียงพอที่จะยับยั้งการแยกเฟสอสัณฐานได้อย่างมีประสิทธิภาพ ดังนั้นรามานสเปกโทรสโกปีสามารถประยุกต์ใช้ในการตรวจสอบและหาปริมาณอันตรกิริยาที่ไม่ชอบน้ำในสารกระจายตัวของแข็งของยาและพอลิเมอร์

ภาควิชา	วิทยาการเภสัชกรรมและเภสัชอุตสาหกรรม	ลายมือชื่อนิสิต	.....
		ลายมือชื่อ อ.ที่ปรึกษาหลัก	.....
สาขาวิชา	เภสัชกรรม	ลายมือชื่อ อ.ที่ปรึกษาร่วม	.....
ปีการศึกษา	2557	ลายมือชื่อ อ.ที่ปรึกษาร่วม	.....

5376960733 : MAJOR PHARMACEUTICS

KEYWORDS: DRUG-POLYMER INTERACTION / GAUSSIAN FUNCTION / MOLECULAR DISPERSION / NIFEDIPINE / RAMAN SPECTROSCOPY

SUJINDA KERATICHEWANUN: AN INVESTIGATION OF INTERACTIONS BETWEEN NIFEDIPINE AND POLYMER IN SOLID DISPERSION USING RAMAN SPECTROSCOPY. ADVISOR: JITTIMA CHATCHAWALSAISIN, Ph.D., CO-ADVISOR: PROF. KATSUHIDE TERADA, Ph.D., NARUEPORN SUTANTHAVIBUL, Ph.D., 115 pp.

Drug-polymer interaction or their miscibility has been known to be a key factor to impede recrystallization of drug dispersed in a polymeric matrix of solid dispersion. The purpose of this study was to demonstrate the feasibility of Raman spectroscopy to determine the extent of drug-polymer interaction in solid dispersions and to investigate whether the present interaction could stabilize the solid state morphology of the drug substance. The solid dispersions of nifedipine and polyvinyl caprolactam - polyvinyl acetate - polyethylene glycol graft copolymer (Soluplus®) with drug loadings of 10, 30, 50, 70 and 90% w/w were prepared by freeze drying, melting and solvent evaporation. The miscibility of solid dispersions was characterized by X-ray powder diffractometry, differential scanning calorimetry, Fourier transform-infrared spectroscopy (FT-IR), solid state-nuclear magnetic resonance spectroscopy (ss-NMR) and Raman spectroscopy. The extent of drug-polymer interaction in X-ray amorphous samples were determined by utilizing Gaussian function fitting of Raman spectra obtained. The results demonstrated that the drug and polymer interacted via hydrogen bonding as indicated by FT-IR and ss-NMR and hydrophobic interaction identified by Raman spectroscopy. The extent of drug-polymer interaction and miscibility levels were found to be more dependent on the amounts of drug loading than preparation methods. The amount of 30% w/w drug loading was shown to be a saturated concentration for the miscibility of nifedipine in the polymer. Crystallization and amorphous phase separation were delayed in the miscible mixtures. When the drug loading was much lower than the saturated concentration, the strength of drug-polymer interaction effectively inhibited the amorphous phase separation. Therefore, Raman spectroscopy could be applied to investigate the extent of hydrophobic interaction in the solid dispersion of drug and polymer both qualitatively and quantitatively.

Department:	Pharmaceutics and Industrial Pharmacy	Student's Signature .....
		Advisor's Signature .....
Field of Study:	Pharmaceutics	Co-Advisor's Signature .....
Academic Year:	2014	Co-Advisor's Signature .....

ACKNOWLEDGEMENTS

I wish to express the deepest gratitude to my family for their encouragement and financial support. Their supports are inestimable and I could not complete the dissertation without my beloved family.

I extend thanks to my advisor, Dr. Jittima Chatchawalsaisin, for the mentor concerning the dissertation, also all advices for daily life over the years we have worked together. I wish to extend my gratitude to Dr. Narueporn Sutanthavibul for valuable suggestions since I was an undergraduate student until now. Thanks also to Dr. John Kendrick for editing and comments on the manuscript.

My sincere appreciation is expressed to Prof. Kasuhide Terada for giving me the opportunity to conduct the research at Toho University, and for considerable supports of the dissertation. I would like to gratefully thank Assoc. Prof. Yasuo Yoshihashi for the expert guidance about the research.

I also thank Assoc. Prof. Parkpoom Tengamnuay, Assoc. Prof. Satit Puttipipatkhachorn, Asst. Prof. Walaisiri Muangsiri and Assoc. Prof. Pornchai Rojsitthisak for their valuable time and supports as being a member of my thesis committee.

I wish to deeply thank Department of Pharmaceutics, Faculty of Pharmaceutical Sciences, Toho University for providing research facilities. I extremely thank the laboratory members there for their assistance of laboratory work, and thank particularly for their friendship.

I extend thanks to Chulalongkorn University Centenary Academic Development Project and Department of Pharmaceutics and Industrial Pharmacy, Faculty of Pharmaceutical Sciences, Chulalongkorn University for providing research facilities, also thank the laboratory members for their help and friendship.

Finally, I would like to specially thank Thammapon Viriyakovitaya for giving me the confidence to go through difficult situations during being a Ph.D. candidate.

This research has been supported by the Ratchadaphiseksomphot Endowment Fund 2013 of Chulalongkorn University (CU-56-649-HR).

CONTENTS

Page

Page

Page

LIST OF TABLES

LIST OF FIGURES

LIST OF ABBREVIATIONS

α-NIF	Crystalline α-form of nifedipine
β-NIF	Crystalline β-form of nifedipine
am-NIF	Amorphous nifedipine
BCS	Biopharmaceutical Classification System
DSC	Differential scanning calorimetry
FD	Freeze drying
FT-IR	Fourier transform-infrared spectroscopy
H	Hour
HPLC	High performance liquid chromatography
IR	Infrared spectroscopy
MAS	Magic angle spinning
ME	Melting
Min	Minute
RH	Relative humidity
RSD	Relative standard deviation
SE	Solvent evaporation
ss-NMR	Solid state-nuclear magnetic resonance spectroscopy
T_c	Crystallization temperature
T_g	Glass transition temperature
T_m	Melting temperature
XPS	X-ray photoelectron spectroscopy
XRPD	X-ray powder diffraction; X-ray powder diffractometry

CHAPTER I
INTRODUCTION

One of the underpinning mechanisms to improve dissolution of poorly water soluble drugs through solid dispersion technique is the conversion of crystalline to its amorphous counterpart (1, 2). However, upon storage, the amorphous state might undergo recrystallization. In a more stable solid dispersion, the drug is miscible with the polymer and hence dispersed in the solid polymer at the molecular level. The miscibility of drug and polymer depends on both drug concentration and preparation method (3-7). In general, the drug could be miscible with the polymer up to its saturated concentration of drug in the solid polymer.

The process of recrystallization from amorphous state is in fact rather complex. Principally, it is involved with nucleation and crystal growth. The factors governing recrystallization from amorphous state could be thermodynamic and kinetic factors. The thermodynamic driving force of supersaturated drug concentration causes the amorphous drug having high free energy to rearrange its structure to a more stable form. The kinetics factors were such as preparation method (i.e. thermal history and mechanical stress) and fragility of the glass (8, 9).

As above mentioned, recrystallization of the drug in the solid dispersion could be delayed if the drug is molecularly dispersed or miscible in the polymer as the single phase solid dispersion (9, 10). In this solid dispersion, the polymer inhibits recrystallization by several mechanisms i.e. drug-polymer interaction via specific interaction (hydrogen bond) (8, 11-17) and/or non-specific interaction (van der Waals force) (18), increase in glass transition temperature (T_g) of the mixture (16, 17), steric hindrance due to bulky structure of a polymer (16, 19) and reduced amorphous free energy (20-23).

Several works have been carried out to investigate the miscibility of drug and polymer by X-ray powder diffractometry (XRPD) (24, 25), differential scanning calorimetry (DSC) (5, 7, 20, 21, 23, 24, 26-29), X-ray photoelectron spectroscopy (XPS) (27), infrared spectroscopy (IR) (5, 7, 20, 23, 24, 26, 30-32), solid state-nuclear

magnetic resonance spectroscopy (ss-NMR) (27, 29) and Raman spectroscopy (14, 28, 32-35). Also, they revealed insight into the drug-polymer interaction involved in the miscible mixtures by using XPS, IR, ss-NMR and Raman spectroscopy.

The principle of Raman spectroscopy is based on light scattering of the vibrational mode which is involved in molecular polarization. Thus, it may be more useful, compared to other methods i.e. IR, for determining non-specific interaction such as hydrophobic interaction in the drug-polymer mixture which is rich in aromatic conjugated systems (18). To date, the application of Raman spectroscopy to detect the hydrophobic interaction between drug and polymer has been limited (18), in particular quantitative characterization of drug-polymer hydrophobic interaction which has not been reported.

In this work, attempts were made to identify and quantify drug-polymer interactions by Raman spectroscopy and other techniques. Recrystallization and amorphous phase separation were also detected in order to confirm the impact of the drug-polymer interaction on solid state stability. The effect of drug loadings and preparation methods i.e. freeze drying, melting and solvent evaporation were also investigated whether the method with or without solvent had influence on the performance of the solid dispersion in terms of states of drug existing in the polymer.

Nifedipine was selected as a model drug, and polyvinyl caprolactam - polyvinyl acetate - polyethylene glycol graft copolymer (Soluplus®) was selected as a polymeric carrier. The solubility parameter of nifedipine and Soluplus® were 21.9 $MPa^{1/2}$ (36) and 19.4 $MPa^{1/2}$ (37), respectively; hence, the binary mixture are likely to be miscible (38). In addition, nifedipine and Soluplus® might form the specific interaction e.g. hydrogen bond because both compounds contained hydrogen bond donors and hydrogen bond acceptors. Also, the drug and the polymer might form the non-specific interaction e.g. van der Waals force via the hydrophobic structures of the two compounds. The presence of molecular interactions between nifedipine and Soluplus® with hydrogen bond and hydrophobic interaction has been evident in the study carried out by Li *et al.* (31) using Fourier transform-infrared spectroscopy (FT-IR) (31).

In the present study, the solid dispersions of nifedipine and Soluplus® were prepared by freeze drying (solvent method with fast solidification rate), melting (non-solvent method with fast solidification rate) and solvent evaporation (solvent method with slow solidification rate). The drug loadings were 10, 30, 50, 70 and 90% w/w. The chemical stability was determined by high performance liquid chromatography (HPLC). The crystallinity was assessed by XRPD. The miscibility limit between nifedipine and Soluplus® was measured by DSC and Raman spectroscopy. The drug-polymer interactions were investigated by FT-IR, ss-NMR and Raman spectroscopy. The quantitative analysis of drug-polymer interactions was carried out by Raman spectroscopy together with Gaussian function fitting method. The solid state stability involved crystallization tendency and the tendency to undergo amorphous phase separation was studied by XRPD and Raman spectroscopy.

Objectives

1. To evaluate drug-polymer interactions in solid dispersion by Raman spectroscopy
2. To identify the correlation between the degree of drug-polymer interactions and solid state stability

CHAPTER II
LITERATURE REVIEW

2.1 Dissolution improvement of poorly water-soluble drugs by solid dispersion

Solid dispersion is one of the most attractive techniques to improve oral bioavailability of the drug in Biopharmaceutical Classification System (BCS) class II i.e. high permeable and low soluble drug. It could be prepared by dispersing the drug into the polymeric matrix via two major methods i.e. solvent evaporation method or melting method. Using the solvent evaporation method (e.g. freeze-drying, spray drying, rotary evaporation, supercritical fluids, spin-coated films), the solid dispersion can be prepared by dissolving the drug and polymeric carrier in common solvents, followed by evaporating the solvent. The advantage of the solvent evaporation method is that the drug is simply homogeneously dispersed. In addition, the method is suitable for thermal labile drugs. However, the common solvents used are often organic solvent; thus, the environment and safety issues are of concern. Through the melting method (e.g. hot melt extrusion), the solid dispersion can be prepared by melting the drug and polymeric carrier, followed by rapidly cooling the molten mixture. The thermostability of the drug and the polymer should be considered when preparing solid dispersion by this method (1, 2).

Based on the solid states of the drug and the polymer present in a mixture, the solid dispersion can be divided into 3 categories, namely, eutectic mixture (crystalline drug and crystalline polymer), solid solution (amorphous drug and crystalline polymer) and glass solution (amorphous drug and amorphous polymer) (39).

The optimized process parameters along with an appropriate polymer type and drug to polymer ratio are contributed to an improvement of drug dissolution via several mechanisms. That is, crystalline state is converted to amorphous state or dispersed in the polymer at a molecular level. Furthermore, dissolution rate is increased by reduction of drug particle size. In addition, drug wettability and porosity can be improved when the drug is dispersed in the polymer (1). However, the development of amorphous solid dispersion to the market is still a challenge

because of the thermodynamically instable of amorphous drug. Thus, it tends to convert to a more stable crystalline counterpart with a decrease in solubility and dissolution.

2.2 Inhibition of drug recrystallization in a solid dispersion

When the drug is homogeneously dispersed in the polymeric matrix at a molecular level, the solid dispersion is denoted as a single phase amorphous system or miscible mixture. Recrystallization of the drug in the miscible mixture could be delayed and/or minimized. While, phase separation of amorphous drug in an immiscible dispersion is prone to rapid nucleation and crystal growth, leading to recrystallization (9, 10).

In the miscible dispersion, the polymer plays a key role in preventing amorphous drug from recrystallization. This may be due to that molecular mobility is decreased by several mechanisms, i.e. drug-polymer interaction including specific interaction such as hydrogen bonding (8, 11-17) and/or non-specific such as van der Waals force (18), anti-plasticizing effect resulting in an increase in T_g of a mixture compared to drug itself (16, 17), and physical barrier caused by the bulky structure of a polymer (16, 19). Furthermore, the polymer is attributed to lowering thermodynamic driving force for recrystallization which might be due to reduced amorphous free energy arisen from drug-polymer interaction (20-23).

The miscibility between the drug and the polymer is affected by drug concentration and preparation method (3-7). In drug concentration aspect, Yuan and Munson (4) found that the extent of drug-polymer interaction between indomethacin and polyvinylpyrrolidone (PVP) K25 in the solid dispersions prepared by melting method was increased with decreasing the drug loading (4). In preparation method aspect, Huang *et al.* (5) revealed that the extent of drug-polymer interaction between nifedipine and ethylcellulose and/or Eudragit RL® 100 in solid dispersions prepared by fast solidification rate method was higher than that prepared by slow solidification rate method. The authors also reported that the extent of drug-polymer interaction was increased with decreasing the drug loading (5). The similar

result was reported by Paudel *et al.* (3) that the miscibility level and the extent of drug-polymer interaction between naproxen and PVP K25 was higher in the solid dispersions prepared by melting compared to those prepared by film casting (3). Janssens *et al.* (7) studied the miscibility level of itraconazole/Eudragit® E100 solid dispersions prepared by spray drying and film casting. The authors found that the miscibility limit of the drug in the polymer prepared by spray drying was higher than that obtained from film casting (7). The similar result was found by Paudel *et al.* (6), that is, the faster evaporation rate in spray drying process resulted in the stronger hydrogen bond between naproxen and PVP K25 (6).

2.3 Intermolecular interactions

Intermolecular interaction could be typically divided into ion-ion forces, ion-dipole forces, dipole-dipole forces and van der Waals forces. The major intermolecular interaction between drug and polymer to stabilize the amorphous drug is hydrogen bond, a special case of dipole-dipole forces. This is because most drug substances possess hydrogen bonding sites (1). Besides hydrogen bond, van der Waals forces are also important in stabilizing amorphous drug. Although van der Waals forces are much weaker than hydrogen bond, they present in all molecules whether they are polar or non-polar (40).

The occurrence of drug-polymer interaction was the parameter indicating the miscible mixture (13, 24). The strength of this molecular interaction between drug and polymer subsequently has an impact on the stability of amorphous solid dispersion (15).

a) Hydrogen bond

A hydrogen bond occurs when hydrogen atom, which intramolecularly forms covalent bond with the highly electronegative atom e.g. O, N, F and Cl, forms intermolecular bond with the electronegative atom. The hydrogen atom is not shared and still covalently bond with its parent atom. The hydrogen bond between XH and Y can be depicted by X–H···Y. This intermolecular bond is similar to dipole-dipole force. However, the size of positively polarized hydrogen atom is relatively

small; hence, the electronegative atom of nearby molecules can come closer and strongly bond to the hydrogen atom.

Hydrogen bond is stronger than a typical dipole-dipole force, yet it is still much weaker than intramolecular forces (ionic or covalent bonds). The strength of most hydrogen bonds range from 10 to 40 kJ/mol; while, that of intramolecular forces is approximately 500 kJ/mol (40). The bond is moderately directional, that is, it is directed at a specific angle, and affecting the orientation of nearby molecules.

The strength of hydrogen bond between drug and polymer in a solid dispersion was indirectly determined by comparing degree of the shift in peak position using several tools e.g. XPS (27), IR (20, 23, 31), ss-NMR (29) and Raman spectroscopy (28). For quantitative analysis, the indirect method was also used. The degree of hydrogen bond was calculated based on peak height ratio (6, 23, 30) or peak area ratio (3, 41) from the IR spectra.

b) Van der Waals force

Van der Waals forces are divided into Keesom force (dipole-dipole), Debye force (dipole-induced dipole) and London force or dispersion force (42). They are the weakest intermolecular forces in which the strength of van der Waals forces is approximately 1 kJ/mol. The dispersion force is the major force contributing to the total van der Waals forces. It arises from electron cloud distribution, resulting in atom or molecule with temporary dipole. The temporary dipole would develop an electric field which can distort the electron clouds of neighboring neutral atoms or molecules, giving rise to the attractive force between atoms or molecules. The possibility of generating dispersion force depends on the polarizability, the ease of electron cloud to be distorted, of the molecules (40).

The dispersion force exists in all atoms and molecules, even neutral molecules e.g. hydrocarbons. It involves most phenomena such as adhesion, physical adsorption, solid strengths, the structures of proteins and polymers (40). In pharmaceutical solid dispersion area, Rawlinson *et al.* (18) reported that the hydrophobic interaction between benzene ring of ibuprofen and alkyl groups of

cross-linked PVP was an important mechanism to enhance crystalline to amorphous conversion of ibuprofen in the physical mixture composed of drug 30% w/w upon 72-week storage at ambient condition (18).

2.4 Characterization of miscibility between drug and polymer

Besides the calculation method, the miscibility between drug and polymer has been characterized by instrumental methods e.g. XRPD (24, 25), DSC (5, 7, 20, 21, 23, 24, 26-29), XPS (27), IR (5, 7, 20, 23, 24, 26, 30-32), ss-NMR (27, 29) and Raman spectroscopy (14, 28, 32-35). Among these methods, XRPD and DSC could not detect drug-polymer interaction. Whereas, XPS, IR, ss-NMR and Raman spectroscopy are the techniques revealing insight into the chemical structures of drug and polymer involving in the drug-polymer interaction by observing the shift in peak position and/or the change in peak shape.

a) X-ray powder diffractometry (XRPD)

XRPD is a standard method to investigate the properties of crystalline materials such as atomic spacing and crystal structure. X-ray diffraction is generated from the interaction between X-ray radiation and electron cloud of atoms. Crystalline material exhibits characteristic diffraction peak (Bragg peak) including 2θ position, peak height, peak area and peak width depending on type of atoms and atomic arrangement. Each crystal lattice exhibits its own *d*-spacing pattern (the spacing between a set of lattice planes) which results in characteristic peak positions. Peak height and peak area reflect the crystal structure such as atomic position; while, peak width reflects the defect of crystalline such as disorder and size of discrete domain. An amorphous material possesses a short range molecular conformation. There is no definite lattice pattern; thus, the XRPD pattern of amorphous material would not appear Bragg peaks, but rather depicts in the continuous halo pattern.

The instrument is typically composed of an X-ray source, incident beam optics, goniometer, diffraction beam optics and a detector. The XRPD technique is a non-destructive and moderately fast method. However, it requires large sample amount.

Furthermore, the contamination or solid state conversion could be concerned during sample preparation (43, 44).

In a solid dispersion sample, an XRPD result with a halo pattern principally suggests the amorphous drug is dispersed in the polymer. It indeed indicates that neither component in the mixture diffracts; hence, the drug may exist as a separated amorphous cluster and/or molecularly dispersed drug. Recently, XRPD has been used to determine the miscibility between drug and polymer by coupling with a computational analysis. The drug-polymer miscibility has been assessed by monitoring the shift of a halo peak, comparing with the pattern of pure amorphous drug (24, 25). However, this technique could not specifically determine the associated functional group of the intermolecular interaction.

b) Differential scanning calorimetry (DSC)

Basically, by this method, the temperatures of sample and reference would be maintained the same when heat is introduced. Once the sample exhibits some thermal events such as desolvation, glass transition, crystallization, melting and decomposition, the heat flow is transferred from the sample (exothermic events) or transferred to the sample (endothermic events). At this stage, there is a difference in the sample and reference temperatures. In case of heat-flux DSC, the different temperature which is resulted from heat capacity of the sample is measured by the separated thermocouples. In case of power compensated DSC, once the difference in temperature between the sample and the reference occurs, the more or less energy is input to maintain the sample and the reference at the same temperature. The power or heat flow required to maintain the temperatures is measured and plotted against temperature or time, and enthalpy change is analyzed (43, 45).

DSC is a destructive technique but it requires small sample size. It is well-established technique to screening miscibility of drug and polymer in solid dispersion. When a solid dispersion has two separated T_gs, the amorphous drug is considered to be immiscible with the polymer. When a single T_g appears between the T_gs of the drug and the polymer, it suggests this mixture is miscible (24, 43). The

occurrence of drug-polymer interaction could be indicated by the deviation from theoretical T_gs calculated from Gordon-Taylor equation (the ideality plot). The positive deviation from the ideality plot indicates that the drug and polymer interact more strongly than the drug itself, and the negative deviation indicates that drug and polymer interact more weakly than drug itself (7, 46). However, similar to the XRPD technique, it could not specifically determine the associated functional group of the intermolecular interaction. In addition, the size of amorphous cluster less than 30 nm generally could not be observed by DSC (29).

c) Infrared spectroscopy (IR)

IR technique is based on light absorption of a fundamental vibration dealing with a change in dipole moment (asymmetric vibration). The energy source wavelength ranges from 250 to 4000 cm^{-1}. The instrumentation can be designed as transmission or reflection geometry. This technique provides excellent fingerprint information but it is difficult to detect symmetric vibration i.e. aromatic compounds, C-C and C-S multiple bonds. Mid-IR is strongly absorbed by water; hence, it is not compatible with aqueous samples. It is also invasive technique as it cannot penetrate into common packaging materials e.g. glass. Furthermore, sample preparation e.g. KBr pellet is needed when using transmission mode (44, 47).

IR technique has been widely employed to qualitatively study drug-polymer interaction because change in chemical environment of a drug in a polymer would affect the spectral pattern i.e. peak position and/or peak shape. The degree of the shift in peak position is affected by the strength of drug-polymer interaction (20, 23, 31). The shift in drug peak position to lower wavenumber indicates stronger drug-polymer interaction than drug-drug interaction and vice versa. The stronger drug-polymer interaction influences on lengthening of the bond between drug-drug molecules; therefore, the vibrational mode of this longer distance of bonding between drug-drug molecules will shift to lower frequency (20, 35, 48).

The technique also has been utilized to quantitatively estimate the extent of hydrogen bond between drug and polymer in solid dispersion based on peak height

ratio (6, 23, 30) and peak area ratio (3, 41) of a non-interacted functional group to an interacted one. For the study of solid state stability, IR spectroscopy was applied to monitor drug-polymer interaction upon exposure to stress conditions. Huang *et al.* (17) and Rumondor *et al.* (13) have utilized this technique to reveal intermolecular interaction of miscible mixture after storage at 40°C/75% relatively humidity (RH) for 3 months (17) or after exposure to 75-94% RH (13). However, the detection was limited to hydrogen bond.

d) Solid state-nuclear magnetic resonance spectroscopy (ss-NMR)

ss-NMR detects the interaction between the spin of nuclear and the magnetic field. When applying the magnetic field to the non-zero nuclear element (e.g. ^{1}H, ^{2}H, ^{13}C, ^{29}Si), the magnetic energy level is split into parallel. The sum of all nuclear spins is called "magnetization". At equilibrium, magnetization is small. When a sample is placed, a small electric current is produced. Thus, nuclear spin is affected by both magnetic field and electric currents of the surrounding electrons. The NMR signal is free induction decay (FID) which is Fourier transformed to frequency or chemical shift (δ). Magic angle spinning (MAS) technique is developed to increase sensitivity of ss-NMR; thus, the sharp peaks are revealed. With MAS technique, the sample is rotated with a high frequency at an angle of 54.74° with respect to the magnetic field (49, 50). ss-NMR is a highly sensitive and non-destructive method. However, it is a very expensive technique and generally requires large sample amount. The operating time is also relatively long.

ss-NMR provides insight into the molecular structure of the drug. The change in chemical shift is resulted from the surrounding of different atoms or functional groups. Yuan *et al.* (29) applied ss-NMR to determine the miscibility between nifedipine and PVP K25 in solid dispersions by measuring relaxation time. The authors also indicated that the hydrogen bond was formed between the drug and the polymer by investigating the change in chemical shift (29). The extent of drug-polymer interaction between indomethacin and PVP K25 in solid dispersions was successfully determined using ss-NMR by measuring the spectral pattern (4).

e) Raman spectroscopy

Raman scattering (inelastic light scattering) was discovered by Krishna and Raman in 1928 (47). Raman spectroscopy is based on light scattering of the vibrational mode dealing with molecular polarization. When electrons are excited by laser light, they will induce polarization, distorting electron cloud from its equilibrium state. The excited electrons will be promoted to a higher energy state (a virtual state). Then the electrons will return to a ground state with scattered light radiation at the frequency of their oscillations. The light from the polarized electrons can be scattered in three frequencies i.e. same frequency as the incident light (Rayleigh scattering or elastic light scattering), lower frequency than the incident light (Stokes Raman scattering) and higher frequency than the incident light (anti-Stokes Raman scattering). The frequency difference between the incident and scattered light is called Raman shift which would occur at the specific wavenumber respecting to the conformation and molecular environment. The intensity of Rayleigh scattered light is 10^4 to 10^6 times stronger than Raman scattered light.

Raman spectroscopy is a complementary technique to IR spectroscopy as the Raman shift occurs at the same frequency observed with IR absorption. Both techniques provide high spectral resolution because they detect fundamental vibration. Raman spectroscopy is a non-destructive, non-invasive and rapid technique. In addition, water does not interfere the measurement as its weak Raman signal. Thus, this technique is compatible with an aqueous sample. The fiber-optic probe of this instrument enables the potential applications in process analytical technology. However, the instrument is expensive for routine use. This tool also has limited application for fluorescent molecules which is a typical interference when using low wavelength laser. Furthermore, Raman spectroscopy is a low sensitivity technique compared to IR because Raman scattering is 10^{10} weaker than mid-IR absorption. Surface-enhance Raman spectroscopy (SERS) and resonance Raman (RR) spectroscopy might be employed in this case to increase Raman intensity. Another limitation of this technique is that a sampling size, a laser focal point, is very small which might not properly represent the average of a bulk sample.

The major components of Raman spectroscopy are an excitation source (laser), a sampling module, a laser rejection filter, a wavelength analyzer and a detector. The instrument can be typically classified into two categories i.e. dispersive Raman spectroscopy and non-dispersive Raman spectroscopy (Fourier transform-Raman spectroscopy; FT-Raman spectroscopy) (Figure 1) based on the technique used in a wavelength analyzer and a detector.

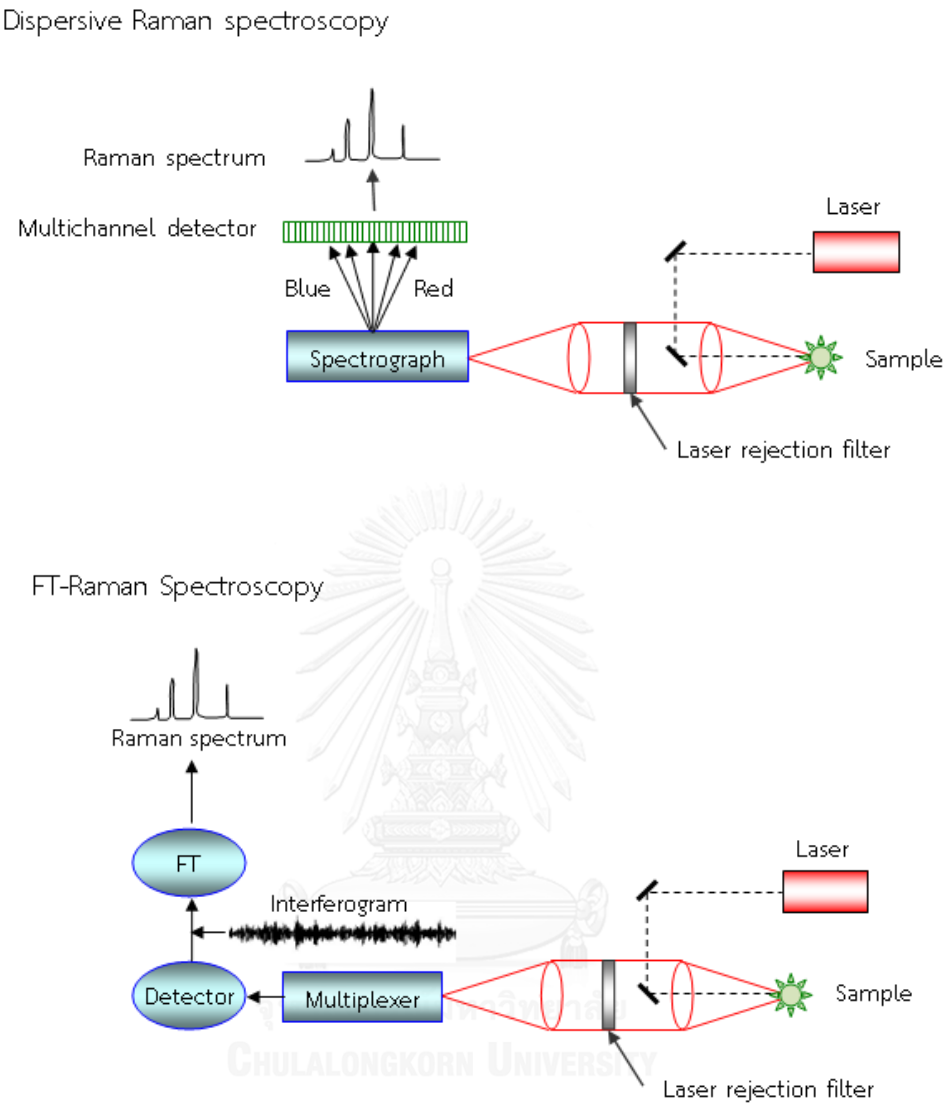

Figure 1 Instrumentation of dispersive Raman spectroscopy and FT-Raman spectroscopy (modified from (47)).

A laser wavelength ranges from UV to near infrared (NIR). Laser wavelengths of 200 - 800 nm is utilized in the dispersive Raman spectroscopy; while, that of 1064 nm is utilized in the FT-Raman spectroscopy. The lower laser wavelength possesses higher signal to noise ratio but it is at higher risk for fluorescence interference. A sampling mode can be backscattering geometry (conventional mode) i.e. 90° backscattering or 180° backscattering and transmission geometry (Figure 2). A similar sampling geometry is used in both dispersive and FT-Raman spectroscopy.

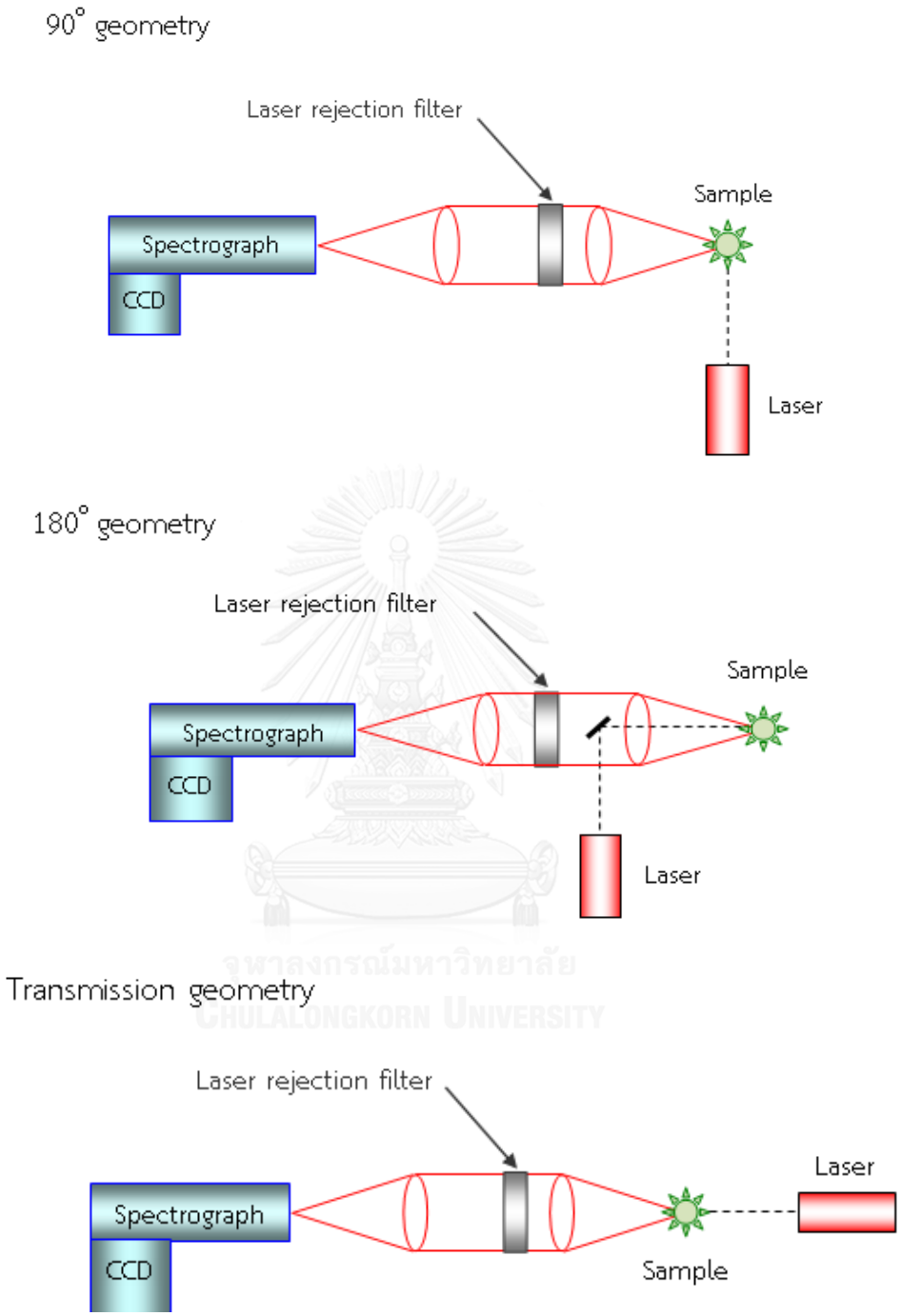

Figure 2 Sampling modes of backscattering geometry and transmission geometry for Raman spectroscopy (modified from (47)).

Transmission geometry is more useful in homogeneity study compared to backscattering geometry (51). Although, homogeneity study by backscattering geometry could be improved by extending sampling area in lateral dimensions (52),

an assessment in a volumetric dimension with this geometry is difficult. A sampling penetration depth by backscattering geometry is limited by the model specification and the magnification of objective lens. However, this obstacle could be encountered by applying confocal microscope to a backscattering geometry of which the sampling depth can be adjusted by using different confocal aperture diameter (47).

A laser rejection filter or notch filter is used for reducing the interference of elastic scattered light which is much more intense than inelastic Raman scattered light. In the dispersive Raman spectroscopy, the scattered light from a laser rejection filter is dispersed by a diffraction grating within a spectrograph to separate wavelengths. Then the separated wavelengths are spread on a charge-coupled devices (CCDs) multichannel detector (Figure 1). In the FT-Raman spectroscopy, several wavelengths pass through a multiplex and these wavelengths are modulated to their characteristic modulation frequency by an interferometer. An interferogram is generated and detected by a single detector, and Fourier transformation is processed to convert an interferogram to a Raman spectrum (Figure 1) (44, 47, 53).

Raman spectroscopy has a wide range of applications in the pharmaceutical area. As with IR, change in chemical environment of a drug in a polymer would affect the Raman spectral pattern in terms of peak position (14, 28, 32-35, 54), peak shape (34) or new peaks (18, 54). Raman scattered radiation is directly proportional to the vibrating species concentration as demonstrated in the equations (1) and (2).

$$S_v = K\sigma_v\upsilon_L(\upsilon_L-\upsilon_\beta)^3P_0C \qquad (1)$$

$$S_v = K\sigma_v(\upsilon_L-\upsilon_\beta)^4P_0C \qquad (2)$$

Where, S_v is the Raman signal; K is a constant depending on laser beam diameter, collection optics, sample volume and temperature; σ_v is the Raman cross section (the constant specific for the material at a particular wavenumber); υ_L is the wavenumber of the laser; υ_β is the wavenumber of the vibrational mode; P_0 is the laser power and C is the sample concentration.

The equation (1) is the relationship between the Raman signal and the sample concentration detected by Raman spectroscopy that measures the number of photons per second (CCD-Raman spectroscopy). While, the equation (2) is applied for Raman spectroscopy that measures optical power (FT-Raman spectroscopy) (44).

The application of Raman spectroscopy to determine intermolecular hydrogen bond has been carried out in binary mixtures containing indomethacin-polyethylene oxide (PEO) and theophylline-PEO (14), sugars-PVP K90 (28), indomethacin-PVP K90, (32) and "API"-cyclodextrins (34). To date, the use of Raman spectroscopy to indicate hydrophobic interaction was limited. Rawlinson *et al.* (18) has reported that molecular interaction between benzene ring of ibuprofen and alkyl groups of cross-linked PVP detected by Raman spectroscopy was an important mechanism to enhance crystalline to amorphous conversion (18).

For quantitative analysis, instead of drug-polymer interaction determination, Raman spectroscopy has been employed to detect polymorphic conversion and/or crystalline-amorphous phase separation of the drug and in solid dispersion (14, 34). In solid state stability aspect, Raman spectroscopy was used to qualitatively study the onset and recrystallization rate of nifedipine under 40°C and 20-80% RH (55).

2.5 Gaussian function fitting

The concept of curve fitting is to convert the experimental curve to the Gaussian distribution function by adjusting undetermined parameters i.e. peak height, peak width and peak position until the best fit is obtained. Gaussian curve fitting is based on nonlinear regression model. The fitting is achieved by iterative calculation using chi^2 (χ^2) minimization method. In the present study, χ^2 is determined by the non-weight method presented in the equation (3).

$$\chi^2 = \sum_{i=1}^{n} (y_i - f(x_i,\theta))^2 \qquad (3)$$

Where y_i is the i^{th} experimental data, x_i is the row vector of the i^{th} independent variable and θ is the parameter.

The Origin software, used in the present study, employs Levenberg-Marquardt algorithm to adjust the parameter values (56). The computing process starts from an initial guess of parameter values and stops by decision loops in order to obtain the parameter values that minimize residuals sum of squares between experimental data and model predictions (56, 57). The Levenberg-Marquardt algorithm was developed by Kenneth Levenberg and Donal Marquardt and it applies the advantages of the steepest descent algorithm and Gauss-Newton algorithm. The algorithm is implemented by two steps i.e. Jacobian matrix calculation and training process design. Once the Jacobian matrix is determined, the update rule of equation (4) is computed during the training process (58).

$$w_{k+1} = w_k - (J_k^T J_k + \mu I)^{-1} J_k e_k \qquad (4)$$

Where w is the weight vector, k is the index of iterations, J is the Jacobian matrix, μ is the combination coefficient, I is the identity matrix and e is the total error.

When the combination coefficient is large, the slow convergence of steepest descent algorithm is applied. The weight vector and combination coefficient are rigorously adjusted until the current error is less than the last total error. Then, the convergence is speed up by switching to Gaussian-Newton algorithm. The training process is iteratively calculated until the current total error is smaller than the required value (58).

The method of curve fitting based on Gaussian model has been demonstrated as an effective tool to resolve an overlapping spectrum for qualitative and quantitative analysis. Hu *et al.* (59) has successfully identified the number of peaks in the seriously overlapped UV/Vis spectrum using the minimum separable peak-peak interval method. Küpper *et al.* (60) has estimated the concentrations of various pigments coexisted in complex mixtures detected by UV/Vis spectroscopy by extracting the spectrum into a series of Gaussian peaks. This method showed an improved accuracy compared to the traditional method of linear equation based on

the absorption coefficient. Dong *et al.* (61) has applied curve fitting technique to indicate the four conformations of hydrogen bond in poly(acrylic acid) film extracted from the spectra of IR, Raman spectroscopy and near infrared spectroscopy (NIR) upon heating the compound from 40 to 140°C.

The application of curve fitting method for solid dispersion samples also has been demonstrated. Moskala *et al.* (41) has determined the strength of intermolecular hydrogen bonding between poly(vinyl phenol) (PVPh) and poly(vinyl acetone) or PVPh and ethylene-vinyl acetate in casted films with various PVPh loadings upon heating the sample from 30 to 190°C. The determination was achieved by using curve fitting method to separate an overlapping IR spectrum into the peaks of non-interacted functional group and interacted one. Then, the relative amount of hydrogen bonding was computed based on peak area ratio. A similar computational method has been reported by Paudel *et al.* (3). The IR spectra of naproxen - PVP K25 solid dispersions with various drug contents prepared by film casting or quench cooling were measured. Then, the relative amount of hydrogen bond between drug and polymer was evaluated by curve fitting method based on peak area ratio.

2.6 Model drug and polymer

a) Nifedipine

Nifedipine [1,4-dihydro-2,6-dimethyl-4-(2-nitrophenyl)-3,5-pyridinedicarboxylate] is a calcium channel blocker used for treatment of cardiovascular disease. The original nifedipine product is Adalat® which is commercially available in Thailand as the immediate-release soft gelatin capsule of 5 or 10 mg/capsule (62). The product is also available as Adalat® CR tablet of 20, 30 or 60 mg/tablet. Adalat® CR is the controlled-release tablet which is based on the osmotic pump delivery system (63).

Nifedipine appears in yellow crystalline powder, and its solution is very light sensitive (64). The solubility of nifedipine is demonstrated in Table I (64). The molecular weight of nifedipine is 346.34 g/mol. Nifedipine is a weak acid and its pK_a is 3.93. The solubility parameter of nifedipine was 21.9 $MPa^{1/2}$ (36).

Table I Solubility of nifedipine in various solvents at 20°C

Solvent	**Solubility (g/L)**
Acetone	250
Methylene chloride	160
Chloroform	140
Ethyl acetate	50
Methanol	26
Ethanol	17

The chemical structure of nifedipine is illustrated in Figure 3. The stable α-form of nifedipine crystallizes in the space group of $P2_1/c$ (65). To date, three polymorphic forms of nifedipine has been reported i.e. a stable α-form, a metastable β-form and γ-form (55). Another naming system was reported by Grooff *et al.* (66) as a stable form A, a metastable form B and form C (66). However, the interchangeability of the polymorphic name was valid only α - A and β - C (65)

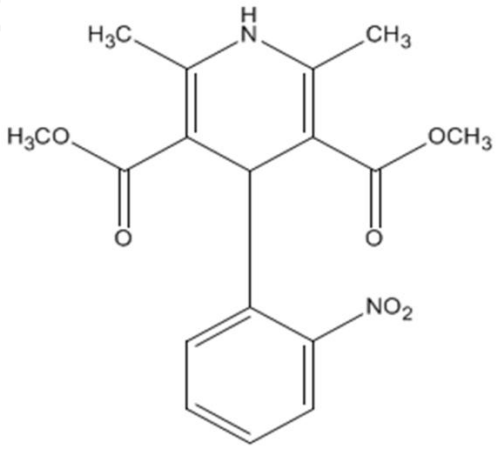

Figure 3 Chemical structure of nifedipine (reproduced from (67) with permission of Springer Science+Business Media).

Nifedipine contains hydrogen acceptors e.g. C=O and NO_2, and hydrogen donor e.g. NH. Tang *et al.* (48) has reported that the intermolecular hydrogen bond between nifedipine molecules occurred at C=O and NH due to the more basicity of C=O compared to NO_2 (48). The drug also contains the hydrophobic structure at the aromatic ring and the pyridine ring. The drug is classified in the BCS class II in which the low solubility of nifedipine is attributed to its low bioavailability. The solubility of crystalline nifedipine was approximately 8.7 μg/mL in water at 37ºC (68), and 11.7 μg/mL in fasted-state simulated intestinal fluid, pH 6.4, at 37ºC (69).

Solid dispersion has been extensively applied to enhance the solubility or dissolution rate of nifedipine. Several mechanisms to improve nifedipine solubility or dissolution rate in solid dispersions included conversion of crystalline to amorphous drug (68-73), reduction of drug particle size (68, 71) and increase of drug wettability (73, 74).

Amorphous nifedipine possessed relatively a low T_g of approximately 45°C (66); thus, it is likely to demonstrate a rapid crystallization. Chan *et al.* (55) found that amorphous nifedipine was crystallized to crystalline metastable β-form after 120 minutes (min) stored under 40°C/20% RH (55). Crystallization of nifedipine in solid dispersions composed of 10% w/w drug in polyethylene glycols were observed in all samples after exposure to different RH varied from 5 to 100% RH at 40°C for 2 hours (h) (75).

The effect of drug loading on miscibility between nifedipine and several polymers was studied. The solid dispersions of nifedipine and PVP K29-32 with drug loadings of 10, 30, 50, 70 and 90% w/w were prepared by solvent evaporation. All samples appeared to be miscible as determined by DSC and XRPD together with pair distribution function calculations. The hydrogen bond between the drug and the polymer in all samples was detected by IR with principal components analysis (24). Huang *et al.* (17) has investigated the miscibility and drug-polymer interaction of nifedipine and the polymers composed of Eudragit RL® 100 and ethylcellulose (2:1 w/w) in solid dispersions prepared by co-precipitation. The authors found that the samples with up to 21% w/w drug were miscible as the detection of a single T_g. The

hydrogen bond between nifedipine and both polymers in the sample with less than 21% w/w drug was detected by FT-IR (17). Furthermore, the extent of drug-polymer interaction, estimated by FT-IR, and the solubilized drug, estimated by DSC, in the polymer were also influenced by the types of polymer and polymer ratios, together with the effect of drug loadings (5).

The effect of preparation method on miscibility between nifedipine and PVP K25 in the solid dispersion was investigated by measuring relaxation time using ss-NMR. The drug and the polymer prepared by melt-quenching in the typical lab were miscible with drug loading up to 75% w/w. While, the samples prepared by spray drying or melt-quenching in ss-NMR rotor appeared to be miscible with drug loadings up to 90% w/w (29).

The influence of preparation method on the degree of drug-polymer interaction in solid dispersion containing nifedipine and polymers was also investigated. The solid dispersions of nifedipine and Eudragit RL® 100 or ethylcellulose were prepared by melting, co-evaporation and co-precipitation. The authors reported that the extent of hydrogen bond between nifedipine and Eudragit RL® 100 or ethylcellulose, identified by FT-IR, was highest in melting sample, and lowest in co-precipitation sample (5).

The influence of miscibility on solid state stability was studied by Ivanisevic (10). The miscible solid dispersions of nifedipine and PVPK29-32 were stored at ambient temperature and RH. Crystallization in the samples, as measured by XRPD, could not be detected up to 267 days (sample with 30% w/w drug), 404 days (sample with 40% w/w drug) and 396 days (sample with 60% w/w drug). For the sample with 70% w/w drug which contained trace amount of crystalline state was also classified as a miscible mixture. It was found that the content of crystalline state was not increased comparing with the initial time point upon storage up to 662 days. The author concluded that, in miscible mixture, the development of more crystallization could be suppressed even in the sample which contained trace crystalline state (10).

b) Soluplus®

Soluplus® is an amphiphilic polymer widely used to improve dissolution of poorly-water soluble drug by hot melt extrusion (26, 31, 76). Soluplus® contains polyethylene glycol 6000 / polyvinyl caprolactam / polyvinyl acetate at a ratio of 13/57/30, and its molecular weight is 90,000-140,000 g/mol. The polymer appears in white to yellowish granules. The solubility of the polymer is demonstrated in Table II (37). The T_g of Soluplus® is approximately 70°C. The solubility parameter of Soluplus® was 19.4 $MPa^{1/2}$ (37, 77).

Table II Solubility of Soluplus® in various solvents at 20°C

Solvent	Solubility (% w/w)
Acetone	40
Dimethylformamide	40
Ethanol	40
Methanol	40
Water	25
Propylene glycol	10

The chemical structure of Soluplus® is displayed in Figure 4. Soluplus® contains hydrogen acceptor e.g C=O and hydrogen donor e.g. OH. The polymer also contains the hydrophobic structure at the polyvinyl caprolactam segment.

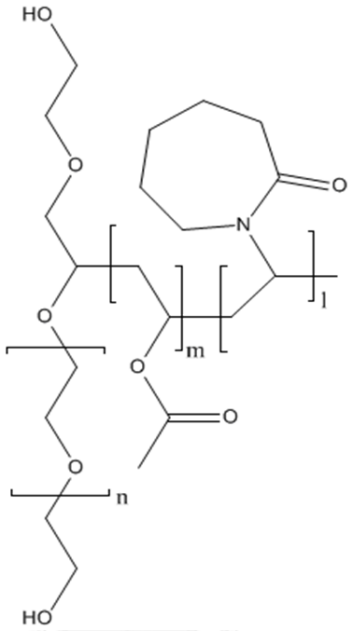

Figure 4 Chemical structures of Soluplus® (reproduced from (67) with permission of Springer Science+Business Media).

Soluplus® has been used to prepared solid dispersion with several drugs including nifedipine. The effect of preparation method on miscibility and drug-polymer interaction was investigated. The solid dispersions between nifedipine and the polymeric matrix composed of Soluplus® and/or Kollidon® SR, with drug loading of 30% w/w and varied ratios of the polymers, were prepared by hot melt extrusion, solvent evaporation and melting. The hydrogen bond between the drug and the polymers was detected in all samples. It was also found that the polymers had a synergistic effect on increasing the strength of hydrogen bond, detected by FT-IR, between the drug and the polymers. The strength of hydrogen bond, determined by the shift in peak position, was strongest in hot melt extrusion samples and weakest in melting samples. After storage at 40°C/75% RH for 15 days, the hydrogen bond was still detected in hot melt extrusion samples. While the hydrogen bond between the drug and the polymer in solvent evaporation and melting samples were

disappeared, and recrystallization was detected. The authors also observed the shifts in peak positions of C-H aliphatic stretching and C-H aromatic of nifedipine in solid dispersion composed of nifedipine and Soluplus® with 30% w/w drug (31).

Djuris *et al.* (26) has studied the miscibility between carbamazepine and Soluplus® in solid dispersions prepared by hot melt extrusion using varied process temperatures. The miscibility limit was determined by melting point depression. The hydrogen bond between the drug and the polymer was identified by FT-IR. It was concluded that carbamazepine was molecularly dispersed in Soluplus® with drug loading up to 5% w/w at all temperatures used in the experiment (26). The solid dispersions of carbamazepine and Soluplus® were also prepared by hot melt extrusion and film casting. The miscible between the drug and the polymer was found in samples with up to 30% w/w drug prepared by both methods as the presence of a single T_g in these samples (78).

CHAPTER III
MATERIALS AND METHODS

3.1 Materials

Chemicals

1 Acetonitrile (lot 505H1258, Kanto Chemical Co., Inc., Tokyo, Japan)
2 Distilled water (Autostill WG220, Yamato Scientific Co., Ltd., Tokyo, Japan)
3 Methanol (lot 505B11731, Kanto Chemical Co., Inc., Tokyo, Japan)
4 Nifedipine (lot TLL2258 and lot PDE4863, Wako Pure Chemical Industries, Ltd., Osaka, Japan)
5 Silica gel, medium granular, blue (lot WKM 6772, Wako Pure Chemical Industries, Ltd., Osaka, Japan)
6 Silicone fluid oil (KF-968-100CS, Shin-Etsu Chemical Co., Ltd., Tokyo, Japan)
7 Sodium chloride (lot AWJ4847, Wako Pure Chemical Industries, Ltd., Osaka, Japan)
8 Soluplus® (lot 20777268E0 and lot 21819647G0, BASF SE, Ludwigshafen, Germany)
9 Tertiary-butyl alcohol (lot 504H1644, Kanto Chemical Co., Inc., Tokyo, Japan)

Equipment

1 Differential scanning calorimeter (DSC) (DSC 8500, PerkinElmer, Inc., MA, USA) with Intracooler 2P (PerkinElmer, Inc., MA, USA), and Pyris software version 11.1.0.0488 (PerkinElmer, Inc., MA, USA)
2 Digital thermometer (TX10, Yokogawa Electric Corporation, Tokyo, Japan)
3 Dynamic vapor sorption (DVS) (DVS Advantage, Surface Measurement Systems Ltd., Middlesex, UK) with software DVS Win version 2.1.8 and DVS Analysis suite version 3.3 (Surface Measurement Systems Ltd., London, UK)

4 Fourier transform-infrared spectroscopy (FT-IR) (FT/IR-4100 equipped with attenuated total reflection (ATR) PRO410-S (JASCO International Co., Ltd., Tokyo, Japan)) with Spectra manager software version 2.2.9.1 (JASCO International Co., Ltd., Tokyo, Japan)

5 Freeze dryer (FD-80, Eyela, Tokyo Rikakikai Co., Ltd., Tokyo, Japan)

6 High performance liquid chromatography instrument (HPLC) composed of SCL-10A system controller, DGU-3A degasser, LC-10AD liquid chromatograph, CTO-10A column oven and SPD-10A UV spectrophotometric detector (Shimadzu Corporation, Kyoto, Japan) with CDS Lite software version 5.0 (DataApex, Prague, Czech Republic)

7 Hot air oven (WFO-450ND, Eyela, Tokyo Rikakikai Co., Ltd., Tokyo, Japan)

8 ISys® Chemical imaging analysis software version 5.0.0.11 (Malvern Instruments, Inc., Maryland, USA)

9 Microcal Origin® software version 3.5 (OriginLab Corporation, MA, USA)

10 Oil bath (OTS-2, Ishii Laboratory Works Co. Ltd., Osaka, Japan)

11 Pycnometer (Quantachrome instruments, FL, USA)

12 Raman spectroscopy (Raman RXN2, Kaiser Optical Systems, Inc., MI, USA) with objective lens (DM2500, Leica Microsystems, Tokyo, Japan), and Hologram software version 4.1 (Kaiser Optical Systems, Inc., MI, USA)

13 Rotary vacuum evaporator (Pair stirrer PS-100, Eyela, Tokyo Rikakikai Co., Ltd., Tokyo, Japan)

14 Single-punch tableting machine (Shimadzu, Kyoto, Japan)

15 Solid-state nuclear magnetic resonance spectroscopy (ss-NMR) (Bruker Avance II 300, Bruker AXS Inc., WI, USA) with Topspin software version 3.1 (Bruker AXS Inc., WI, USA)

16 Thermogravimetric analysis instrument (TGA) (TG8120, Rigaku Corporation, Tokyo, Japan) with Thermo plus 2 software (Rigaku Corporation, Tokyo, Japan)

17 X-ray powder diffractometer (XRPD) (Bruker D8 Discovery, Bruker AXS Inc., WI, USA) with GADDS software version 4.1.36 (Bruker AXS Inc., WI, USA)

18 Variable-temperature X-ray powder diffractrometer (VT-XRPD) (RINT 2000 Ultima^{+}, Riguku Corporation, Tokyo, Japan) and Windmax software (Riguku Corporation, Tokyo, Japan) coupled with X-ray powder diffractometer-differential scanning calorimeter (XRPD-DSC II, Riguku Corporation, Tokyo, Japan) and ThermoPlus 2 software version 4.208 (Riguku Corporation, Tokyo, Japan)

3.2 Methods

3.2.1 Preparation of standards of nifedipine and miscible solid dispersion

A commercial crystalline α-form of nifedipine (α-NIF) was used as received. An amorphous state and metastable crystalline β-form of nifedipine (β-NIF) which might occur during sample preparation were prepared to be reference standards for characterization. Solid dispersions where the drug was molecularly dispersed in the polymeric matrix with low and high drug concentrations were also prepared and applied for quantitative analysis of drug-polymer interaction in the solid dispersion.

a) Standard of amorphous nifedipine (am-NIF)

am-NIF was prepared by placing α-NIF in a stainless steel beaker and heating at 182±2°C for 15-30 min in an oil bath (OTS-2, Ishii Laboratory Works Co. Ltd., Osaka, Japan). The molten drug was quenched by removing the beaker from the oil bath. Then, the drug was equilibrated at room temperature for 15 min. The solid state of am-NIF was confirmed by XRPD and Raman spectroscopy. Its Raman spectrum was also used to establish a Gaussian function model for quantitative analysis of drug-

polymer interaction in the solid dispersion. The chemical stability of am-NIF was investigated by HPLC.

b) Standard of crystalline β-form of nifedipine (β-NIF)

β-NIF was generated by modifying the method reported by Grooff *et al.* (66). am-NIF was placed in a stainless steel beaker and heated at 92 ± 1°C for 3 min in an oil bath. Then, the beaker was removed from the heat source and stored at room temperature (~25°C) for 15 min. The solid state of β-NIF was confirmed by XRPD and Raman spectroscopy.

c) Standards of miscible solid dispersion

The standards of miscible solid dispersion were prepared at low and high drug concentrations. At the low drug concentration, drug-polymer interaction in the miscible solid dispersion was presumably dominant. At the high or saturated drug concentration, the drug-polymer interaction and drug-drug interaction in the miscible solid dispersion were assumed to be balanced.

Standard of miscible solid dispersion with the low drug concentration

Solid dispersions of nifedipine and Soluplus® with drug loadings of 0.1, 0.5, 1, 3 and 5% w/w were prepared by freeze drying (FD). This range was designated in order to determine a minimum drug concentration in the solid dispersion from which its signal could be sufficiently detected by Raman spectroscopy.

An accurate weight of α-NIF was dissolved in tertiary-butyl alcohol and Soluplus® was dissolved in methanol. The amount of methanol did not exceed 10% v/v of the total amount of solvent. After thoroughly dissolved, the two solutions were mixed in a polytetrafluoroethylene beaker with constant agitation. Then, quenching was carried out by adding liquid nitrogen into the solutions. The freezing solutions were placed under vacuum (FD-80, Eyela, Tokyo Rikakikai Co., Ltd., Tokyo, Japan) at approximately 0°C for 4 days. Then, the samples were vacuum dried over silica gel for at least 24 h at room temperature and 15-20% RH for residual solvent

removal. The batch sizes of the standards were 0.5 to 3 g which was adequate for characterization.

Each solid dispersion was measured by Raman spectroscopy. The solid dispersion which exhibited the most shift in peak position comparing with the peak position of a pure am-NIF was selected as the standard of miscible solid dispersion with the low drug concentration. Its spectrum was used to establish a Gaussian function model for quantitative analysis of drug-polymer interaction in the solid dispersion.

Standard of miscible solid dispersion with the high drug concentration

Solid dispersions of nifedipine and Soluplus® with drug loadings of 10, 30 and 50% w/w were prepared by FD as described above. This range of drug concentrations was designated based on the preliminary study of film casting. A clear film, suggesting miscibility between drug and polymer, could be obtained with the drug loading up to 35% w/w. The solid dispersion with 50% w/w drug was also prepared because it was postulated that fast solidification rate of FD might provide the higher saturated drug concentration in the miscible solid dispersion than that prepared by slow solidification rate of film casting.

Each solid dispersion was measured by Raman spectroscopy. The maximum drug concentration of solid dispersion which did not show characteristic spectra of am-NIF and/or crystalline nifedipine was chosen as the standard of miscible solid dispersion with the high or saturated drug concentration. Its spectrum was used to establish a Gaussian function model for quantitative analysis of drug-polymer interaction in the solid dispersion.

3.2.2 Preparation of solid dispersion samples

Solid dispersion samples composed of 10, 30, 50, 70 and 90% w/w of nifedipine in Soluplus® were prepared by three methods, i.e. FD, melting (ME) and solvent evaporation (SE) as follows:

a) FD

The samples were prepared as described above for the standards of miscible solid dispersions.

b) ME

Accurate weights of α-NIF and Soluplus® were mixed using a mortar and pestle about 3 min. The mixture was then placed in a stainless steel beaker and heated at 182 ± 2°C for 15-30 min in an oil bath until completely melted. The molten mixture was quenched by removing the beaker from the oil bath and equilibrated at room temperature for approximately 10 min. After solidification, the sample was gently ground using a mortar and pestle.

c) SE

Accurate weights of α-NIF and Soluplus® were dissolved in methanol. The solvent removal was done in a vacuum rotary evaporator (Pair stirrer PS-100, Eyela, Tokyo Rikakikai Co., Ltd., Tokyo, Japan) at 50-55°C. The sample was vacuum dried over silica gel for not less than 24 h at room temperature and 15-20% RH for residual solvent removal. Then, the dried sample was gently ground using a mortar and pestle.

All FD, ME and SE samples were kept in amber bottles at -20°C before characterization. The residual solvent and chemical stability were determined by TGA and HPLC, respectively. The crystallinity was investigated by XRPD. The miscibility of the drug and the polymer was studied by DSC, FT-IR, ss-NMR and Raman spectroscopy.

3.2.3 Characterization of solid dispersions

a) High performance liquid chromatography (HPLC)

As nifedipine is a light sensitive drug, the chemical stability of am-NIF and the drug in solid dispersions was assessed by an HPLC method according to the United States Pharmacopeia 36 (USP 36) (79). A chromatographic system was composed of

an SCL-10A system controller, a DGU-3A degasser, an LC-10AD liquid chromatograph, a CTO-10A column oven and a SPD-10A UV spectrophotometric detector (Shimadzu Corporation, Kyoto, Japan). The separation was accomplished by the following conditions:

Column	:	C_{18}, 5-µm particle size, 4.6x250 mm (Inertsil® ODS-3, GL Sciences Inc., Tokyo, Japan)
Column temperature	:	Ambient
Mobile phase	:	Water : Acetonitrile : Methanol (50:25:25)
Flow rate	:	1 ml/min
Injection volume	:	25 µl
Detector	:	UV 265 nm

The instrument was controlled by CDS Lite version 5.0 (DataApex, Prague, Czech Republic) software.

Analytical method verification

Specificity, linearity, range, accuracy and precision of the analytical method were verified (79).

Specificity

An accurate weight of Soluplus® was transferred to a volumetric flask. The polymer was dissolved with the mobile phase to obtain Soluplus® concentration of 1 mg/ml

Linearity

Stock standard solution

An accurate weight of α-NIF was transferred to a volumetric flask. The drug was dissolved with methanol (not exceeding 10% v/v of the total amount of diluent). Then, the solution was diluted to the volume with the mobile phase to obtain nifedipine concentration of 1 mg/ml.

Standard solutions

A series of standard solutions were prepared by diluting the stock standard solution with the mobile phase to obtain nifedipine concentrations of 0.02, 0.04, 0.06, 0.08, 0.10 and 0.12 mg/ml.

The solutions were prepared in triplicate. The calibration parameters i.e. slope (a), intercept (b), coefficient of regression (R) and coefficient of determination (R^2) were calculated.

Range

The values between the lowest and the highest concentrations of linearity were determined as a range.

Accuracy

Stock standard solution

Accurate weights of α-NIF and Soluplus® were transferred to a volumetric flask. The drug and the polymer were dissolved with methanol (not exceeding 10% v/v of the total amount of diluent). Then, the solution was diluted to the volume with the mobile phase to obtain nifedipine concentration of 0.55 mg/ml and Soluplus® concentration of 4.95 mg/ml.

Standard solutions

A series of standard solutions were prepared by diluting the stock standard solution with the mobile phase to obtain the following solutions:

a) Nifedipine 0.011 mg/ml and Soluplus® 0.1 mg/ml

b) Nifedipine 0.055 mg/ml and Soluplus® 0.5 mg/ml

c) Nifedipine 0.110 mg/ml and Soluplus® 1.0 mg/ml

The solutions were prepared in triplicate. An added amount of nifedipine was plotted against a found amount of nifedipine. Then, the slope, y-intercept and R^2 were determined. Accuracy was present as % recovery.

Precision

Standard stock solution

Accurate weights of α-NIF and Soluplus® were transferred to a volumetric flask. The drug and the polymer were dissolved with methanol (not exceeding 10% v/v of the total amount of diluent). Then, the solution was diluted to the volume with the mobile phase to obtain nifedipine concentration of 1 mg/ml and Soluplus® concentration of 9 mg/ml.

Standard solutions

The stock standard solution was diluted with the mobile phase to obtain nifedipine concentration of 0.1 mg/ml and Soluplus® concentration of 0.9 mg/ml. Repeatability was determined from six replications, and intermediate precision was determined by the repeatability of three different days. The relative standard deviation (RSD) of measured concentration of the drug was calculated.

Assay

The chemical stability of am-NIF and the drug in the prepared solid dispersion, and that in the stressed solid dispersion which were stored at 98°C or 60°C/75%RH were measured by transferring an accurate weight of sample to a volumetric flask. The sample was dissolved with methanol and diluted to the volume with the mobile phase to obtain nifedipine concentration of 0.1 mg/ml. The measurements were done in duplicate. System suitability was determined by 6 replicate injections. The column efficiency was not less than 4000 theoretical plates. The tailing factor was not more than 1.5 and the RSD for replicate injections was not more than 1.0%. Each sample contained not less than 90.0% and not more than 110.0% of the labeled amount of nifedipine.

b) X-ray powder diffractometry (XRPD)

XRPD

XRPD was used to confirm the solid state of a commercially available α-NIF, prepared am-NIF, prepared β-NIF, also to characterize the solid state of Soluplus®, the prepared solid dispersions and the stressed miscible solid dispersions which were stored at 60°C/75% RH.

The sample powder was placed on a quartz sample holder. An XRPD pattern was measured by a Bruker D8 Discovery (Bruker AXS Inc., WI, USA) controlled by GADDS version 4.1.36 (Bruker AXS Inc., WI, USA) using Cu K-α radiation with the voltage and current of 40 kV and 40 mA, respectively. Each sample was measured from 2θ of 3.8 to 27.5° with a step size of 0.02°.

Variable-temperature X-ray powder diffractometry (VT-XRPD)

VT-XRPD was used to study the crystallization tendency in the miscible and immiscible solid dispersions. The onset of detectable crystallization was real time monitored.

The experiment was done by VT-XRPD (RINT 2000 Ultima+, Riguku Corporation, Tokyo, Japan) controlled by Windmax software (Riguku Corporation, Tokyo, Japan). The sample powder was placed on an aluminium pan (Riguku Corporation, Tokyo, Japan) and heated from room temperature to 98 ± 2°C with a rate of 10°C/min by XRPD-DSC II (Riguku Corporation, Tokyo, Japan) controlled by ThermoPlus 2 version 4.208 (Riguku Corporation, Tokyo, Japan). Nitrogen with a flow rate of 100 ml/min was supplied. An XRPD pattern was collected using Cu K-α radiation with the voltage and current of 40 kV and 40 mA, respectively. The sample was measured from 2θ of 5.0 to 30.0° with a step size of 0.02° and a scan speed of 20°/min. The onset time for observable crystallization was determined after reaching the maximum temperature.

c) Differential scanning calorimetry (DSC)

A conventional DSC method was used to determine the miscibility between the drug and the polymer in the prepared solid dispersions.

The thermal analysis was measured by a DSC 8500 (PerkinElmer, Inc., MA, USA) equipped with Intracooler 2P (PerkinElmer, Inc., MA, USA), and controlled by Pyris version 11.1.0.0488 (PerkinElmer, Inc., MA, USA). The temperature and enthalpy was calibrated using indium. Nitrogen was supplied at a flow rate of 20 ml/min. The sample powder was sealed in a standard aluminium pan (PerkinElmer, Inc., MA, USA).

For the thermal analysis of am-NIF and β-NIF, they were primarily generated in situ in a DSC pan. am-NIF was formed by heating α-NIF from 0 to 178°C with a rate of 10°C/min and holding for 15 min, followed by cooling to 0°C with a rate of 50°C/min. β-NIF was formed by modifying the method reported by Grooff *et al.* (66). The in situ formed am-NIF was heated from 0 to 120°C with a rate of 10°C/min, and cooling to 0°C. Then, the thermal events of α-NIF, β-NIF and am-NIF including T_g, crystallization temperature (T_c) and melting temperature (T_m) were measured by heating from 0 to 200°C with a rate of 10°C/min.

For the thermal analysis of Soluplus® and solid dispersion samples, the material was heated from 0 to 80°C with a rate of 10°C/min, held for 20 min and cooled to 0°C with a rate of 50°C/min. Then, it was reheated from 0 to 200°C with a rate of 10°C/min. The first heating run was carried out to reduce the effect of plasticizing solvent on T_g (7). The thermal events including T_g, T_c and T_m were examined from the reheating run.

The experiment was done in triplicate. The reported values are midpoint T_g, onset T_c and onset T_m. The miscible solid dispersion was classified by the presence of single T_g between the T_gs of nifedipine and Soluplus®, and the absence of T_m.

Modulated temperature differential scanning calorimetry (MDSC)

The instrument and software for MDSC measurement was the same as used in the conventional DSC measurement. A sample was sealed in a standard aluminium pan (PerkinElmer, Inc., MA, USA) and heated from 0 to 180°C. A heating rate

between steps was 1°C/min and a temperature increment between steps was 0.5°C with a holding time of 1 min.

The measurements were done in triplicate. The midpoint T_g, was extracted from a reversing heat flow curve.

Calculation of T_g using Gordon-Taylor equation

The observed T_gs of samples were plotted against polymer contents and compared with the theoretical T_gs calculated from the Gordon-Taylor equation using the equations (5) and (6) (80). The deviation of the observed T_gs from the theoretical T_gs suggests the molecular interaction between the drug and the polymer.

$$T_g = \frac{w_1 T_{g1} + K w_2 T_{g2}}{w_1 + K w_2} \quad (5)$$

$$K = \frac{\rho_1 T_{g1}}{\rho_2 T_{g2}} \quad (6)$$

Here, w and ρ are the weight fractions and true densities, respectively, and T_g is the glass transition temperature. The true density of Soluplus® was determined by helium pycnometer and that of am-NIF was reported by Forster *et al.* (80).

d) Fourier transform-infrared spectroscopy (FT-IR)

FT-IR was used to examine drug-polymer interactions including specific and non-specific interaction in the solid dispersions.

The experiment was performed by a FT/IR-4100 with an attenuated total reflection (ATR) PRO410-S (JASCO International Co., Ltd., Tokyo, Japan) controlled by Spectra manager software version 2.2.9.1 (JASCO International Co., Ltd., Tokyo, Japan). The sample powder was measured from 400 to 4,000 cm^{-1} with a resolution of 4 cm^{-1}. Each spectrum was averaged from 64 scans. The occurrence of drug-polymer interaction was proved by the shift in peak position of the drug.

e) Solid state-nuclear magnetic resonance spectroscopy (ss-NMR)

ss-NMR was used to investigate drug-polymer interactions including specific and non-specific interaction in the solid dispersions.

The experiment was carried out by a Bruker Avance II 300 (Bruker AXS Inc., WI, USA), and controlled by Topspin software version 3.1 (Bruker AXS Inc., WI, USA). The instrument was operated on ^{13}C cross-polarization/magic angle spinning (CPMAS) with a transmitter frequency of 75 MHz. A CPMAS standard bore probe (Bruker AXS Inc., WI, USA) with 5 kHz for ^{13}C and 62 kHz for ^{1}H, and a two pulse phase modulation (TPPM) of 15 decoupling was run at 300 kelvin. A chemical shift was calibrated using glycine. The sample powder was inserted in a MAS 7-mm zirconia rotor and covered with a Kel-F cap (Bruker AXS Inc., WI, USA). The spinning rate was set at 5 kHz. The contact time was 1.75 milliseconds and the amplitude ramp on ^{1}H channel was approximately 49 Watts (from 50 to 100%). The spectra were visually investigated. The occurrence of drug-polymer interaction was proved by the shift in peak position of the drug.

f) Raman spectroscopy

Raman spectroscopy was applied to examine the spectral pattern of Soluplus® and to qualitatively and quantitatively determine drug-polymer interactions including specific and non-specific interaction in the solid dispersion samples. The tool was also used to verify the solid state of a commercially available α-NIF, am-NIF and β-NIF by comparing to the spectra reported by Chan *et al.* (55).

The sample surface was flattened by a tableting machine (Shimadzu, Kyoto, Japan) with a compression force of 0.5 ton/cm^2 before measuring. The measurement was performed by a Raman RXN2 (Kaiser Optical Systems, Inc., MI, USA), and controlled by Hologram version 4.1 (Kaiser Optical Systems, Inc., MI, USA). The instrument was a dispersive Raman spectrometer consisting of a 1,000-nm laser wavelength, a 180° backscattering sampling geometry and an InGaAs array detector. The spectrum was measured from 200 to 2,400 cm^{-1} with a resolution of 5 cm^{-1} and an exposure time of 5 seconds. A wavenumber was calibrated using naphthalene.

The objective lens (DM2500, Leica Microsystems, Tokyo, Japan) was 50x with a 16-μm sampling diameter and a 32-μm sampling depth. The spectra of α-NIF, β-NIF, am-NIF and Soluplus® were averaged from a 100-point map (200 x 200 μm^2); while, that of the standards of solid dispersion with the low and high drug concentrations and solid dispersion samples for qualitative analysis were averaged from a 1,200-point map (800 x 600 μm^2).

The spectra were then visually investigated. The occurrence of drug-polymer interaction was determined by the shift in peak position of the drug. The quantitative analysis of drug-polymer interactions was carried out on the solid dispersion samples which showed X-ray halo pattern i.e. X-ray amorphous sample. The spectra of these samples were averaged from a 100-point map. Nifedipine presenting as amorphous state, and molecularly dispersed within the polymer at the low and high drug concentrations were quantified by calculating the average of 6 maps.

The qualitative analysis of drug-polymer interactions

Spectral data preprocessing

The Raman spectra of α-NIF, am-NIF, β-NIF, Soluplus®, the standards of miscible solid dispersion with the low and high drug concentrations and the solid dispersion samples were preprocessed by ISys® Chemical imaging analysis version 5.0.0.11 (Malvern Instruments, Inc., MD, USA). The spectra covering 550 to 1800 cm^{-1} were averaged. Then, the averaged spectrum was baseline corrected at 660 and 872 cm^{-1}, and normalized by standard normal variate (SNV). The shift in peak position was visually inspected to identify drug-polymer interactions.

The quantitative analysis of drug-polymer interactions

The quantitative analysis of drug-polymer interactions in the prepared solid dispersions and the stressed solid dispersions which were stored at 60°C/75% RH were implemented with the following steps:

Spectral data preprocessing

The spectra of am-NIF, Soluplus®, the standards of miscible solid dispersion with the low and high drug concentrations and the X-ray amorphous solid dispersion samples were preprocessed by average and baseline correction as the same procedures as described above for the qualitative analysis.

Gaussian function fitting

Microcal Origin® version 3.5 (OriginLab Corporation, MA, USA) was employed to generate the model spectrum consisting of a series of Gaussian peaks which represented the experimental spectrum. The parameters i.e. peak height, peak width and peak position were incorporated to construct the Gaussian peaks, and the Gaussian function model of the spectrum was obtained by a linear combination of all Gaussian peaks as expressed in the equation (7).

$$f(x) = \sum_{i=1}^{N} (abs(P_1) \cdot \exp(-abs(P_2) \cdot (x - abs(P_3))^2))_i \qquad (7)$$

Where, f(x) is a series of Gaussian peaks describing the model spectrum; abs is absolute; exp is exponential; P_1 is the peak height; P_2 is the peak width; P_3 is the peak position and x is the experimental peak position.

The experimental spectrum of am-NIF and Soluplus® was directly converted to their model spectrum by fitting with Gaussian function.

The standard of miscible solid dispersion with the low drug concentration was selected among the FD samples consisting of 0.1, 0.5, 1, 3 and 5% w/w drug, which showed the most shifts in drug peak position compared to am-NIF's peak. Then the experimental spectrum of the selected sample was converted to the Gaussian function model of the standard of miscible solid dispersion with the low drug concentration.

The experimental spectrum of the standard of miscible solid dispersion with the low drug concentration was also subtracted by the model spectrum of Soluplus®. The remaining portion was converted to the Gaussian function model.

The model was defined here as model “M”. The model “M” therefore solely represented the spectra of the drug molecules which were molecularly dispersed in the polymer. This model would be used in calculation of the standard of miscible solid dispersion with the high drug concentration.

The standard of miscible solid dispersion with the high drug concentration was selected as the following step. The experimental spectra of the solid dispersion with drug loadings of 10, 30 and 50% w/w were subtracted by the model spectra of am-NIF and model “M”, and the resulting spectrum was converted to new Gaussian function models for each drug loading. The new model, model spectra of am-NIF and model “M” was then used to calculate the fractional area of each state under the experimental spectrum of solid dispersion. The fractional area of each is calculated relative to the total area which is normalized to 100% as described in equation (8).

$$\text{Normalized peak area of A} = \frac{\text{(Fractional area of A) x 100}}{\text{Area of A + area of B + area of C}} \qquad (8)$$

Where, A, B and C are the new model, model spectra of am-NIF and model “M”, respectively.

The solid dispersion which did not contain the fractional area of am-NIF and had the greatest remaining area under the experimental spectrum after subtracting by each model was chosen to be the miscible solid dispersion with a saturated drug concentration. Its “new Gaussian function model” was designated to be the model spectrum of the standard of miscible solid dispersion with the high drug concentration.

The model spectra of the standards of miscible solid dispersion with the low and high drug concentrations and am-NIF were further applied to estimate the proportion of these states in the X-ray amorphous samples prepared by FD, ME and SE. First, the experimental spectra of X-ray amorphous samples were converted to the model spectra by linear summation of the model spectra of low and high drug concentrations and am-NIF. Then, the best fit was obtained by varying the

coefficient of each state, justified by the minimal chi^2 value, as expressed in equation (9).

$$g(x) = a \cdot f(x)_{low} + b \cdot f(x)_{high} + c \cdot f(x)_{am\text{-}NIF} + d \quad (9)$$

Where, g(x) is a function describing the model spectrum of a sample; a, b, c are the coefficients of the Gaussian function models of the standards of miscible solid dispersions with the low and high drug concentrations and amorphous state, respectively; f(x) is the Gaussian function model of each state and d is y-intercept of baseline.

The weight fraction of the drug dispersed in each state was computed based on the fractional area under the peak, relative to the total area which is normalized to 100% w/w drug loading as shown in equation (10)

$$\text{Normalized weight fraction of A} = \frac{\text{(Fractional area of A) x 100}}{\text{Area of A + area of B + area of C}} \quad (10)$$

Where, A and B are the miscible solid dispersions with the low and high drug concentration states, respectively and C is the amorphous state.

3.2.4 Solid state stability study of solid dispersion samples

a) Crystallization tendency

An effect of miscibility between drug and polymer in the FD, ME and SE solid dispersion on the crystallization tendency was investigated. The immiscible solid dispersions which might exhibit rapid crystallization were monitored in real time by VT-XRPD. The study was conducted at 98 ± 2°C and relative time to detectable crystallization was observed. The miscible solid dispersions which might present slow crystallization were stored at 98 ± 2°C in a hot air oven (WFO-450ND, Eyela, Tokyo Rikakikai Co., Ltd., Tokyo, Japan). The onset time for observable crystallization was determined. The experiment was terminated when the content of nifedipine in the sample was less than 90.0% w/w or at the maximum time of 3 months. The measurements were done in triplicate. The correlation between the relative amount

of nifedipine molecularly dispersed in the polymer and the onset time for observable crystallization was investigated.

b) Tendency to undergo amorphous phase separation

An effect of drug-polymer interaction on tendency for the miscible solid dispersion to undergo amorphous phase separation was investigated. The miscible solid dispersions with the low and high drug concentrations were subjected to this experiment. The samples were stored in a desiccator containing a saturated sodium chloride solution to obtain approximately 75% RH and placed at 60 ± 2°C in a hot air oven (WFO-450ND, Eyela, Tokyo Rikakikai Co., Ltd., Tokyo, Japan) for 3 months. The fractions of drug dispersed in miscible solid dispersions with the low and high drug concentrations and am-NIF in stressed samples were periodically investigated by Raman spectroscopy. The crystallinity of samples was investigated by XRPD. The experiment was terminated when either the chemical stability of nifidipine in the samples was less than 90.0% w/w or the Raman spectral pattern of the sample was not fitted with the standard patterns.

3.2.5 Other characterization

a) Dynamic vapor sorption (DVS)

Moisture could influence on the properties of amorphous material e.g. T_g. Thus, the hygroscopicity including adsorption and absorption behaviors of am-NIF and Soluplus® was studied.

The vapor sorption isotherms were investigated by DSV apparatus (DVS Advantage, Surface Measurement Systems Ltd., Middlesex, UK) at room temperature. The experiment was controlled by software DVS Win version 2.1.8 and DVS Analysis suite version 3.3 (Surface Measurement Systems Ltd., London, UK). Samples of approximately 3 mg were placed on an aluminium pan and exposed to water vapor from 0 to 98% RH with a step size of 5% RH. The equilibrium of each humidity level was determined when the change in mass within a minute (dm/dt) was not exceeded 0.004%.

b) Thermogravimetric analysis (TGA)

The amount of residual solvent in a solid dispersion sample was measured by TGA. The value was applied to calculate the chemical stability of nifedipine in solid dispersion sample determined by HPLC.

The experiment was carried out by TGA apparatus (Thermo plus TG8120, Rigaku Corporation, Tokyo, Japan). Samples of approximately 3 mg were placed in a 70-µl aluminium cup (Rigaku Corporation, Tokyo, Japan). Nitrogen at a flow rate of 50 ml/min was used as the purge gas. The sample was heated from room temperature (~25°C) to 120°C with a rate of 10°C/min.

c) Pycnometry

Pycnometry was applied to measure the true density of Soluplus® which was used to calculate the theoretical T_g based on Gordon-Taylor equation as described in DSC section.

The true density was determined by a helium displacement pycnometer (Quantachrome instruments, FL, USA). Approximately 1 g sample was filled in a microcell and covered with a lid. The experiment was conducted at room temperature using 99.999% helium with a pressure of 17.0 psi. The measurements were done with five replications.

CHAPTER IV
RESULTS AND DISCUSSIONS

4.1 Characterization of solid dispersions

a) X-ray powder diffractometry (XRPD)

A commercial α-NIF exhibited diffraction peaks at 8.4, 10.7, 12.0, 16.4, 19.9 and 24.9°; while, β-NIF presented the characteristic peaks at 7.8, 9.5, 11.1, 12.6, 17.2 and 24.3°. am-NIF showed a halo pattern. These diffraction patterns corresponded to the values reported by Grooff *et al.* (66). The FD, ME and SE samples with drug loadings up to 70, 90 and 30% w/w, respectively showed X-ray halo patterns as depicted in Figure 5a (FD samples), Figure 5b (ME samples) and Figure 5c (SE samples). The FD sample composed of 90% w/w possessed the characteristic peaks of β-NIF; while, the SE samples with 50, 70 and 90% w/w drug showed the diffraction peaks identical to α-NIF.

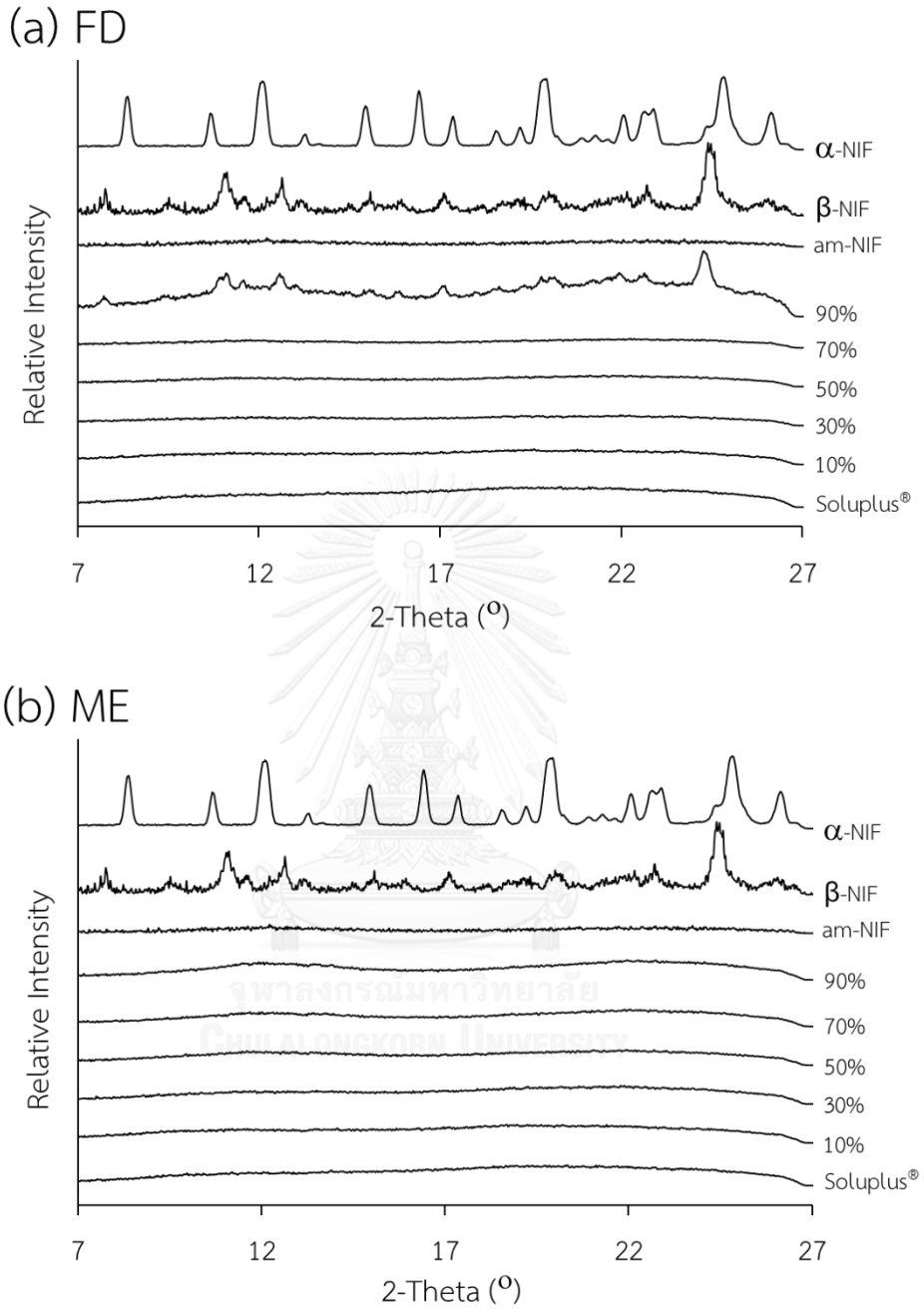

Figure 5 XRPD patterns of Soluplus®; solid dispersions with drug loadings of 10, 30, 50, 70, 90% w/w; am-NIF; β–NIF and α-NIF. The samples were prepared by (a) FD, (b) ME and (c) SE methods. Reproduced from (67) with permission of Springer Science+Business Media.

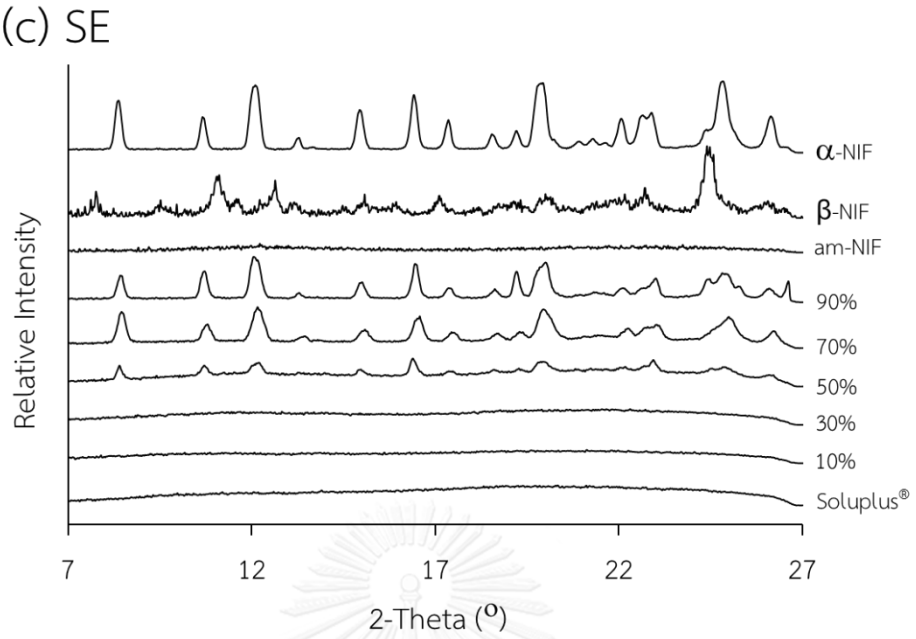

Figure 5 (continued) XRPD patterns of Soluplus®; solid dispersions with drug loadings of 10, 30, 50, 70, 90% w/w; am-NIF; β–NIF and α-NIF. The samples were prepared by (a) FD, (b) ME and (c) SE methods. Reproduced from (67) with permission of Springer Science+Business Media.

Crystalline phase separation was found in samples with high drug content prepared by solvent method i.e. FD and SE. While, the recrystallization phenomenon could not be observed in the samples with the entire range of drug loadings prepared by melt quenching technique. This was probably due to the rearrangement of drug molecules from am-NIF to a more stable crystalline form, either α-NIF or β–NIF, before the completion of solvent removal. The SE method possessed a slower rate of solvent removal, compared with the FD method. This allowed more time for the drug molecules in SE samples to rearrange themselves and form the more stable α-NIF form at lower drug concentrations.

XRPD is the primary tool to identify the solid state of the drug in a solid dispersion. When the diffraction events are present, the drug in the mixture is a crystalline state. When the halo pattern is observed, it indicates that neither component in the mixture diffracts. In the latter case, the drug might exist in amorphous state or be dispersed at the molecular level in the polymeric matrix.

Therefore, the drug-polymer miscibility in X-ray amorphous sample could not be justified by XRPD.

b) Differential scanning calorimetry (DSC)

The thermal analysis was measured by a conventional DSC. The thermal events of Soluplus®, am-NIF, β-NIF and α-NIF are depicted in Figure 6. The values shown in the figure are an example of one measurement; while, the reported values in the text are averaged from three measurements. A stable crystalline α-NIF was melted at 172.3°C. A metastable β-NIF was transformed to an another metastable form at 61.2°C, followed by the conversion to a stable α-NIF at 118.5°C which was melted at 170.3°C. The T_g of am-NIF was found at 44.8°C. It was crystallized to a metastable form at 96.0°C, and further converted to α-NIF at 119.1°C, followed by melting at 170.2°C. These results were in agreement with the values reported by Grooff *et al.* (66, 81). Soluplus® exhibited T_g at 76.2°C; while crystallization and melting events were not observed.

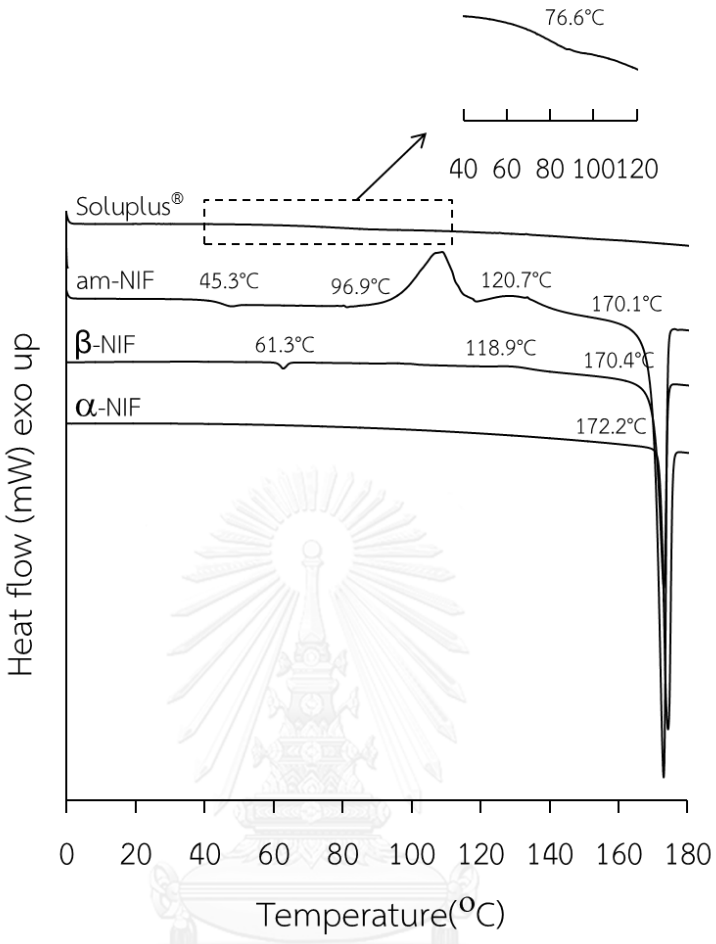

Figure 6 Thermal events of Soluplus®, am-NIF, β-NIF and α-NIF heated from 0 to 200°C with a heating rate of 10°C/min. The thermograms and values in the figure were obtained from one measurement.

For solid dispersions, the samples were first heated to 80°C to reduce the effect of plasticizing solvent on T_g. This temperature was chosen as it was at least 10°C lower than the crystallization temperature. The single T_g of FD samples was shifted from 72.7 to 46.7°C with increased weight fractions of the drug from 10 to 70% w/w as demonstrated in Figure 7a. The sample with 70% w/w drug also exhibited crystallization and melting events at 93.6 and 158.2°C, respectively. The FD sample with 90% w/w drug did not exhibit the glass transition but it had the thermal event pattern similar to that of β-NIF. This sample showed an endothermic

transformation at 57.8°C, followed by an exothermic conversion at 134.9°C and melting at 169.9°C.

The ME samples exhibited a decrease in single T_gs from 70.2 to 47.0°C upon increasing the drug concentrations from 10 to 90 % w/w as shown in Figure 7b. In addition to the presence of T_g, crystallization events were observed at 98.3 and 85.6°C in the samples composed of 70 and 90% w/w drug, respectively. Melting events were also detected at 158.0, 166.3 and 171.1°C in the samples composed of 50, 70 and 90% w/w drug, respectively.

The similar trend of downward shifts of a single T_g as increasing drug loadings was also present in the SE samples as shown in Figure 7c. When the drug loadings were increased from 10 up to 70% w/w, the single T_g was decreased from 71.8 to 50.6°C. The sample with 50% w/w drug also showed melting at 143.5°C. The sample with 70% w/w drug demonstrated crystallization at 111.2°C followed by melting at 160.3°C. The observation of T_gs in these samples suggested that the drug was remained in am-NIF, together with α-NIF in the polymeric matrix as detected by XRPD. The SE sample consisting of 90% w/w drug exhibited melting at 170.9°C without the detection of glass transition and crystallization, similar to the thermal event of α-NIF.

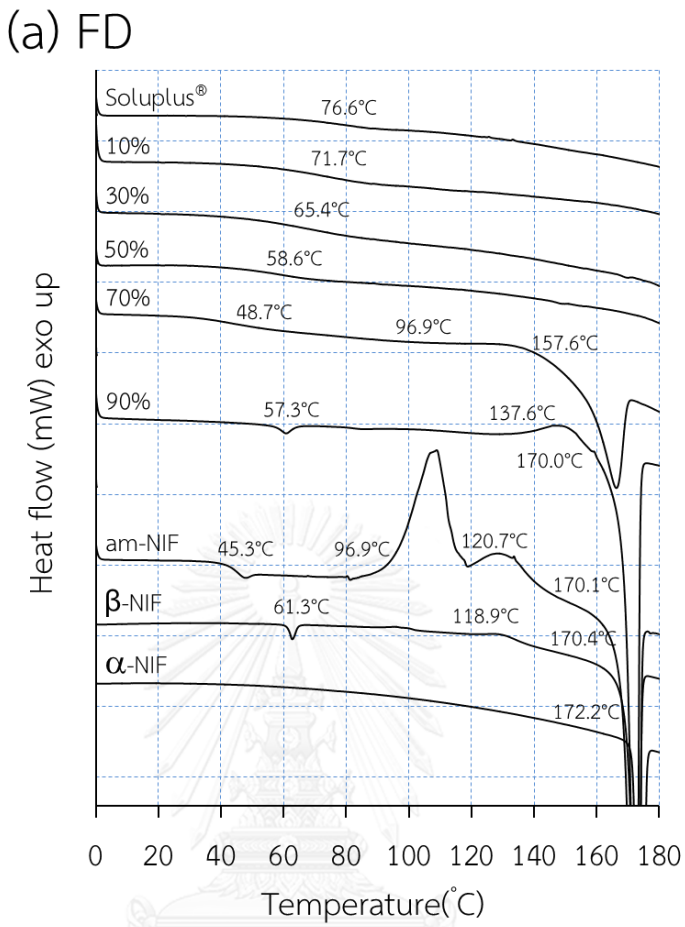

Figure 7 Thermal events of Soluplus®; solid dispersions with drug loadings of 10, 30, 50, 70, 90% w/w; am-NIF; β–NIF and α-NIF heated from 0 to 200°C with a heating rate of 10°C/min. The samples were prepared by (a) FD, (b) ME and (c) SE methods. The thermograms and values in the figure were obtained from one measurement.

(b) ME

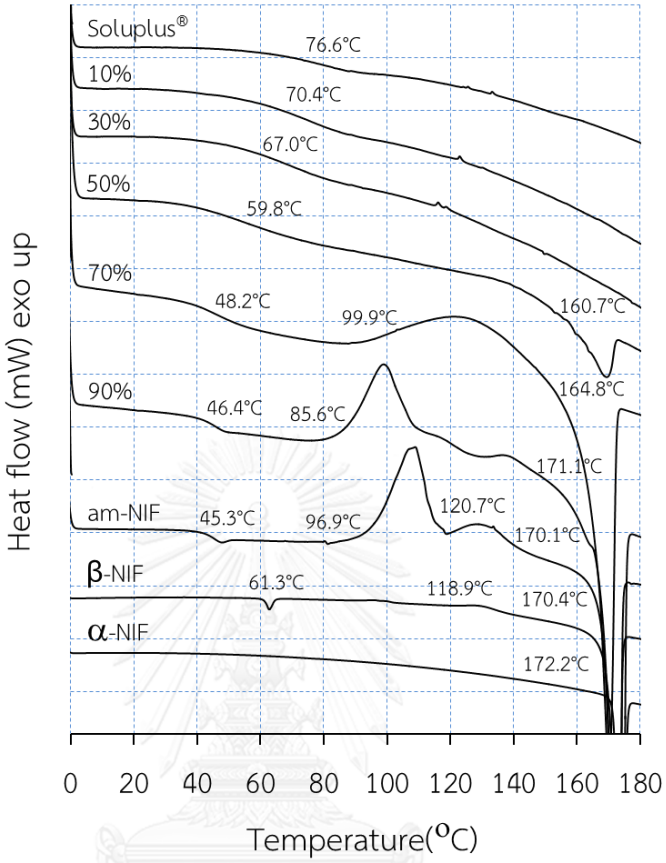

Figure 7 (continued) Thermal events of Soluplus®; solid dispersions with drug loadings of 10, 30, 50, 70, 90% w/w; am-NIF; β–NIF and α-NIF heated from 0 to 200°C with a heating rate of 10°C/min. The samples were prepared by (a) FD, (b) ME and (c) SE methods. The thermograms and values in the figure were obtained from one measurement.

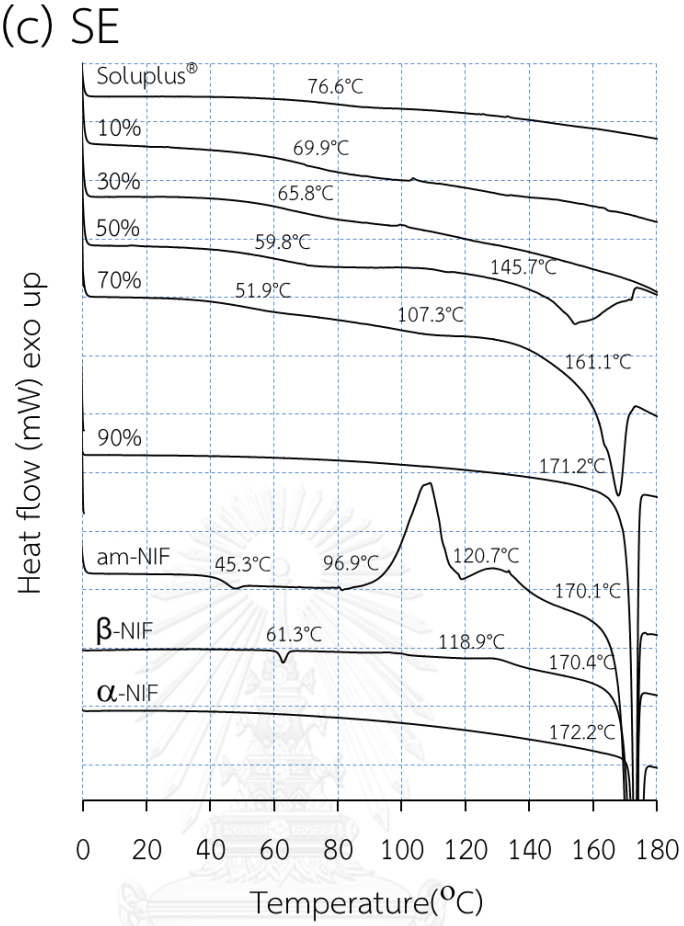

Figure 7 (continued) Thermal events of Soluplus®; solid dispersions with drug loadings of 10, 30, 50, 70, 90% w/w; am-NIF; β–NIF and α-NIF heated from 0 to 200°C with a heating rate of 10°C/min. The samples were prepared by (a) FD, (b) ME and (c) SE methods. The thermograms and values in the figure were obtained from one measurement.

The samples of all preparation methods demonstrated the similar T_g values at equivalent drug loadings up to 50% w/w as present in Table III. However, at 70% w/w drug, the SE sample showed the higher T_g than that of FD and ME samples. This was due to the crystallization of some am-NIF portions to the more stable α-NIF during the solvent removal process of SE. As a result, the remaining fraction of am-NIF was less than those in the samples prepared by FD and ME, leading to the shift

of T_g toward the T_g of polymer. The T_g of SE sample with drug loading of 50% w/w was not affected by this phenomenon.

It has been reported that the slower cooling rate for glass forming resulted in the lower T_gs of prepared glass (82). In the present study, the cooling rate of DSC which was different from the cooling rates of sample preparations might alter the T_gs of samples detected from the second heating run. Therefore, a MDSC was applied to investigate the influence of cooling rate using in the conventional DSC on T_g deviation. The T_g of FD sample with 30% w/w drug was measured using conventional DSC and MDSC methods described in the DSC section. The detected T_gs from the two methods were not different, that is, 66.2 ± 0.7°C for the conventional DSC and 67.1 ± 1.1 for the MDSC. This result indicated that the cooling rate used in the conventional DSC had no significant effect on the T_g detected at the second heating run.

Table III The T_gs of solid dispersions of nifedipine and Soluplus® composed of 10, 30, 50, 70 and 90% w/w drug prepared by FD, ME and SE. The reported values are midpoint T_g detected during heating from 0 to 200°C.

Drug loading (% w/w)	**T_g (°C)**		
	FD	**ME**	**SE**
10	72.7 ± 1.0[a]	70.2 ± 0.2	71.8 ± 1.7
30	66.2 ± 0.7	66.7 ± 0.4	65.3 ± 0.5
50	58.2 ± 0.9	59.1 ± 0.9	59.9 ± 1.2
70	46.7 ± 1.8	48.1 ± 0.2	50.6 ± 1.1
90	-[b]	47.0 ± 1.7	-

[a] Standard deviation (n=3)

[b] No T_g could be observed

DSC is a more useful technique than XRPD to evaluate drug-polymer miscibility in the solid dispersion. A solid dispersion which shows a single T_g between the T_gs of the drug and the polymer is typically classified as a miscible mixture. Based on the

criteria, the maximum drug concentrations in solid dispersions prepared by FD, ME and SE which provided the miscible mixtures were 70, 90 and 70% w/w drug, respectively. However, the detection of subsequent melting events in the FD sample composed of 70% w/w drug, ME samples composed of 50, 70 and 90% w/w drug and SE samples composed of 50 and 70% w/w suggested that these samples contained amorphous clusters, which eventually crystallized to α-NIF during heating. The amorphous drug in ME and SE samples with 50% w/w drug crystallized to α-NIF without the observation of crystallization event. The observation of melting event without crystallization detection in amorphous solid dispersion has been reported (29). This might be due to the detection limit of the DSC and the improper condition to detect crystallization in the solid dispersion. From this point, the samples which exhibited a single T_g without the presence of melting event including the FD, ME and SE samples with drug loadings up to 50, 30 and 30% w/w, respectively were classified as miscible mixtures.

The experimental T_gs of the solid dispersions are plotted against the polymer contents as shown in Figure 8. The true density of Soluplus® determined by helium pycnometry was 1.16 ± 0.01 g/cm^3 (n=5). The theoretical T_gs were computed using the equations (5) and (6) with the true densities of am-NIF and Soluplus® of 1.36 g/cm^3 (80) and 1.16 g/cm^3 respectively. The graph demonstrates minor negative deviations from ideality which reflected the weaker drug-polymer interaction compared to drug-drug interaction (7, 46). The deviations from the ideality basically imply the occurrence of molecular interaction between the drug and the polymer but it could not reveal the chemical structures dealing with such interaction.

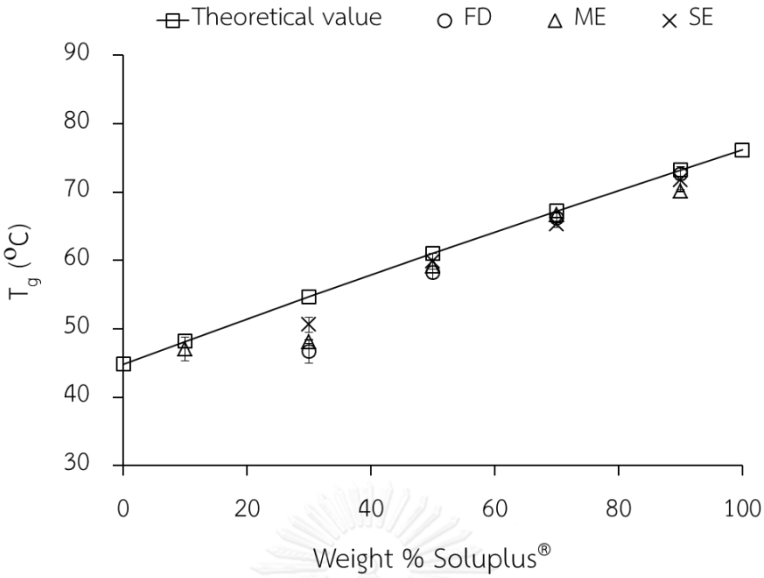

Figure 8 The theoretical and observed T_gs of solid dispersions containing nifedipine and Soluplus® with Soluplus® content of 0 to 100% w/w prepared by FD, ME and SE methods. The T_g of FD and SE samples with 10% w/w of Soluplus® could not be detected (n=3). Reproduced from (67) with permission of Springer Science+Business Media.

c) Fourier transform-infrared spectroscopy (FT-IR)

The FT-IR spectra between 400 and 4000 cm^{-1} were visually inspected. The systematic shift of nifedipine peak positions of the samples with varied drug loadings was observed over the spectral range of 1450 to 1600 cm^{-1}. The peak positions in this region were assigned to the NO_2 asymmetric vibration of the drug (55). α-NIF, β-NIF and am-NIF had the characteristic peaks at 1526.4, 1522.5 and 1527.4 cm^{-1}, respectively. Peak positions of the drug in FD samples were gradually shifted toward the characteristic peaks of am-NIF, from 1531.2 to 1528.3 cm^{-1}, with increasing the drug loading from 10 to 90% w/w as shown in Figure 9a. The ME and SE samples exhibited the same peak positions at equivalent drug loadings. Their peak positions were shifted from 1531.2 to 1528.3 cm^{-1} with increasing the drug fractions from 10 to 70% w/w as present in Figure 9b for the ME samples and Figure 9c for the SE samples. At 90% w/w drug loading, the peak positions of ME and SE samples were

identical to that of am-NIF and α-NIF, respectively. In general, there was no significant shift of nifedipine peak position over other IR regions.

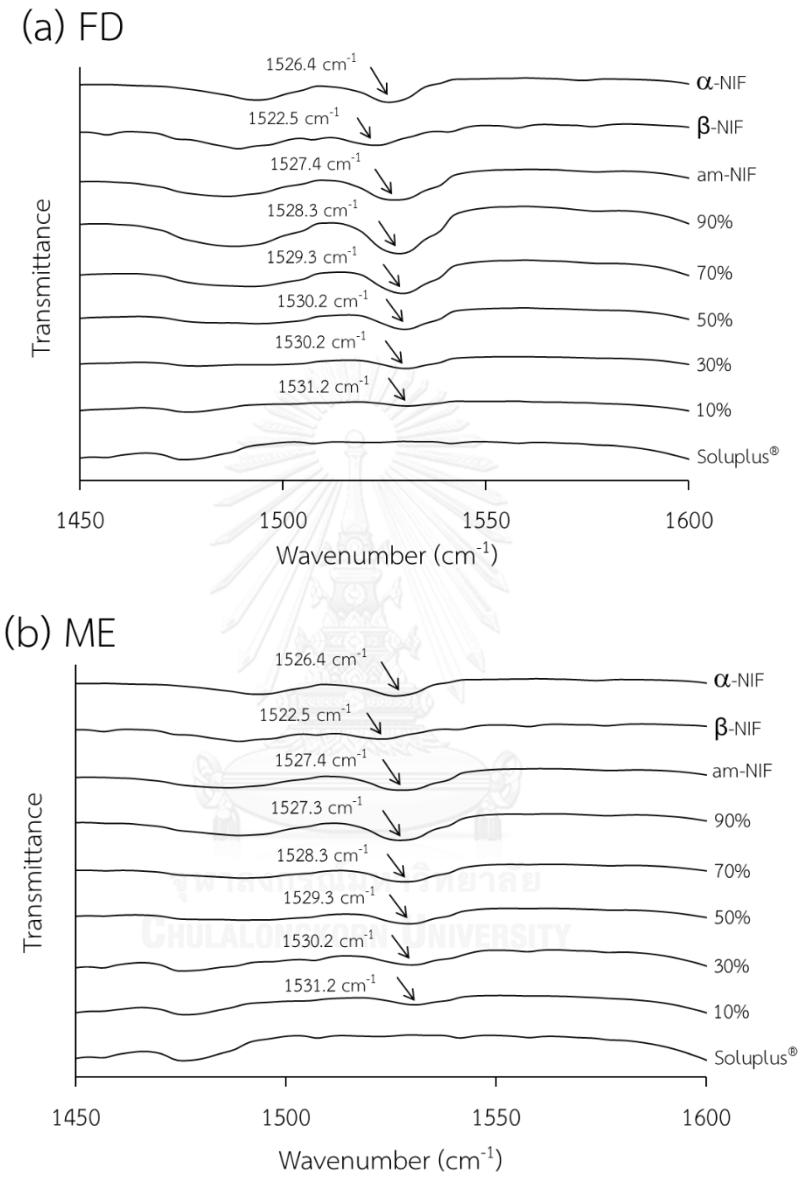

Figure 9 FT-IR spectra over the region of 1450 to 1600 cm^{-1} of Soluplus®; solid dispersion samples with drug loadings of 10, 30, 50, 70, 90% w/w; am-NIF; β–NIF and α-NIF. The samples were prepared by (a) FD, (b) ME and (c) SE methods. Figure 9(a) was reproduced from (67) with permission of Springer Science+Business Media.

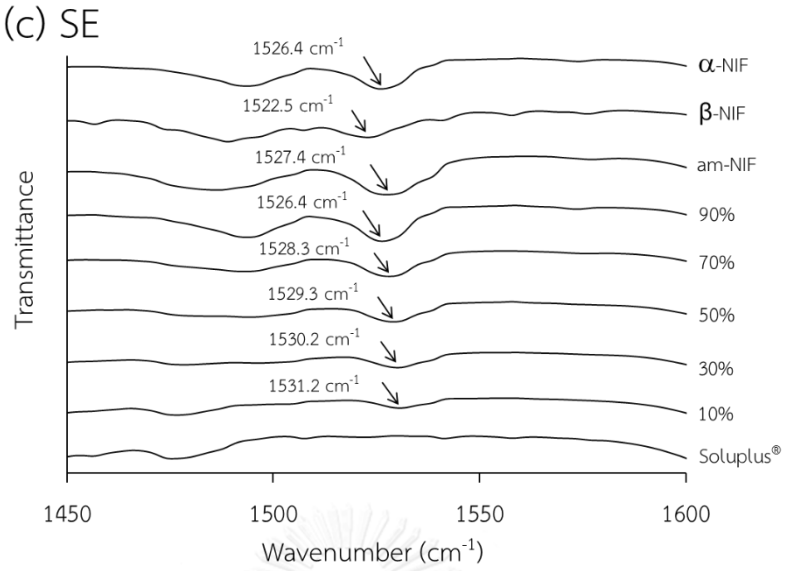

Figure 9 (continued) FT-IR spectra over the region of 1450 to 1600 cm^{-1} of Soluplus®; solid dispersion samples with drug loadings of 10, 30, 50, 70, 90% w/w; am-NIF; β–NIF and α-NIF. The samples were prepared by (a) FD, (b) ME and (c) SE methods. Figure 9(a) was reproduced from (67) with permission of Springer Science+Business Media.

The shift in IR peak position of nifedipine in the solid dispersions implied that the chemical environment of the drug was different from a pure drug. This might arise from a hydrogen bond between the nitro group of nifedipine and the OH of Soluplus®. Furthermore, it revealed that the specific interaction between nifedipine and Soluplus® was weaker than the interaction between nifedipine itself because the peak positions of the drug were shifted to higher wavenumber (20, 35, 48). These findings corresponded to the DSC results which also indicated the weaker drug-polymer interaction than drug-drug interaction.

The shift in Soluplus® peak position involving in the hydrogen bond was also investigated. However, this was inconclusive since the spectral region of 3300 to 3650 cm^{-1} which was assigned to OH stretching vibration of Soluplus® (83) exhibited a broad FT-IR pattern as depicted in Figure 10.

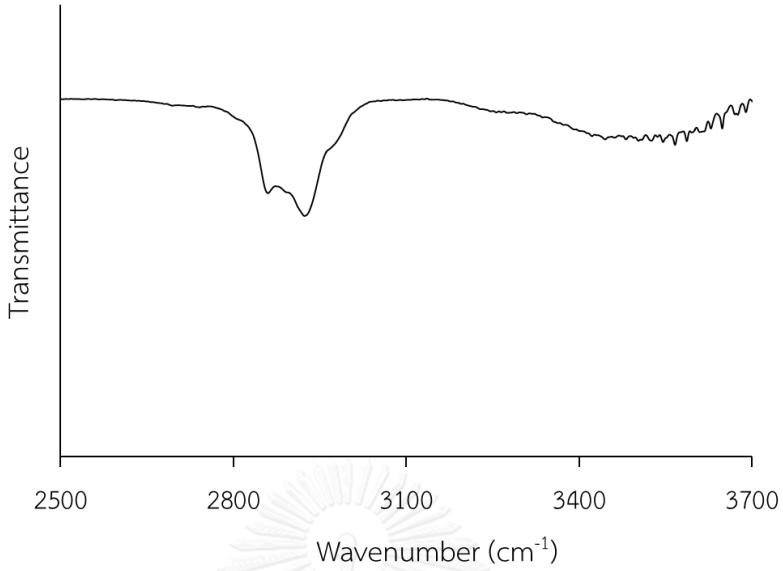

Figure 10 FT-IR spectrum of Soluplus® showing the broad pattern of OH stretching over the region of 3300 to 3650 cm^{-1}.

FT-IR is generally a standard tool to indicate an occurrence of a hydrophilic interaction. In this case, a subtle change in the peak position indicating hydrogen bond between nifedipine and Soluplus® was recognized in the samples prepared by all three methods. The hydrophobic interaction was not observed for all samples due to the limited capability of IR detection.

d) Solid state-nuclear magnetic resonance spectroscopy (ss-NMR)

The change in chemical shift of nifedipine in the solid dispersions with respect to the drug concentration was observed at around 147 to 148 ppm. This region corresponded to C-12 carbon at $-C-NO_2$ of aromatic rings (84, 85). The characteristic peaks of α-NIF and am-NIF were at 148.3 and 147.5 ppm, respectively. β-NIF possessed the characteristic peaks at 148.0 and 146.6 ppm. The peak positions of nifedipine in FD and ME samples with drug loading from 10 up to 70 and 90% w/w, respectively, were slightly shifted from 147.9 to the characteristic peak of am-NIF at 147.6 ppm with increasing the drug fractions. The ss-NMR spectra of FD and ME samples are shown in Figure 11a and 11b, respectively. The FD sample with 90%

w/w drug showed the chemical shift at 148.0 and 146.6 ppm, identical to the characteristic peaks of β-NIF.

For SE samples, the samples with 10 and 30% w/w drug exhibited the peak positions at 147.8 ppm, and the spectral patterns were similar to that of am-NIF as shown in Figure 11c. When increasing the drug loading from 50 to 90% w/w, the peak positions were shifted from 148.1 to 148.3 ppm. The spectral patterns of these samples were therefore similar to that of α-NIF.

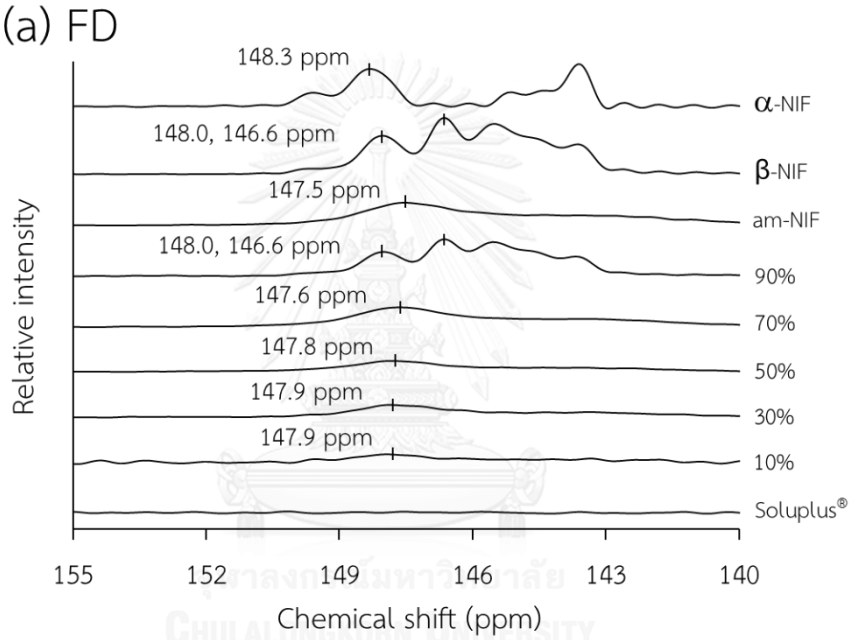

Figure 11 ss-NMR spectra over the region of 155 to 140 ppm of Soluplus®; solid dispersion samples with drug loadings of 10, 30, 50, 70, 90% w/w; am-NIF; β–NIF and α-NIF. The samples were prepared by (a) FD, (b) ME and (c) SE methods. Figure 11(a) was reproduced from (67) with permission of Springer Science+Business Media.

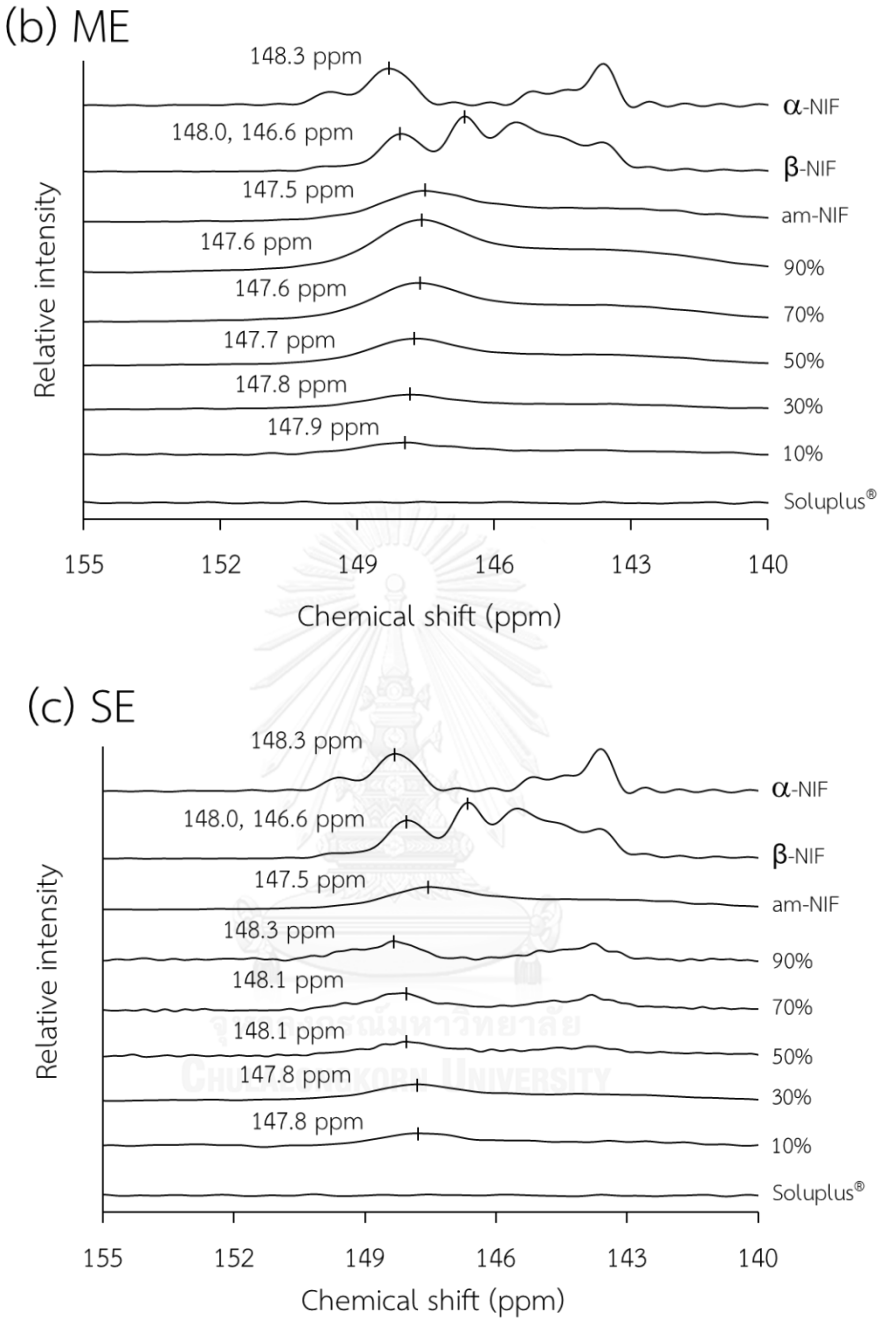

Figure 11 (continued) ss-NMR spectra over the region of 155 to 140 ppm of Soluplus®; solid dispersion samples with drug loadings of 10, 30, 50, 70, 90% w/w; am-NIF; β–NIF and α-NIF. The samples were prepared by (a) FD, (b) ME and (c) SE methods. Figure 11(a) was reproduced from (67) with permission of Springer Science+Business Media.

As with IR, the peak position detected by ss-NMR provides the information of molecular structure of the drug. In the present study, the change in nifedipine peak position at around 148 ppm with varied drug concentrations was evident. The peak positions of X-ray amorphous samples prepared by three different methods demonstrated the similar trends. These peaks showed the gradually downfield shifted from the characteristic peak of am-NIF with decreasing the drug loadings. The shift in C-12 carbon at $-C-NO_2$ detected by ss-NMR resulted from such hydrogen bond between the drug and the polymer. The findings were consistent with the FT-IR results and confirmed the occurrence of hydrogen bond between the NO_2 of nifedipine and the OH of Soluplus®.

The alteration of peak position was as small extent as 0.4 ppm. It was shifted from the characteristic peak of am-NIF at 147.5 ppm to the maximum observation at 147.9 ppm in the sample composed of 10% w/w drug. Yoshie *et al.* (86) has reported that the hydrogen bond between poly(3-hydroxybutyrate) and PVP caused the change in PVP chemical shift of approximately 1 ppm (86). Similar finding has been reported by Aso *et al.* (84) that the hydrogen bond between phenobarbitol and PVP led to the change in PVP chemical shift of approximately 2 ppm (84). Thus, the subtle change in the chemical shift (less than 0.5 ppm) in the present study pointed out that the hydrogen bond between nifedipine and Soluplus® was relatively weak.

Overall results of FT-IR and ss-NMR suggested that there might be other molecular interactions e.g. hydrophobic interaction which possibly played an important role in the miscibility between nifedipine and Soluplus® at a molecular level. As with IR, it was unable to detect such interactions by ss-NMR technique because the chemical shifts of nifedipine other than the C-12 carbon region were not shown the significant change in peak position.

e) Raman spectroscopy

The qualitative analysis of drug-polymer interactions

The Raman spectra between 200 and 2400 cm^{-1} were visually inspected. Raman spectroscopy could not detect the systematic shifts in nifedipine peak positions over the region of 1450 to 1600 cm^{-1} as observed by FT-IR. Over this region, α-NIF, β-NIF and am-NIF exhibited Raman peak positions at 1531.8, 1529.4 and 1531.5 cm^{-1}, respectively in which the values corresponded to those reported by Chan *et al.* (55).

The peak positions of nifedipine in FD samples with drug loadings of 10, 30 50 and 70% w/w occurred at 1531.2 cm^{-1}, similar to the characteristic peak of am-NIF. While, the peak obtained from FD sample with 90% w/w drug was shifted to the characteristic peak of β-NIF (Figure 12a).

The characteristic peak of nifedipine in ME sample with 10% w/w drug was overlapped with the Soluplus® peak at 1530.9 cm^{-1}. While, the peaks obtained from ME sample with 30, 50 70 and 90% w/w drug were present at around the characteristic peak of am-NIF at 1531.2 and 1531.5 cm^{-1} (Figure 12b).

The peak position of nifedipine in SE sample with a drug loading of 10% w/w was also overlapped with Soluplus® peak at 1530.9 cm^{-1}. This peak was slightly shifted to 1531.2 cm^{-1} when the drug loading was increased to 30% w/w. Then, it was shifted to the characteristic peak of am-NIF at 1531.5 cm^{-1} with the drug loadings of 50 and 70% w/w. The SE sample with a drug loading of 90% w/w showed a peak position at 1531.8 cm^{-1} which corresponded to α-NIF (Figure 12c).

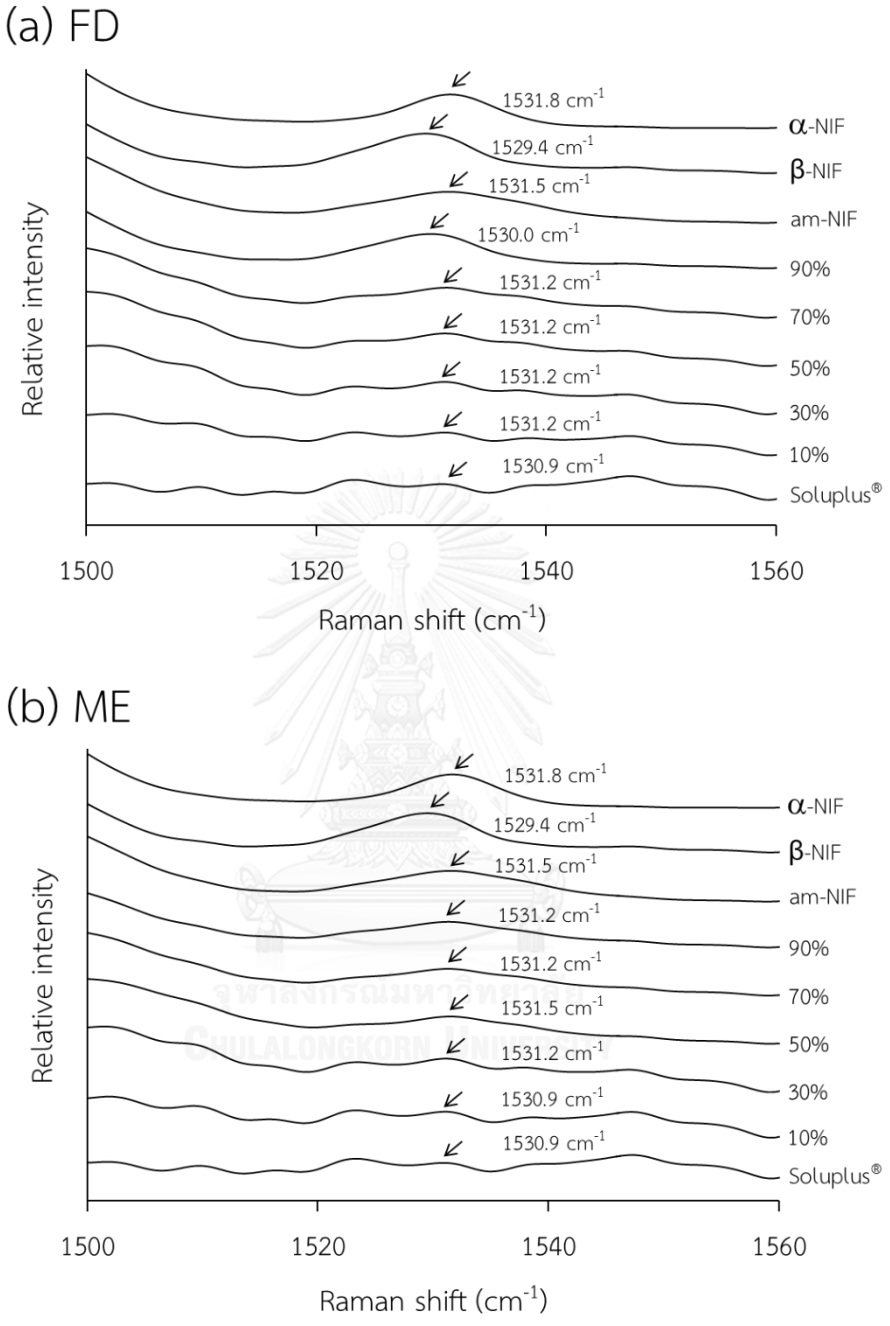

Figure 12 Raman spectra over the region of 1500 to 1560 cm^{-1} of Soluplus®; solid dispersion samples with drug loadings of 10, 30, 50, 70, 90% w/w; am-NIF; β-NIF and α-NIF. The samples were prepared by (a) FD, (b) ME and (c) SE methods.

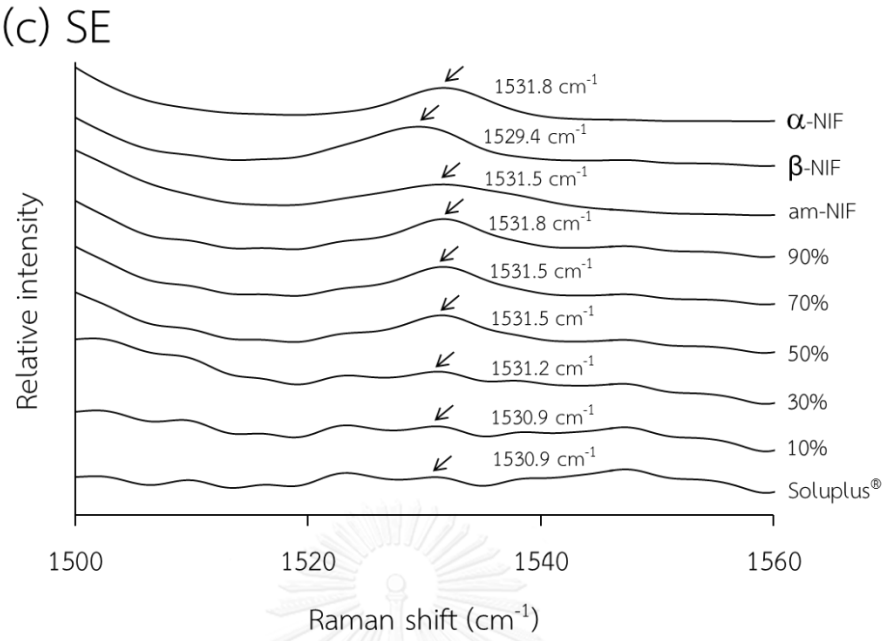

Figure 12 (continued) Raman spectra over the region of 1500 to 1560 cm^{-1} of Soluplus®; solid dispersion samples with drug loadings of 10, 30, 50, 70, 90% w/w; am-NIF; β-NIF and α-NIF. The samples were prepared by (a) FD, (b) ME and (c) SE methods.

Interestingly, the systematic shifts in nifedipine peak positions were observed over the spectral region of 790 to 820 cm^{-1} which was the characteristic vibration of aromatic hydrocarbon of the drug (18). α-NIF, β-NIF and am-NIF possessed the characteristic peaks at 810.6, 806.7 and 807.3 cm^{-1}, respectively as illustrated in Figure 13. Soluplus® had the characteristic peak at 795.6 cm^{-1}. Within this spectral region, the peaks positions of β-NIF and am-NIF were relatively closed. Thus, the analysis region was extended covering 775 to 850 cm^{-1}. Over the extended region, β-NIF had a broad spectral pattern from 825 to 835 cm^{-1}; while, am-NIF exhibited a sharp peak at 831.9 cm^{-1} as shown in Figure 13. The characteristic peaks and spectral patterns of α-NIF, β-NIF and am-NIF were consistent with the results reported by Chan *et al.* (55).

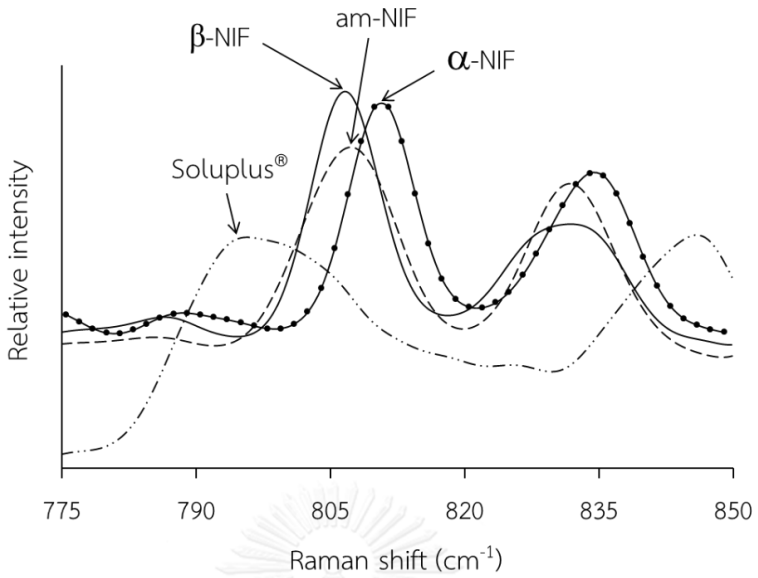

Figure 13 Raman spectra over the region of 775 to 850 cm^{-1} showing the characteristic peaks of α-NIF, β-NIF, am-NIF and Soluplus®. Intensity was normalized and re-scaled to compare peak positions.

Teraoka *et al.* (87) has reported that the photodegradation products of nifedipine including nitroso-derivative and nitro-derivative exhibited the IR peak positions at 1729 cm^{-1} and 1728 cm^{-1}, respectively (87). In the present study, the Raman peaks of photodegradation products, if any, did not interfere the results analyzed from the Raman region of 775 to 850 cm^{-1}.

For solid dispersion samples, the peak positions of FD samples were gradually upward shifted from 802.5 to 805.8 cm^{-1} with increasing the drug content from 10 to 70% w/w. The FD samples with drug loadings of 10, 30, 50 and 70% w/w demonstrated the peaks at 802.5, 804.0, 804.9 and 805.8 cm^{-1}, respectively. The spectral patterns of these samples did not correspond to the patterns of α-NIF or β-NIF. FD sample with drug loading of 90% w/w showed the peak at 807.6 cm^{-1} and the broad spectral pattern between 825 and 835 cm^{-1}, corresponding to the characteristic pattern of β-NIF as demonstrated in Figure 14a.

A similar trend was observed in the ME samples. When the drug loading was increased from 10% w/w to 30, 50, 70 and 90% w/w, the peak positions were shifted

from 802.8 cm^{-1} to 804.0, 804.9, 805.5 and 807.0 cm^{-1}, respectively as depicted in Figure 14b. The spectral patterns of all ME samples did not correspond to α-NIF or β-NIF.

For SE samples, the peak positions of samples composed of 10 and 30% w/w drug were at 802.5 and 804.0 cm^{-1}, respectively. The spectral patterns were dissimilar to the patterns of α-NIF or β-NIF as shown in Figure 14c. The SE samples with 50, 70 and 90% w/w exhibited the peaks at 810.6, 810.9 and 810.9 cm^{-1}, respectively, which were similar to the characteristic pattern of α-NIF.

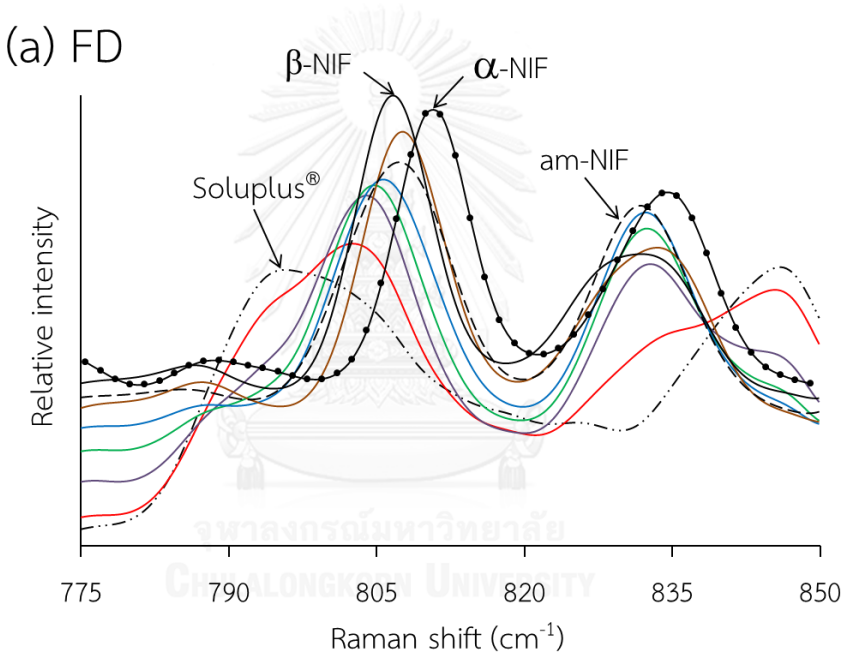

Figure 14 Raman spectra over the region of 775 to 850 cm^{-1} of solid dispersion samples with drug loadings of 10% (red), 30% (purple), 50% (green), 70% (blue) and 90% (brown) w/w. The samples were prepared by (a) FD, (b) ME and (c) SE methods. Intensity was normalized and re-scaled to compare peak positions.

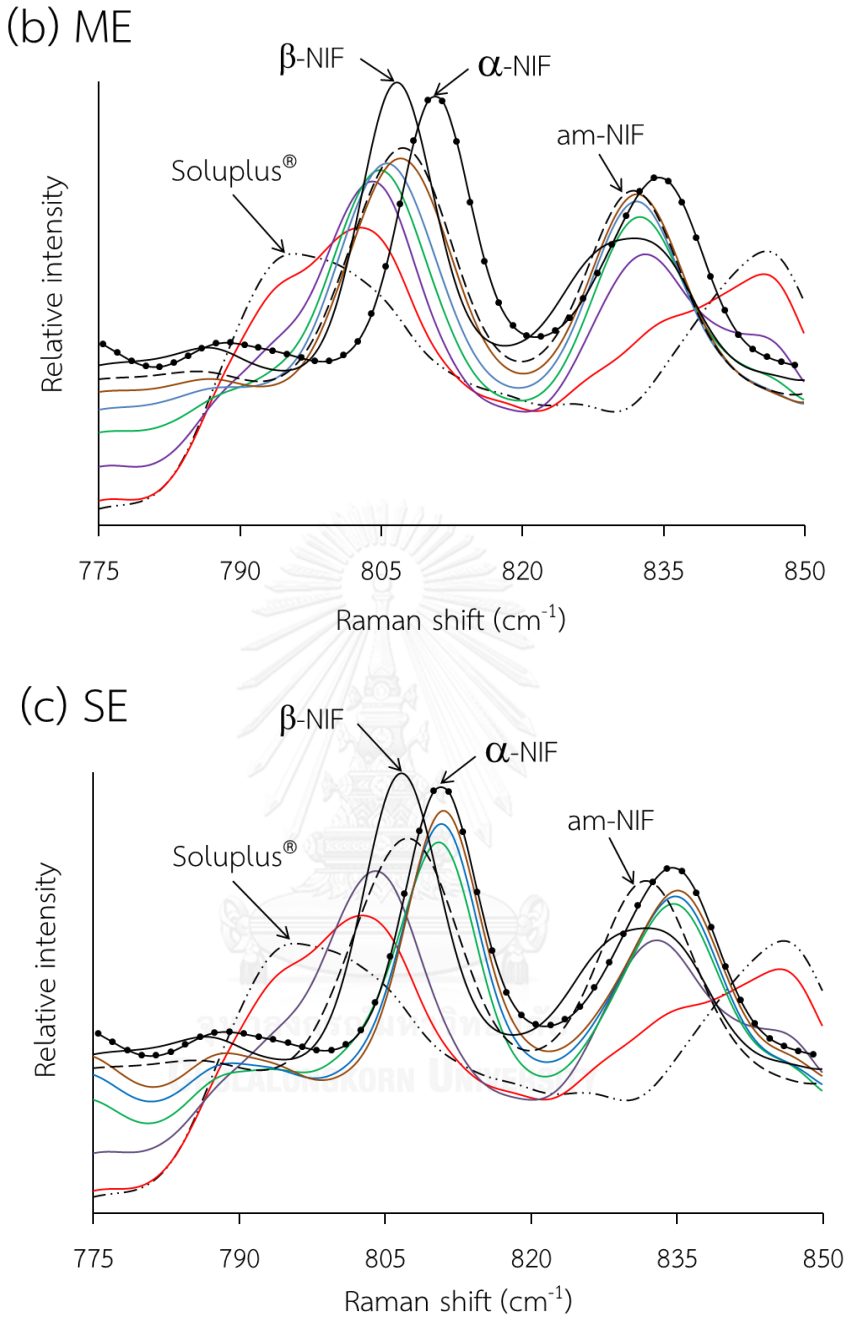

Figure 14 (continued) Raman spectra over the region of 775 to 850 cm^{-1} of solid dispersion samples with drug loadings of 10% (red), 30% (purple), 50% (green), 70% (blue) and 90% (brown) w/w. The samples were prepared by (a) FD, (b) ME and (c) SE methods. Intensity was normalized and re-scaled to compare peak positions.

The solid state of nifedipine in solid dispersion samples detected by Raman spectroscopy agreed with the results obtained from XRPD. Nifedipine in the FD sample with 90% w/w drug demonstrated the nature of β-NIF; while, those in the SE samples with 50, 70 and 90% w/w drug existed in α-NIF. Nifedipine in other samples were neither α-NIF nor β-NIF.

The shift in peak position implied the difference in chemical environment of the drug. In the present study, the shift occurred between 790 and 820 cm^{-1} which was assigned to the vibration of aromatic hydrocarbon of nifedipine. Soluplus® also contained the hydrophobic group at the cyclic amide in polyvinyl caprolactam segment. Therefore, the shift in the nifedipine peak position between 790 and 820 cm^{-1} might result from the weak van der Waals interactions between the aromatic hydrocarbon of nifedipine and the cyclic amide of Soluplus®. Among X-ray amorphous samples, the peak positions of nifedipine in the solid dispersions prepared by FD, ME and SE were gradually shifted out of the characteristic peak of am-NIF to the lower wavenumber with a decrease in drug loading. This indicated that the hydrophobic interaction between the drug and the polymer was stronger than the drug-drug interaction.

In general, the degree of the shift in IR or Raman peak position is affected by the strength of drug-polymer interaction (23, 28, 34). The larger shift suggests the stronger interaction (28). The peak positions obtained from the FD, ME and SE samples with drug loadings of 10, 30, 50, 70 and 90% w/w are illustrated in Figure 15. Recrystallization in the FD sample with 90% w/w drug, and in the SE samples with 50, 70 and 90% w/w drug was attributed to the deviation of their peak positions. Huang *et al.* (5) has found that the extent of molecularly dispersed nifedipine in the solid dispersion containing nifedipine and ethylcellulose and/or Eudragit RL® 100 depended on the preparation method. The fusion method of fast solidification rate provided a higher extent of molecular nifedipine than co-evaporation method of slow solidification rate (5). However, the X-ray amorphous samples (FD samples with 10 to 70% w/w, ME samples with 10 to 90% w/w drug and SE samples with 10 to 30% w/w drug) demonstrated the similar degrees of the shifts in peak positions at

equivalent drug loadings. The decrease in nifedipine weight fractions gave rise to the stronger drug-polymer interaction. These findings pointed out that the strength of nifedipine and Soluplus® interaction was strongly influenced by the drug concentration than the preparation methods.

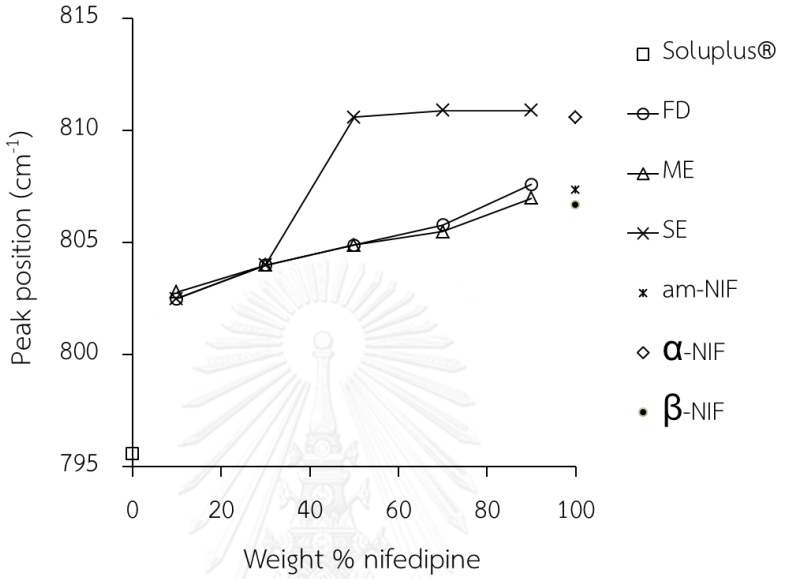

Figure 15 The shifts in Raman peak positions over the spectral region of 795 to 815 cm^{-1} of solid dispersion samples with drug loadings of 10, 30, 50, 70 and 90% w/w prepared by FD, ME and SE methods. Reproduced from (67) with permission of Springer Science+Business Media.

The Raman peaks of α–NIF at 810.6 cm^{-1}, β–NIF at 806.7 cm^{-1} and am-NIF at 807.3 cm^{-1} corresponded to the FT-IR peaks at 793.6, 788.7 and 783.0 cm^{-1}, respectively. These IR peak positions were comparable to the values reported by Chan *et al.* (55). In the IR region of 775 to 850 cm^{-1}, the peak positions of nifedipine in solid dispersion samples did not exhibit the systematic shifts. The IR peak position of nifedipine in FD sample with a drug loading of 10% w/w occurred at 783.0 cm^{-1} (Figure 16a). The FD samples with drug loadings of 30 and 50% w/w showed peak positions at 783.9 cm^{-1}. The peak was shifted to the peak position of am-NIF at 783.0 cm^{-1} as the drug loading was increased to 70% w/w. The FD sample with the drug loading of 90% w/w showed the peak position at 782.0 cm^{-1} which did not correspond to am-NIF, β-NIF or α-NIF.

The IR peak position of nifedipine in the ME sample with a drug loading of 10% w/w could not be observed (Figure 16b). The ME samples with drug loadings of 30 and 50% w/w showed the peak position at 783.9 and 783.0 cm^{-1}, respectively. The peak position of ME sample was shifted to 782.0 cm^{-1} when the drug loadings was increased to 70 and 90% w/w. For SE samples (Figure 16c), the peak positions of samples with drug loadings of 10 and 30% w/w occurred at 785.9 and 783.9 cm^{-1}, respectively, and were shifted to the characteristic peak of α-NIF as the drug loading was increased to 50 and 90% w/w. The peak position of SE sample with 70% w/w drug was present at 783.9 cm^{-1}.

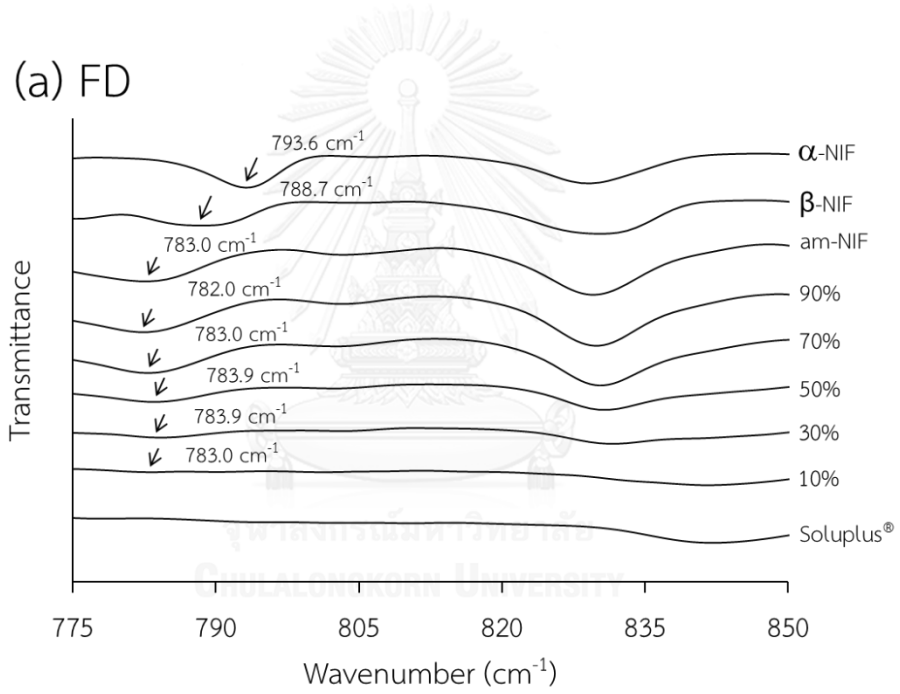

Figure 16 FT-IR spectra over the region of 775 to 850 cm^{-1} of Soluplus®; solid dispersion samples with drug loadings of 10, 30, 50 70, 90% w/w; am-NIF; β-NIF and α-NIF. The samples were prepared by (a) FD, (b) ME and (c) SE methods.

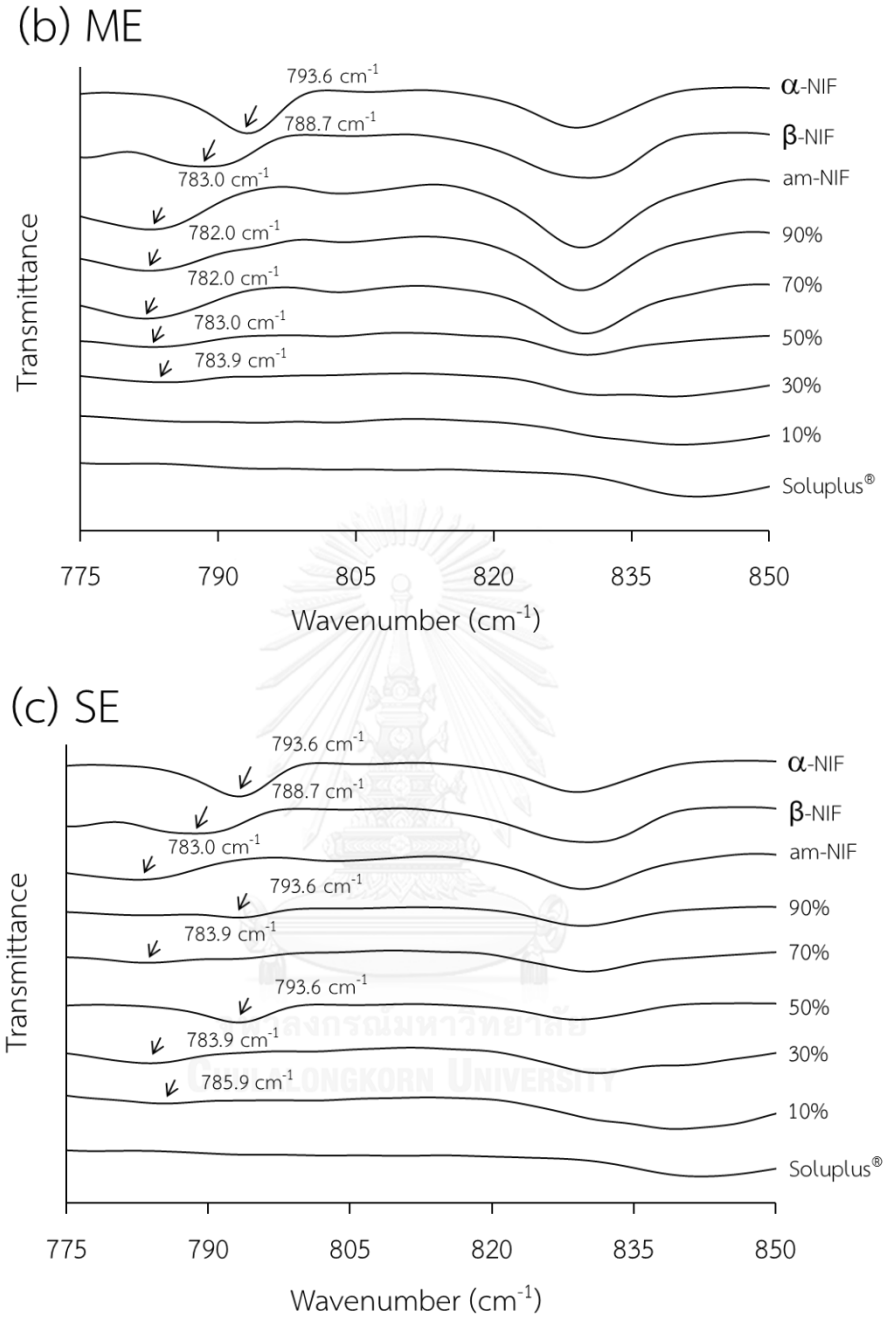

Figure 16 (continued) FT-IR spectra over the region of 775 to 850 cm^{-1} of Soluplus®; solid dispersion samples with drug loadings of 10, 30, 50 70, 90% w/w; am-NIF; β-NIF and α-NIF. The samples were prepared by (a) FD, (b) ME and (c) SE methods.

The shift of peak positions observed for the drug in FD, ME and SE samples over the FT-IR region of 775 to 820 cm^{-1} was not systematic. This was due to the limitation of IR technique. The hydrophobic interaction between the drug and the

polymer might not show the change in dipole moment; hence, the interaction was IR inactive.

The quantitative analysis of drug-polymer interactions

Raman spectroscopy technique could not identify the hydrogen bond between nifedipine and Soluplus®. However, this tool could detect the varied strength of hydrophobic interaction, based on the systematic shift of the peak positions with respect to the drug loadings in the solid dispersions. Raman spectroscopy was further applied to determine the amount of drug-polymer interactions in the X-ray amorphous samples. These samples included the FD samples composed of 10, 30, 50 and 70% w/w drug, ME samples composed of 10, 30, 50, 70 and 90% w/w drug, and SE samples composed of 10 and 30% w/w drug. The level of miscibility between nifedipine and Soluplus® was determined based on the relative amounts of each state of nifedipine existing in the samples.

As it was postulated earlier, the drug in the X-ray amorphous samples could be present as amorphous state or molecularly dispersed in the polymeric matrix or both. Within these samples, when the drug loading was below the saturated drug's concentration in the solid polymer, the drug was dissolved in and miscible with the polymer. When the drug loading was excess, above the saturated drug's concentration in the polymeric carrier, there was not sufficient space for molecular drug and the amorphous drug was the results under the conditions that have been used. The latter case led to the immiscible solid dispersion where a great extent of drug-drug interactions is present, i.e. the drug molecules stayed in amorphous state.

Among the miscible solid dispersions, the drug concentration can be varied from a very low level to the saturated concentration. At the very low concentration, much lower than its saturated concentration, the drug molecules are presumed to be completely surrounded by a polymeric substance. All drug molecules interact only with polymer networks and exist in "monomolecularly dispersed state". Being in this state, the drug-polymer interaction (adhesive force) extensively exists. The interaction between drug-drug molecules (cohesive force) is rare.

At the high drug concentration, especially at a saturated concentration, the drug molecules possibly interact with both polymeric matrix and drug molecules itself. The drug in this state is termed here as “molecularly dispersed state”. The strength of drug-polymer interaction is weaker than that in monomolecularly dispersed state. Drug-drug interaction and drug-polymer interaction are balanced to maintain as a miscible mixture, and a cluster of amorphous drug does not occur (7, 9). The drug molecules presenting as monomoleculuarly dispersed state and molecularly dispersed state can appear as the schematic representations illustrated in Figure 17a and Figure 17b.

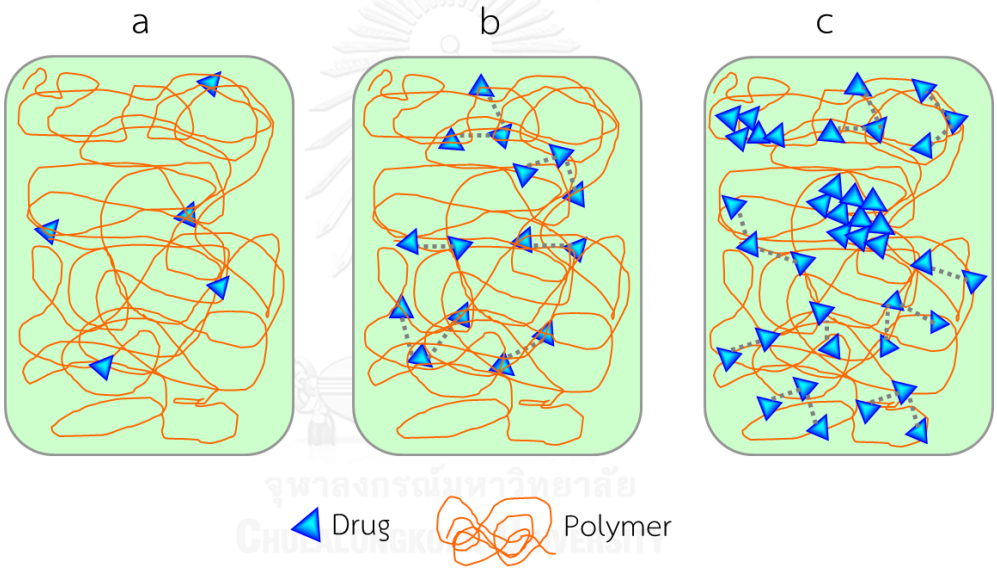

Figure 17 The conceptual models of (a) monomolecularly dispersed state, (b) molecularly dispersed state and (c) combination of molecularly dispersed state and amorphous clusters. The balance between drug-drug interaction and drug-polymer interaction is represented by the dot lines. Reproduced from (67) with permission of Springer Science+Business Media.

Therefore, the standards of miscible solid dispersions with the low and high concentrations as described earlier were established for the standards of monomolecularly and molecularly dispersed states, respectively. The FD method was utilized to prepare the standards; since, the fast solidification of FD should provide a homogeneous product.

To obtain the standard of nifedipine existing in the monomolecular state, the spectral patterns of FD solid dispersions consisting low drug concentrations, 0.1, 0.5, 1, 3 and 5% w/w drug were investigated. The spectral pattern of solid dispersion with 0.1% w/w drug showed the identical pattern to that of Soluplus®. When the drug content was increased to 0.5% w/w, the distinct shoulder at 798.6 cm^{-1} was observed. The similar spectral pattern was found in the solid dispersion with 1% w/w drug. The distinct shoulder was developed to 800.1 and 801.6 cm^{-1} with increasing the weight fraction of the drug to 3 and 5% w/w, respectively as illustrated in Figure 18. The observed shoulder peak was overlapped with the Soluplus® peak but it was possible to differentiate from the polymer peak.

The development of the shoulder peak was assigned to nifedipine peak which was shifted from the characteristic peak of am-NIF. The most shift in peak position further away from the characteristic peak of am-NIF was found in the solid dispersions with 0.5 and 1% w/w drug. Thus, this indicated strong drug-polymer interaction. The molecular environment of solid dispersions with 0.5 and 1% w/w drug was similar as the identical peak position was present. This could be postulated that the molecular interaction in these two samples was only drug-polymer interaction. As the peak positions in the solid dispersions with 3 and 5% w/w drug were shifted toward that of am-NIF, the drug in these solid dispersions had different chemical environment from the drug in the solid dispersions with 0.5 and 1% w/w drug, and possessed relatively stronger drug-drug interaction. According to the results, the FD solid dispersion with 0.5% w/w drug was selected as the standard for monomolecularly dispersed state because its spectrum showed the most shift of peak position from the characteristic peak of am-NIF and yet could be distinguished from the Soluplus® peak. It was also composed of the lower drug concentration, and hence this minimized the extent of drug-drug interaction, compared with the solid dispersion with 1% w/w drug.

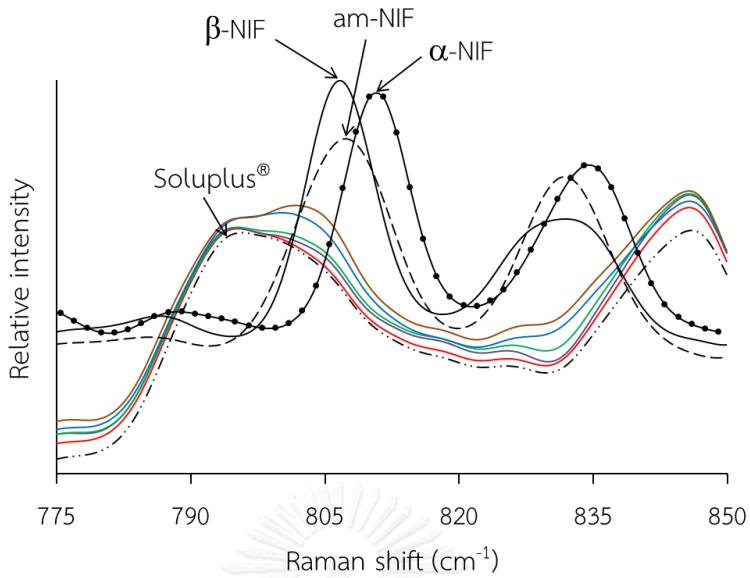

Figure 18 Raman spectra over the region of 775 to 850 cm^{-1} of FD solid dispersions with drug loadings of 0.1% (red), 0.5% (purple), 1% (green), 3% (blue) and 5% (brown) w/w. Intensity was normalized and re-scaled to compare peak positions.

To obtain the standard of molecularly dispersed state, the spectral patterns of FD solid dispersions consisting of high drug concentrations, 10, 30 and 50% w/w drug, were investigated.

The remaining spectrum of the solid dispersions with the high drug concentrations after subtracted by the model spectra of am-NIF and model M was converted to the new Gaussian function model. The spectra of solid dispersions with 10 and 30% w/w drug contained neither model spectrum of am-NIF nor model M as demonstrated in Figure 19a (10%) and Figure 19b (30%). Their experimental spectra could be fitted with a new series of five Gaussian peaks. While the spectrum of solid dispersion with 50% w/w drug could be fitted with the fraction of model spectrum of am-NIF combined with a new series of five Gaussian peaks as depicted in Figure 19c. The amount of am-NIF present in this sample was accounted for 10% w/w based on the area fraction.

Therefore, the FD solid dispersion with drug loading of 30% w/w was selected as the standard for molecularly dispersed state as it did not include am-NIF and

model M. In addition, it provided more opportunity for achieving in the saturated concentration of miscible mixture, comparing with the lower drug concentration of 10% w/w.

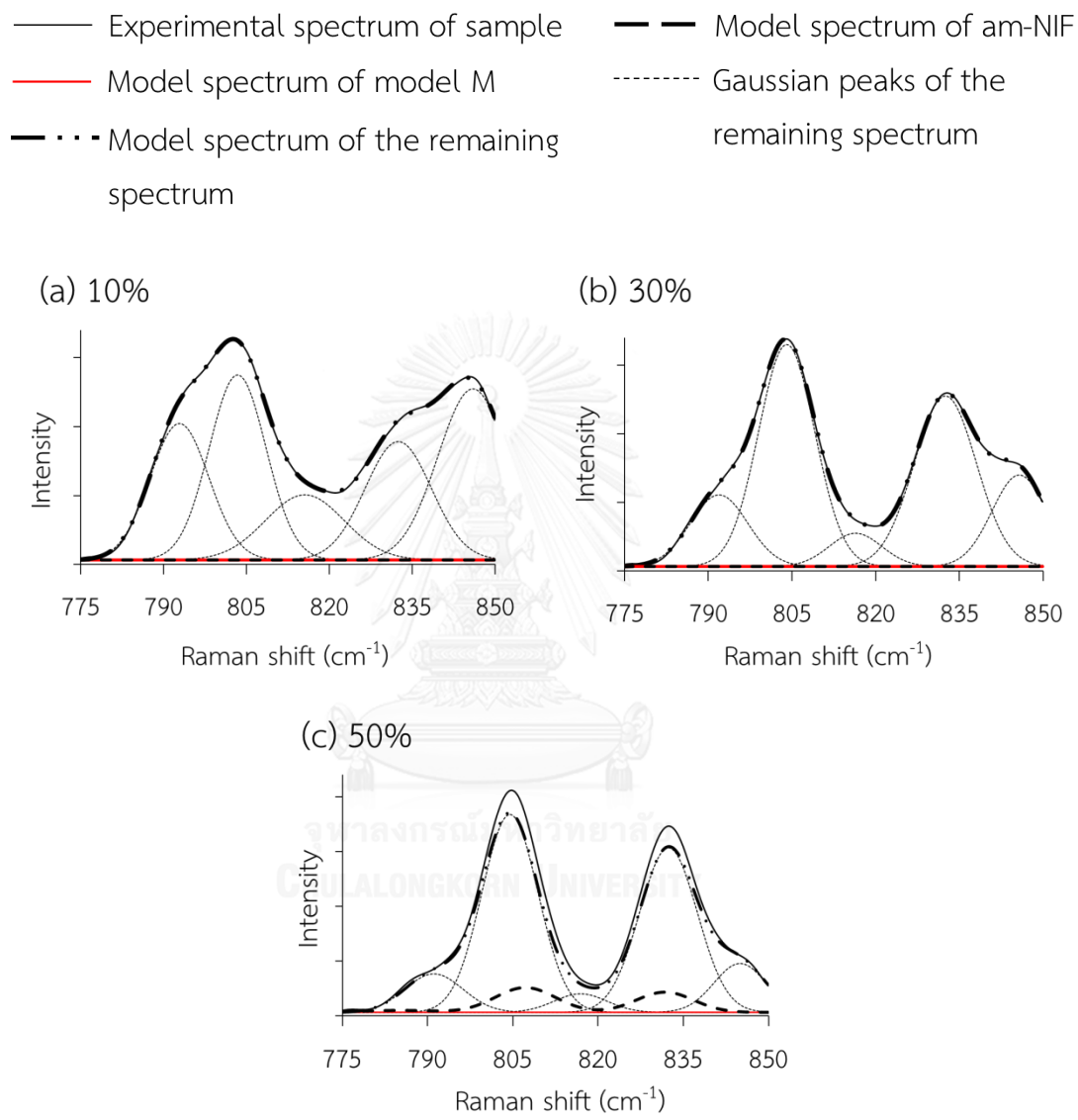

Figure 19 A new series of Gaussian peaks fitted to the remaining spectra of FD solid dispersions with drug loadings of (a) 10%, (b) 30% and (c) 50% w/w after subtracted by model spectra of am-NIF and model M. Figure 19(b) was reproduced from (67) with permission of Springer Science+Business Media.

The method of curve fitting was used to estimate the amounts of each state in the samples. The experimental spectra of the standards of monomolecularly and molecularly dispersed states, and amorphous state could be fitted with a series of seven, five and three Gaussian peaks as demonstrated in Figure 20. These three Gaussian function models were applied to estimate the amounts of nifedipine presenting as monomolecularly and molecularly dispersed states, as well as amorphous clusters in X-ray amorphous samples.

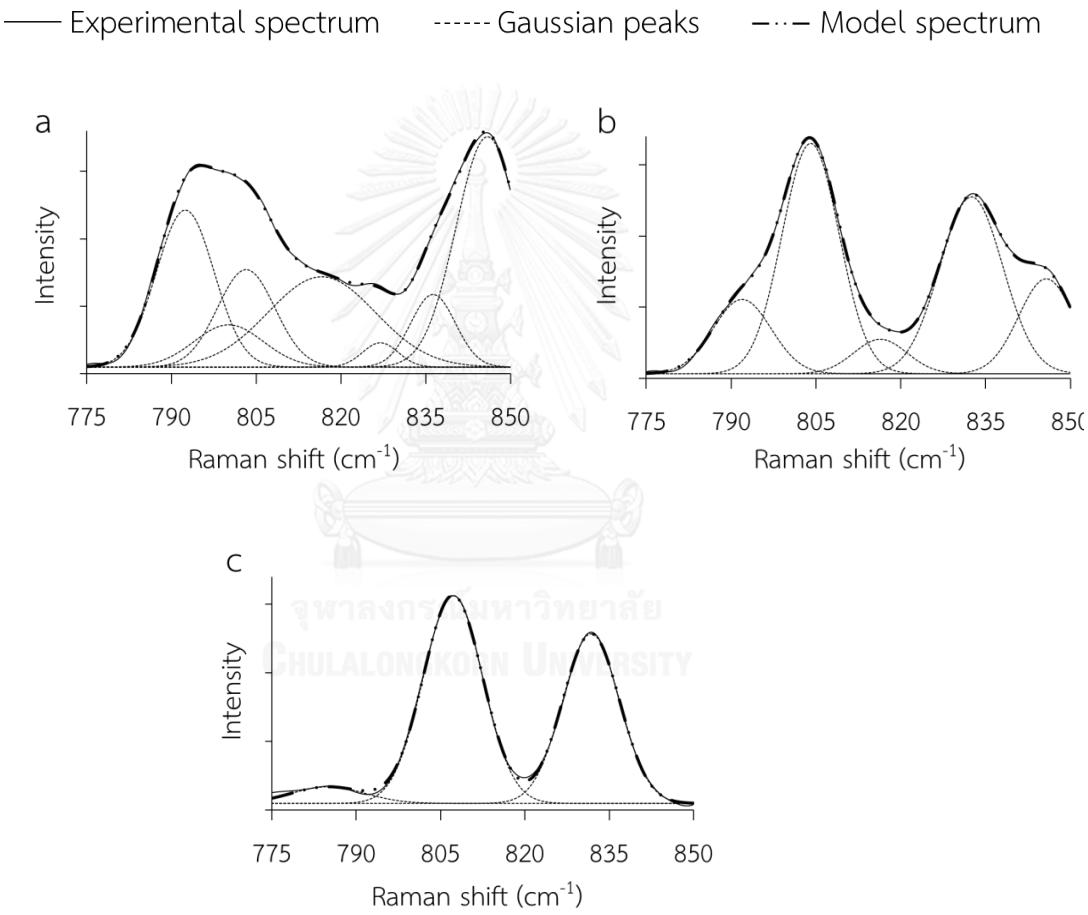

Figure 20 A series of Gaussian peaks fitted to the experimental Raman spectra of nifedipine (a) monomolecularly dispersed state, (b) molecularly dispersed state and (c) amorphous state. Reproduced from (67) with permission of Springer Science+Business Media.

X-ray amorphous samples were analyzed by fitting the model spectra of nifedipine in three states i.e. monomolecular, molecular and amorphous states to the experimental spectra of the samples. The model spectra of standards for monomolecularly and molecularly dispersed states prepared by FD were also used to estimate the amount of drug-polymer interactions in the solid dispersion samples prepared by ME and SE. The standards prepared by FD could properly fit to the spectra of ME and SE samples. The example fitting of Gaussian function models of standards to ME samples composed of drug 10, 30, 50, 70 and 90% w/w are illustrated in Figure 21.

The relative amounts of each state in a sample were calculated based on its area fraction. The values of each state were averaged from 6 different areas. The homogeneity of sample was indicated by standard deviation.

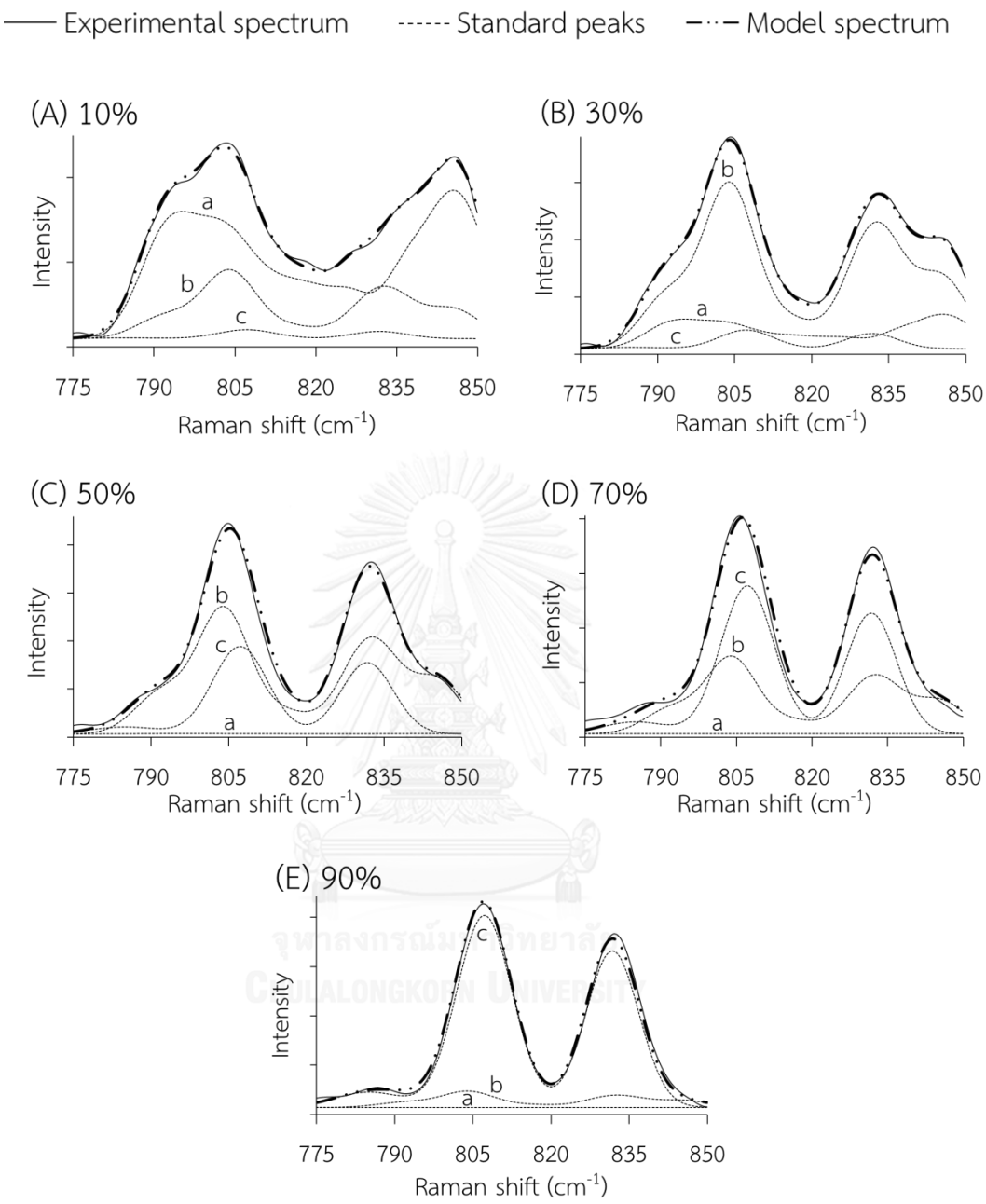

Figure 21 Model spectra of (a) monomolecularly dispersed state, (b) molecularly dispersed state and (c) amorphous state of nifedipine fitted to the experimental spectra of ME samples with drug loadings of (A) 10, (B) 30, (C) 50, (D) 70 and (E) 90% w/w.

The proportions of nifedipine in each state were computed from the fractional area of each. The values of each state in samples with different drug concentrations were normalized to the drug loading of 100% w/w. The results are present in Table IV and Figure 22.

Table IV The relative amounts of nifedipine presenting as monomolecularly dispersed state, molecularly dispersed state, and amorphous states in X-ray amorphous samples determined by curve fitting method.

Preparation method	Drug loading (% w/w)	Content (% w/w)		
		Monomolecularly dispersed state	Molecularly dispersed state	Amorphous
FD	10	59.7 ± 2.2[a]	40.3 ± 2.3	0.0 ± 0.1
	30	0.6 ± 0.6	98.5 ± 1.5	0.8 ± 1.6
	50	0.1 ± 0.1	71.1 ± 4.1	28.9 ± 4.1
	70	0.0 ± 0.0	39.8 ± 1.8	60.2 ± 1.8
ME	10	62.3 ± 6.6	37.1 ± 7.1	0.6 ± 1.0
	30	8.1 ± 7.1	86.9 ± 7.8	5.0 ± 2.0
	50	0.1 ± 0.1	68.4 ± 10.4	31.5 ± 10.4
	70	0.0 ± 0.0	40.5 ± 7.2	59.5 ± 7.2
	90	0.0 ± 0.0	8.3 ± 3.7	91.7 ± 3.7
SE	10	59.9 ± 3.6	40.0 ± 3.7	0.1 ± 0.1
	30	2.7 ± 1.3	96.1 ± 1.7	1.2 ± 1.4

[a] Standard deviation (n=6)

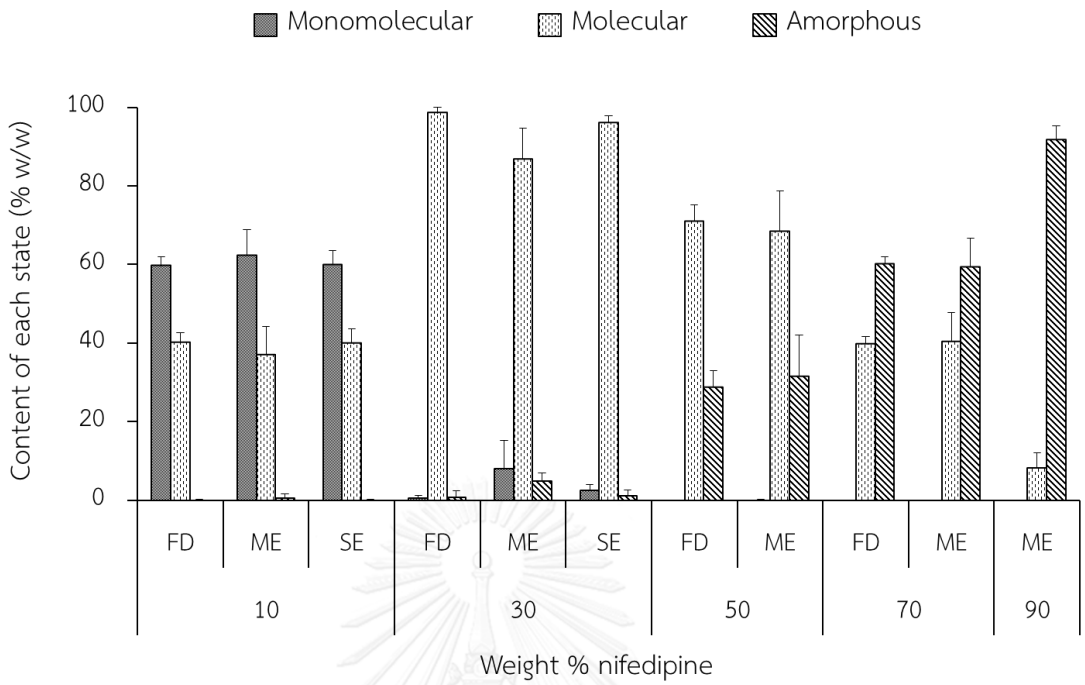

Figure 22 The content of nifedipine existing as monomolecularly dispersed state, molecular dispersed state and amorphous state in the studied X-ray amorphous samples prepared by FD, ME and SE methods. The content of each state in different drug loading samples was normalized to 100% w/w (n=6). Reproduced from (67) with permission of Springer Science+Business Media.

The relative amount of each state in the solid dispersion samples would suggest the degree of drug-polymer interaction. The higher portion of the monomolecularly dispersed stated in the solid dispersion implied the greater opportunity of strong drug-polymer interaction.

The contents of each state in the samples prepared by three different methods showed a similar trend. The average amounts of each state at equivalent drug loadings were comparable, irrespective to the preparation methods. The results were consistent with the approximate degree of the shift in nifedipine peak positions from FD, ME and SE samples at the same drug content (Figure 15). The similar peak positions implied that the strength of drug-polymer interactions among these samples were not different.

For the FD, ME and SE samples with drug loading of 10% w/w, all drug molecules were dispersed in the polymer at the molecular level. Most drug molecules existed in the monomolecularly dispersed state and the remaining fractions were in the molecularly dispersed state. For the samples with 30% w/w drug, almost all drug molecules in the FD, ME and SE sample were in the molecularly dispersed state. Thus, the strength of adhesive force between drug and polymer in the sample with 30% w/w drug was weaker than that in the samples with 10% w/w. The trace amorphous drug of about 1 and 5% w/w could be detected in SE and ME samples, respectively.

When the drug loadings were increased from 30 to 90% w/w, the proportions of drug dispersed at the molecular level were substantially decreased; while amorphous clusters were sharply increased. With the drug loading up to 50% w/w, the majority portion of the drug in FD and ME samples was in the molecularly dispersed state, together with increased amount of amorphous state. The nifedipine amorphous clusters might coexist with the molecularly dispersed drug as illustrated in Figure 17c. There was no monomoleculary dispersed state detected in these samples. At the drug content of 70% w/w, the fraction of the amorphous state was higher than the molecularly dispersed state for both FD and ME samples. This suggested the extensive amorphous clusters in these samples. The predominant drug molecules were interacted with itself. For ME sample with 90% w/w drug, almost all drug molecules were in amorphous state. The strength of drug-polymer interaction was therefore weakest.

The FD and SE samples with up to 30% w/w drug, and the ME sample with 10% w/w drug did not contain amorphous state. These drug contents could be the maximum concentration of nifedipine in Soluplus® to maintain the miscible mixture of the drug and the polymer. The trace amount of amorphous state was detected in the ME sample with 30% w/w drug; hence, this sample might not be clearly classified as miscible mixture. The samples with 50, 70, 90% w/w drug prepared by the three methods were categorized into immiscible mixture because there were substantial amorphous and/or crystalline drugs detected in these immiscible mixtures.

Even with this, ME appeared to be the most effective method to prepare the solid dispersions without the presence of crystalline drug. The crystalline drug was not found in the samples with the entire ranges of drug loadings (10, 30, 50, 70 and 90% w/w). Furthermore, the molecularly dispersed drug was observed even in the ME sample with 90% w/w drug. However, the ME samples were inhomogeneous. The amounts of each state showed the greatest variation, indicated by the higher standard deviation comparing with the FD and SE samples as shown in Table IV and Figure 22. The insufficient mixing of nifedipine and Soluplus® in powders and/or in the molten states might be attributed to the inhomogeneity of the ME samples.

The DSC results indicated that the FD sample with 50% w/w drug and ME sample with 30% w/w drug were miscible mixtures as a single T_g without melting event was present. However, Raman spectroscopy could detect the existence of amorphous cluster in these samples, especially a large amount in the FD sample with 50% w/w drug loading. It was possibly due to the detection limit of the DSC. Generally, the size of amorphous cluster less than 30 nm, or tens of microns, could not be observed by DSC (88, 89). Also, heat introduced to the sample during DSC measurement might cause the movement of molten sample, and the detection of melting event became obstructed (90). This led to the misleading classification of the sample as a miscible mixture. In addition, it might be due to the poor mixing of the ME sample. Thus, the distribution of amorphous clusters was not homogeneous (as the high standard deviation shown in Table IV and Figure 22), resulting in sampling error.

4.2 Solid state stability study of solid dispersion samples

4.2.1 Crystallization tendency

Crystallization tendency of the drug in the solid dispersions which were classified as miscible and immiscible mixtures were investigated by storing the samples at an elevated temperature (98°C), which was much higher than sample T_gs in order to induce molecular mobility. At this temperature the sample were in rubbery state. The influence of the molecular mobility of the glassy state on

crystallization was minimized and the effect of sample T_g on crystallization could be neglected. Therefore, crystallization inhibition was assumed to be affected by only drug-polymer interaction. If there was a strong drug-polymer interaction, this should retard amorphous agglomeration, and hence, an onset of crystallization should be delayed. In addition, the results will be discussed based on the assumption that the saturated concentration of nifedipine in Soluplus® did not increase at the elevated studied temperature.

The immiscible samples included in the study were the FD and ME samples with 50 and 70% w/w drug. These samples contained the varied amounts of drug in each state and hence different degrees of drug-polymer interaction. The majority of the drug molecules in the sample with 50% w/w drug were molecularly dispersed state; while, that of 70% w/w were amorphous state. The onset of crystallization was real time monitored in VT-XRPD.

The miscible samples subjected to the study were the FD and SE samples with 30% w/w drug. Although the ME sample with 30% w/w drug was still ambiguously to be classified as the miscible mixture as above discussed, it was also included for comparison. The preliminary study suggested that these samples were relatively stable in the oven at 98°C for 6 days. Thus, to monitor the crystallization tendency, these samples were stored in an oven, instead of real time monitoring. The onset of detectable crystallization was periodically monitored with XRPD until nifedipine content, determined by HPLC, was less than 90.0% w/w. It was found that the drug content in FD, ME and SE samples with 30% w/w drug were 86.7% w/w (FD sample), 78.4% w/w (ME sample) and 76.2% w/w (SE sample) after storage for 28 days. Therefore, the study of crystallization tendency in samples with 30% w/w drug was terminated at 28 days.

The time to detectable crystallization of FD, ME and SE samples containing 30, 50 and 70% w/w drug stored at 98°C are summarized in Table V.

Table V Time to detectable crystallization of FD, ME and SE samples containing 30, 50 and 70% w/w drug stored at 98°C.

Sample	Onset of crystallization
FD 30% w/w	≥ 28 ± 0[a] days
FD 50% w/w	10 ± 2 h
FD 70% w/w	6 ± 1 min
ME 30% w/w	≥ 28 ± 0 days
ME 50% w/w	11 ± 3 min
ME 70% w/w	7 ± 2 min
SE 30% w/w	≥ 28 ± 0 days

[a] Standard deviation (n=3)

The time to detectable crystallization of FD and ME samples containing 50 and 70% w/w drug stored at 98°C are shown in Figure 23.

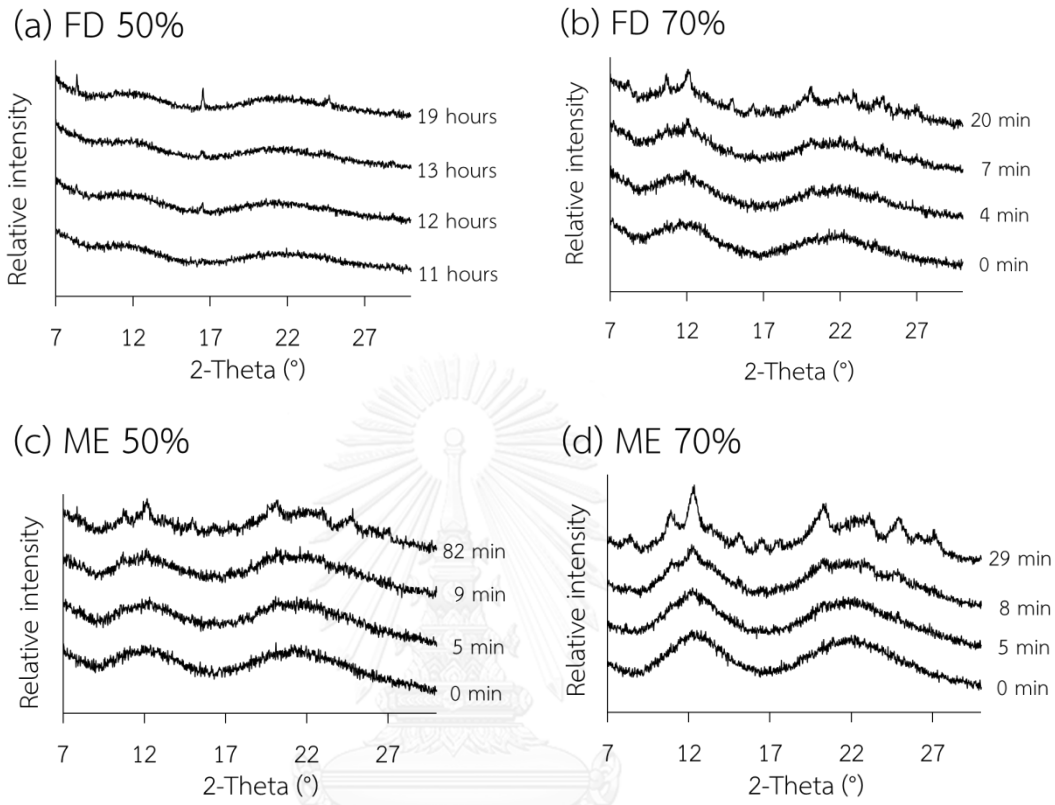

Figure 23 XRPD diffractograms of FD samples with drug loadings of (a) 50 and (b) 70% w/w and ME samples with drug loadings of (c) 50 and (d) 70% w/w stored at 98°C. The diffractograms were obtained from one measurement. Reproduced from (67) with permission of Springer Science+Business Media.

No sign of crystallization could be observed in the samples with drug loading of 30% w/w prepared by all three methods. The average onset time to detectable crystallization of FD and ME samples with 50% w/w were 10 h and 11 min, respectively. The FD and ME samples with 70% w/w drug showed the onset time to detectable crystallization at 6 and 7 min, respectively.

The relative amount of the drug dispersed in the polymer at the molecular level is plotted against the onset time for observable crystallization. The correlation between the sum of monomolecularly and molecularly dispersed states,

(normalized to 100% w/w drug loading) and the onset time of crystallization showed natural exponential function relationship as depicted in Figure 24. Within the homogeneous FD samples, the onset time of crystallization was substantially increased when the degree of molecular interaction was slightly increased. The data set of FD samples provided well fitted to the model as indicated by the R^2 of 1.0000 (Figure 24a); while, the model obtained from ME samples showed relatively low R^2 of 0.7772 (Figure 24b). This might due to the inhomogeneity of ME samples. There were some large amorphous clusters in sample with 50% w/w drug rapidly inducing crystallization.

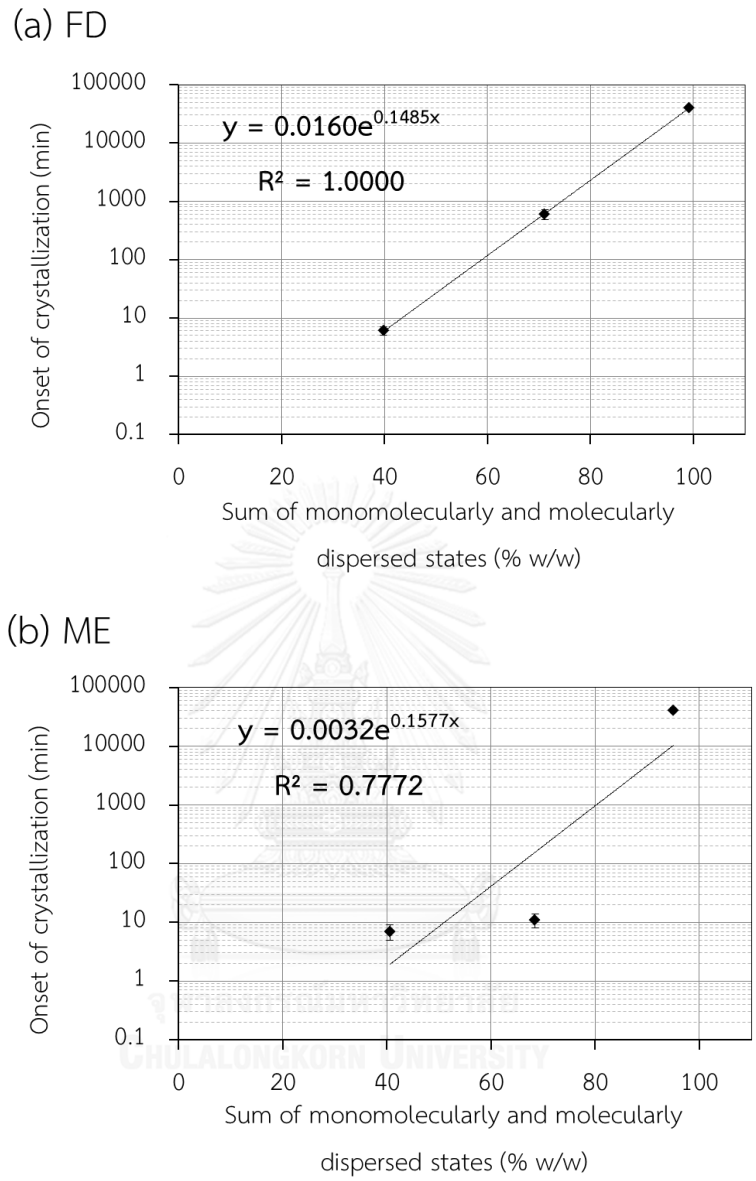

Figure 24 The correlation of sum of monomolecularly and molecularly dispersed states and time to detectable crystallization of (a) FD and (b) ME samples stored at 98°C.

Recrystallization in solid dispersion could be delayed when the amorphous drug is homogeneously and molecularly dispersed in the polymer (9, 10, 21). The stability of amorphous drug depended on the thermodynamic factor such as drug concentration and the kinetic factor such as preparation method (8, 9). These

findings suggested that the crystallization tendency of nifedipine in the solid dispersion was influenced by both factors.

The FD and ME samples with 70% w/w drug exhibit rapid crystallization as the nature of immiscible mixture. The large amount of amorphous clusters caused an accelerated nucleation and crystal growth. The FD and ME sample with 50% w/w contained the comparable amount of molecularly dispersed drug and drug in amorphous state. However, the ME sample demonstrated the much rapid onset of crystallization than the FD sample. This was possibly due to the high variation of each state distributed in the ME sample. Some large amorphous clusters could expedite nucleation, followed by the crystal growth. This also indicated that recrystallization could be better delayed in homogeneous molecular dispersion sample, FD sample for this instant. The FD sample with 50% w/w drug showed rapid crystallization, although it contained higher amount of monomolecularly and molecularly dispersed states, indicating higher drug-polymer interaction. This because the drug loading was above the saturated concentration introduced the thermodynamic driving force for crystallization. The thermodynamic factor was therefore able to overcome the kinetic factor of drug-polymer interaction.

The crystallization of samples with drug loading of 30% w/w prepared by all three methods could not be observed, even monitoring for 28 days. In these samples, the thermodynamic driving force was not high as the drug content was within the saturated concentration. In addition, the considerable amount of drug-polymer interactions detected at an ambient temperature was adequate to suppress molecular mobility of the drug molecules even at the elevated temperature. Hence, the crystallization was inhibited. The failure to observe crystallinity may be also because a trace amount of crystalline occurred at a lower level than the detection limit of the XRPD. Besides, the degradation products of 15-20% w/w did not diffract under the studied conditions.

According to crystallization tendency, the small amount of amorphous state in the ME sample with 30% w/w drug (Table IV and Figure 22) was inadequate to induce crystallization up to the storage time of the study. This ME sample could be

justified as miscible mixture similar to FD and SE samples at the same drug concentration.

It must be noted that, the temperature used in the study was much higher than the conventional stability. The results only suggested the influence of the extent of molecularly dispersed drug in homogeneous samples on crystallization retardation. It did not point out the solid state stability of the drug at ambient conditions.

4.2.3 Tendency to undergo amorphous phase separation

The purpose of this study was to investigate whether the varied degrees of drug-polymer interaction in the miscible mixtures could contribute to inhibition of amorphous phase separation. The samples subjected to this study were the FD samples with drug concentrations of 10 and 30% w/w. In these samples, the sample with 10% w/w drug contained approximately 60% w/w of monomolecularly dispersed state and 40% w/w of molecularly dispersed state. While, the sample with 30% w/w drug rarely contained the monomolecularly dispersed state; almost all drug, 99% w/w of the nifedipine content exhibited in the molecularly dispersed state.

After 22 days, the chemical stability of nifedipine in FD samples with drug loadings of 10 and 30% w/w stored at 60°C/75% RH were 98.3% (10% w/w drug concentration) and 105.2% (30% w/w drug concentration), within the USP 36's specification. The relative amounts of monomolecularly and molecularly dispersed states, and amorphous drug at each time point were calculated based on the method described earlier.

The content of each state in the FD sample with drug loading of 10% w/w was similar to that presented at the beginning of the study as shown in Table VI and Figure 25a. There was a slight amorphous state in these samples in which it was insignificantly different from the initial point (α = 0.05, p-value = 0.07). This implied that the extent of drug-polymer interaction in these samples were sufficient to inhibit the amorphous phase separation. For the FD sample with drug loading of 30% w/w,

marked increase in amorphous and monomolecularly dispersed states were detected; while, the molecularly dispersed state was decreased as demonstrated in Table VI and Figure 25b. This can be explained that the balance of drug-drug and drug-polymer interactions, reflected by approximately 99% w/w of the nifedipine content being molecularly dispersed state at the beginning, was failed. At the temperature close to T_g, the molecules were highly mobile. The kinetic energy induced the drug molecules to move closer and hence drug-drug interaction could overcome drug-polymer interaction. Some drug molecules were detached from the polymer and formed amorphous clusters. Consequently, the rest of drug molecules were surrounded by the polymer as defined by the monomolecularly dispersed state.

Table VI The content of nifedipine presenting as monomolecularly and molecularly dispersed states, and amorphous state in FD sample with drug loadings of 10 and 30% w/w stored at 60°C/75%RH.

Duration (day)	Content (% w/w)					
	Monomolecularly dispersed state		Molecularly dispersed state		Amorphous	
	10% w/w	30% w/w	10% w/w	30% w/w	10% w/w	30% w/w
0	61.3 ± 1.4[a]	0.6 ± 0.7	38.6 ± 1.6	98.0 ± 2.2	0.1 ± 0.2	1.3 ± 2.3
4	62.6 ± 2.2	11.8 ± 1.8	35.7 ± 3.6	78.1 ± 2.0	1.7 ± 1.7	10.1 ± 1.3
8	62.7 ± 1.3	16.4 ± 2.4	35.5 ± 1.8	70.7 ± 3.1	1.7 ± 0.6	12.9 ± 0.7
12	63.7 ± 1.1	18.3 ± 1.1	34.2 ± 1.1	65.4 ± 1.8	2.2 ± 0.1	16.3 ± 0.8
17	63.1 ± 0.4	25.6 ± 4.5	35.2 ± 0.5	53.9 ± 9.5	1.7 ± 0.4	20.6 ± 5.0
22	63.1 ± 0.5	33.6 ± 3.3	35.4 ± 0.5	32.5 ± 9.0	1.5 ± 0.1	33.9 ± 6.7

[a] Standard deviation (n=3)

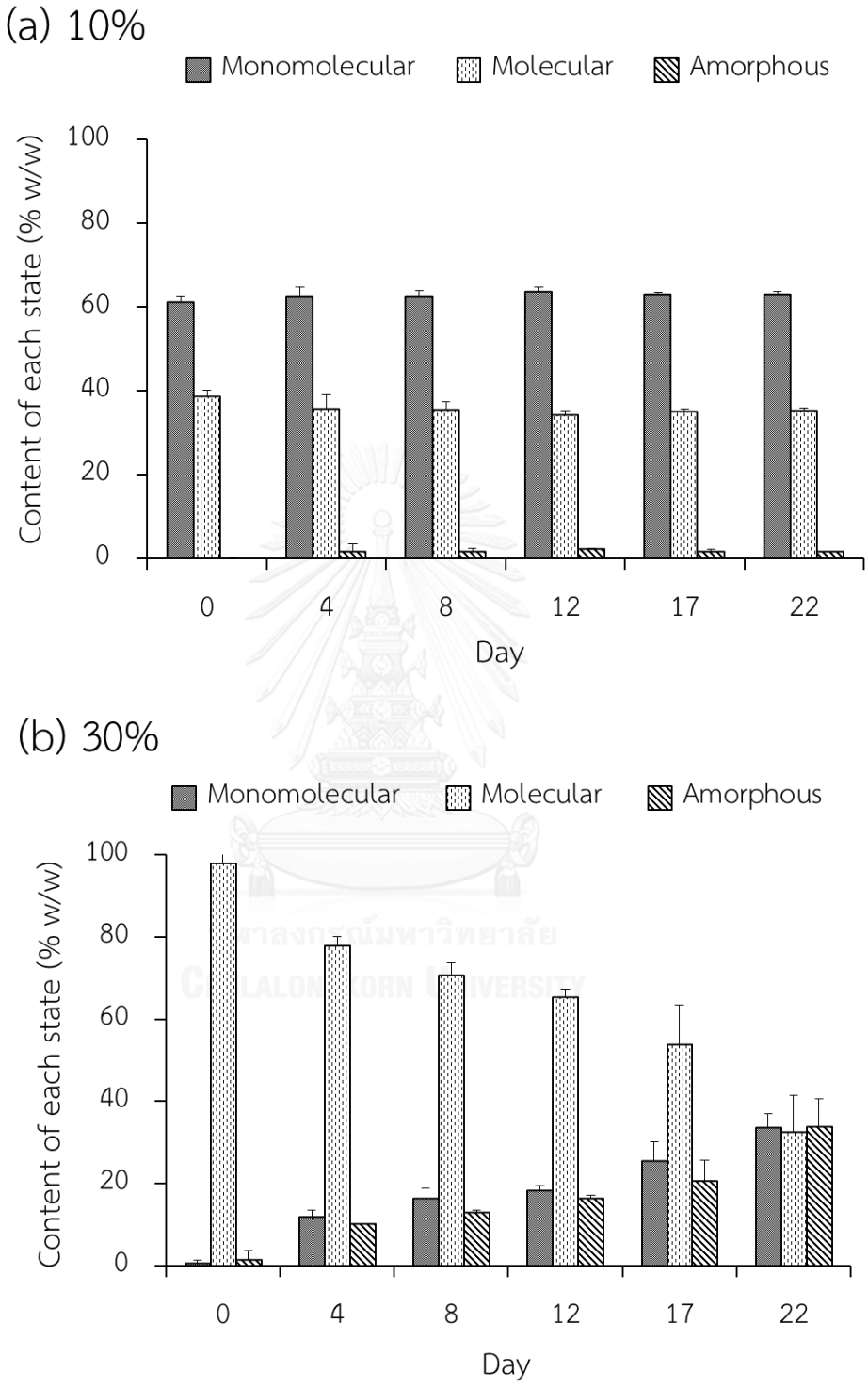

Figure 25 The content of nifedipine presenting as monomolecularly and molecularly dispersed states, and amorphous states in FD samples with drug loadings of (a) 10 and (b) 30% w/w stored at 60°C/75% RH (n=3).

The FD sample with 30% w/w drug stored for 17 days exhibited distorted spectral pattern which was not fitted with the model spectra of monomolecular, molecular and amorphous standards comparing with the model spectrum of 12 days as shown in Figure 26. The distorted spectrum was more pronounced upon storage for 22 days. The amounts of each state in the samples of 17 and 22 days showed a relatively high standard deviation, as demonstrated in Table VI and Figure 25. The experiment was therefore terminated at 22 days.

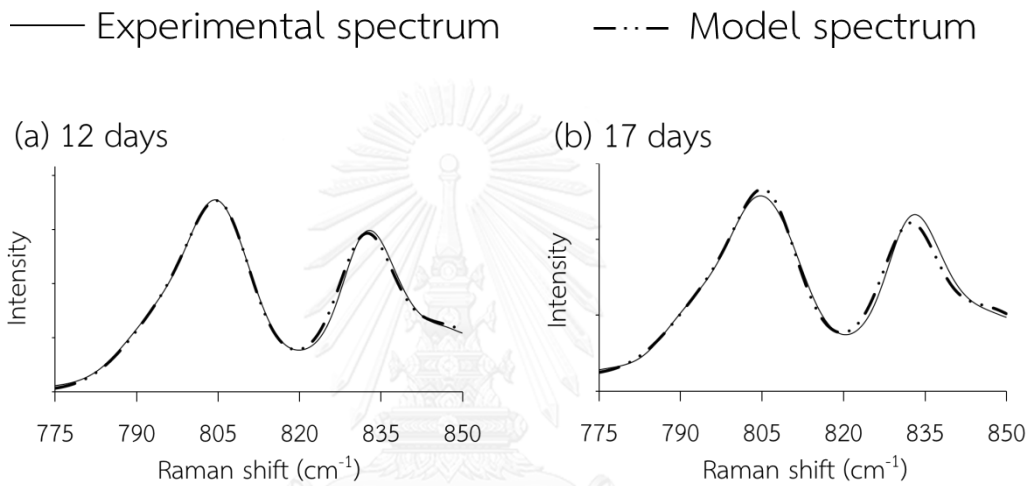

Figure 26 The model spectrum fitted to the experimental Raman spectrum of FD samples with 30% w/w drug stored at 60°C/75% RH for (a) 12 and (b) 17 days.

It was supposed that the distorted Raman spectral pattern was possibly due to an occurrence of nucleation and crystal growth. A relatively large fraction of am-NIF existing in the samples were converted to a trace of crystalline nifedipine, either α-NIF or β-NIF. Thus, an attempt was made to fit the sample's spectrum with the additional model spectra of α-NIF or β-NIF.

The model spectrum of α-NIF or β-NIF was obtained by Gaussian function fitting as described in the equation (7). An attempt was made to fit the experimental spectra of FD sample with 30% w/w drug stored for 17 and 22 days with five standard model spectra including monomolecularly and molecularly dispersed states, am-NIF state, α-NIF and β-NIF, as the method described in the equation (9). However, due to the limitation of the software, the experimental spectrum of

sample could be fitted with the maximum of three model spectra at a time. Each set of fitting was designated as shown in Table VII. The chi^2 values obtained from each set of fitting were compared as demonstrated in Table VII. The model of standards which provided the minimal chi^2 was selected to be the final set of model spectra to fit to the experimental spectra of FD sample with 30% w/w stored at 60°C/75% RH for 17 and 22 days.

Table VII Chi^2 values obtained from fitting experimental spectrum of the FD sample with 30% w/w drug stored at 60°C/75% RH for 22 days with varied standard models.

Set	Monomolecular	Molecular	am-NIF	α-NIF	β-NIF	Chi^2
1	+[a]	+	+	-[b]	-	633
2	+	-	+	+	-	1647
3	-	+	+	+	-	426
4	+	+	-	+	-	113
5	+	-	+	-	+	1584
6	-	+	+	-	+	1361
7	+	+	-	-	+	1446

[a] Included in Gaussian function fitting

[b] Excluded in Gaussian function fitting

The minimal chi^2, indicating the best fit, was obtained from the standard models of monomolecularly and molecularly dispersed states, and α-NIF. Therefore, these model spectra were used to calculate the amount of monomolecularly and molecularly dispersed states, and α-NIF in the samples as the method described in the equation (9) and (10). The results are shown in Figure 27

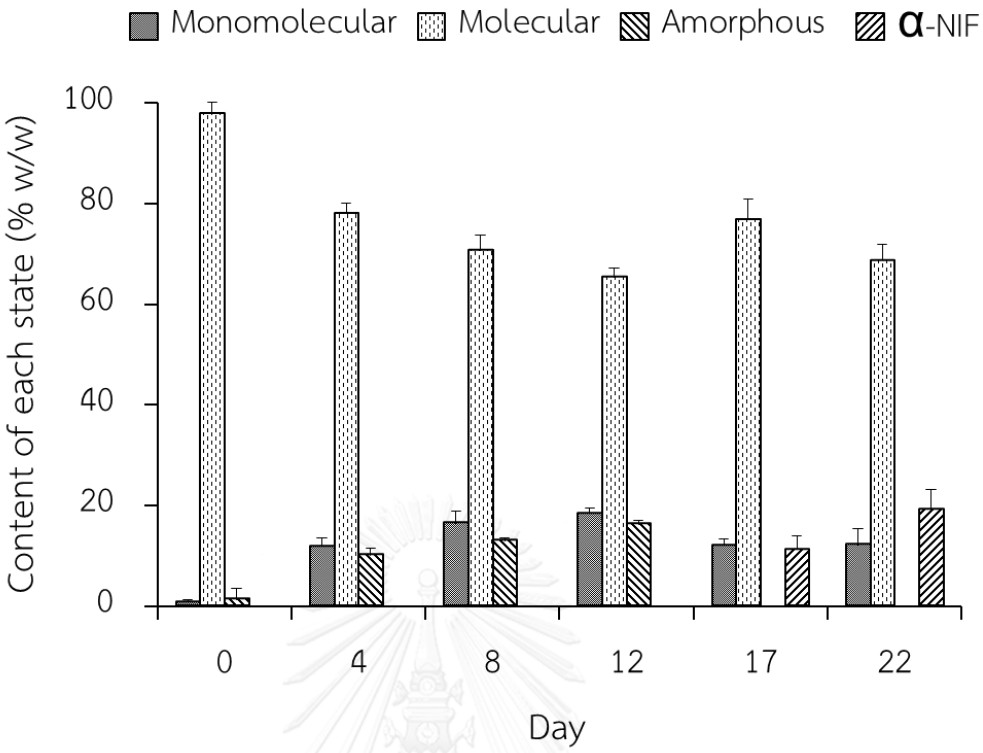

Figure 27 The content of nifedipine presenting as monomolecularly and molecularly dispersed states, amorphous state and α-NIF in the FD sample with drug loading of 30% w/w stored at 60°C/75% RH (n=3).

These results pointed out that there was some amorphous nifedipine in the FD sample with 30% w/w drug converted to α-NIF upon storage to 17 and 22 days. The contents of α-NIF in the samples were 11.2 ± 2.8% w/w (17 days) and 19.2 ± 4.1% w/w (22 days) of the nifedipine content. The contents of molecularly dispersed states in the samples at 17 and 22 days were higher than that of 12 days. This was probably due to the limitation of calculation. Although there might be am-NIF in the samples at 17 and 22 days, it could not be calculated when the experimental spectra were only fitted to the model spectra of monomolecularly and molecularly dispersed states, and α-NIF. The missing amount of am-NIF might cause error in the amount of molecularly dispersed state.

The existence of calculated α-NIF in the FD samples with 30% w/w drug stored at 60°C/75% RH for 22 days, being 19.2% of nifedipine content or approximately 6%

w/w of the total sample weight, however, could not be detected by XRPD as depicted in Figure 28.

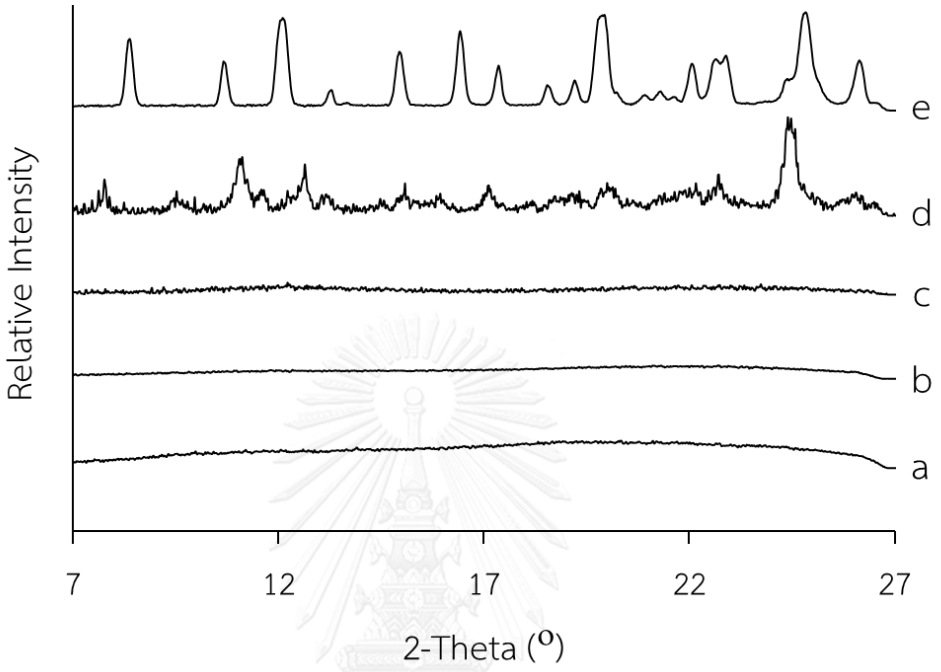

Figure 28 XRPD diffractograms of (a) Soluplus®, (b) FD sample with 30% w/w drug stored at 60°C/75% RH for 22 days, (c) am-NIF, (d) β–NIF and (e) α-NIF.

CHAPTER V
CONCLUSIONS

The results of the present study indicated that Raman spectroscopy was a useful tool to detect the hydrophobic interaction between the aromatic hydrocarbon of nifedipine and the cyclic amide of Soluplus®. The application of Gaussian function to establish the model of the Raman spectra allowed the extent of drug-polymer interaction to be determined based on the solid state morphology of drug dispersed in the polymer.

The hydrophobic interaction between the drug and the polymer was found to be stronger than the drug-drug interaction in the miscible mixtures until up to 30% w/w drug loading. The present study also proved that the drug loading affected the extent of drug-polymer interaction; the more drug was diluted, the stronger drug-polymer interaction would be. This further resulted in the inhibition of recrystallization and hindered the drug to undergo amorphous phase separation.

The preparation methods had an insignificant effect on the miscibility of solid dispersion but rather on homogeneity of the states of drug existing in the solid dispersions. The melting method employed in the solid dispersion preparation caused inhomogeneous matrix, leading to rapid recrystallization at high temperature studied.

Raman spectroscopy was also shown to be a potential tool to monitor the tendency to undergo amorphous phase separation in miscible mixture at the early stage. This tool revealed that to prevent the miscible mixture from amorphous phase separation, the concentration of the drug in the polymer should be much lower than the saturated concentration. Then, the strength of drug-polymer interaction could efficiently impede amorphous drug agglomeration, and the crystallization could eventually be delayed.

However, the quantification of the extent of drug-polymer interaction could be improved if the calculation at a time is applied to the model spectra of the solid

dispersion at low and saturated drug concentration, am-NIF, α-NIF and β-NIF for this case. In addition, the effect of drug-polymer interaction on the solid state stability of sample should be implemented under conventional stability conditions e.g. 30°C/75% RH or 40°C/75% RH. Finally, the feasibility of quantifying the extent of drug-polymer interaction in samples prepared by industrial scale processing, i.e. spray drying or hot melt extrusion, should be further investigated.

REFERENCES

1. Vasconcelos T, Sarmento B, Costa P. Solid dispersions as strategy to improve oral bioavailability of poor water soluble drugs. Drug Discov Today. 2007;12(23-24):1068-1075.
2. Leuner C, Dressman J. Improving drug solubility for oral delivery using solid dispersions. Eur J Pharm Biopharm. 2000;50(1):47-60.
3. Paudel A, Nies E, Van den Mooter G. Relating hydrogen-bonding interactions with the phase behavior of naproxen/PVP K 25 solid dispersions: Evaluation of solution-cast and quench-cooled films. Mol Pharmaceutics. 2012;9(11):3301-3317.
4. Yuan X, Munson E. Investigating molecular interactions of indomethacin and PVP in amorphous solid dispersions using ssNMR spectroscopy. AAPS Annual Meeting and Exposition; November 13; San Antonio 2013
5. Huang J, Li Y, Wigent RJ, Malick WA, Sandhu HK, Singhal D, et al. Interplay of formulation and process methodology on the extent of nifedipine molecular dispersion in polymers. Int J Pharm. 2011;420(1):59-67.
6. Paudel A, Loyson Y, Van den Mooter G. An investigation into the effect of spray drying temperature and atomizing conditions on miscibility, physical stability, and performance of naproxen-PVP K 25 solid dispersions. J Pharm Sci. 2013;102(4):1249-1267.
7. Janssens S, De Zeure A, Paudel A, Van Humbeeck J, Rombaut P, Van den Mooter G. Influence of preparation methods on solid state supersaturation of amorphous solid dispersions: A case study with itraconazole and Eudragit E100. Pharm Res. 2010;27(5):775-785.
8. Bhugra C, Pikal MJ. Role of thermodynamic, molecular, and kinetic factors in crystallization from the amorphous state. J Pharm Sci. 2008;97(4):1329-1349.
9. Qian F, Huang J, Hussain MA. Drug-polymer solubility and miscibility: Stability consideration and practical challenges in amorphous solid dispersion development. J Pharm Sci. 2010;99(7):2941-2947.

10. Ivanisevic I. Physical stability studies of miscible amorphous solid dispersions. J Pharm Sci. 2010;99(9):4005-4012.
11. Matsumoto T, Zografi G. Physical properties of solid molecular dispersions of indomethacin with poly(vinylpyrrolidone) and poly(vinylpyrrolidone-co-vinylacetate) in relation to indomethacin crystallization. Pharm Res. 1999;16(11):1722-1728.
12. Al-Obaidi H, Buckton G. Evaluation of griseofulvin binary and ternary solid dispersions with HPMCAS. AAPS PharmSciTech. 2009;10(4):1172-1177.
13. Rumondor ACF, Marsac PJ, Stanford LA, Taylor LS. Phase behavior of poly(vinylpyrrolidone) containing amorphous solid dispersions in the presence of moisture. Mol Pharmaceutics. 2009;6(5):1492-1505.
14. Schmidt AG, Wartewig S, Picker KM. Polyethylene oxides: Protection potential against polymorphic transitions of drugs? J Raman Spectrosc. 2004;35(5):360-367.
15. Kestur US, Van Eerdenbrugh B, Taylor LS. Influence of polymer chemistry on crystal growth inhibition of two chemically diverse organic molecules. CrystEngComm. 2011;13(22):6712-6718.
16. Gupta P, Thilagavathi R, Chakraborti AK, Bansal AK. Role of molecular interaction in stability of celecoxib–PVP amorphous systems. Mol Pharmaceutics. 2005;2(5):384-391.
17. Huang J, Wigent RJ, Schwartz JB. Drug-polymer interaction and its significance on the physical stability of nifedipine amorphous dispersion in microparticles of an ammonio methacrylate copolymer and ethylcellulose binary blend. J Pharm Sci. 2008;97(1):251-262.
18. Rawlinson CF, Williams AC, Timmins P, Grimsey I. Polymer-mediated disruption of drug crystallinity. Int J Pharm. 2007;336(1):42-48.
19. Yoshioka M, Hancock BC, Zografi G. Inhibition of indomethacin crystallization in poly(vinylpyrrolidone) coprecipitates. J Pharm Sci. 1995;84(8):983-986.
20. Konno H, Taylor LS. Influence of different polymers on the crystallization tendency of molecularly dispersed amorphous felodipine. J Pharm Sci. 2006;95(12):2692-2705.

21. Marsac PJ, Shamblin SL, Taylor LS. Theoretical and practical approaches for prediction of drug-polymer miscibility and solubility. Pharm Res. 2006;23(10):2417-2426.

22. Li YC, Pang HS, Guo ZF, Lin L, Dong YX, Li G, et al. Interactions between drugs and polymers influencing hot melt extrusion. J Pharm Pharmacol. 2014;66(2):148-166.

23. Marsac PJ, Konno H, Taylor LS. A comparison of the physical stability of amorphous felodipine and nifedipine systems. Pharm Res. 2006;23(10):2306-2316.

24. Rumondor ACF, Ivanisevic I, Bates S, Alonzo DE, Taylor LS. Evaluation of drug-polymer miscibility in amorphous solid dispersion systems. Pharm Res. 2009;26(11):2523-2534.

25. Ivanisevic I, Bates S, Chen P. Novel methods for the assessment of miscibility of amorphous drug-polymer dispersions. J Pharm Sci. 2009;98(9):3373-3386.

26. Djuris J, Nikolakakis I, Ibric S, Djuric Z, Kachrimanis K. Preparation of carbamazepine-Soluplus® solid dispersions by hot-melt extrusion, and prediction of drug-polymer miscibility by thermodynamic model fitting. Eur J Pharm Biopharm. 2013;84(1):228-237.

27. Maniruzzaman M, Morgan DJ, Mendham AP, Pang J, Snowden MJ, Douroumis D. Drug-polymer intermolecular interactions in hot-melt extruded solid dispersions. Int J Pharm. 2013;443(1-2):199-208.

28. Taylor LS, Zografi G. Sugar–polymer hydrogen bond interactions in lyophilized amorphous mixtures. J Pharm Sci. 1998;87(12):1615-1621.

29. Yuan X, Sperger D, Munson EJ. Investigating miscibility and molecular mobility of nifedipine-PVP amorphous solid dispersions using solid-state NMR spectroscopy. Mol Pharmaceutics. 2014;11(1):329-337.

30. Yuasa H, Ozeki T, Takahashi H, Kanaya Y, Ueno M. Application of the solid dispersion method to the controlled release of medicine. VI. Release mechanism of a slightly water-soluble medicine and interaction between flurbiprofen and hydroxypropyl cellulose in solid dispersion. Chem Pharm Bull. 1994;42(2):354-358.

31. Li X, Jiang C, Pan L, Zhang H, Hu L, Li T, et al. Effects of preparing techniques and aging on dissolution behavior of the solid dispersions of NF/Soluplus/Kollidon SR: Identification and classification by a combined analysis by FT-IR spectroscopy and computational approaches. Drug Dev Ind Pharm. 2015;41(1):2-14.
32. Taylor LS, Zografi G. Spectroscopic characterization of interactions between PVP and indomethacin in amorphous molecular dispersions. Pharm Res. 1997;14(12):1691-1698.
33. Breitenbach J, Schrof W, Neumann J. Confocal Raman-spectroscopy: Analytical approach to solid dispersions and mapping of drugs. Pharm Res. 1999;16(7):1109-1113.
34. Vajna B, Farkas I, Farkas A, Pataki H, Nagy Z, Madarász J, et al. Characterization of drug–cyclodextrin formulations using Raman mapping and multivariate curve resolution. J Pharm Biomed Anal. 2011;56(1):38-44.
35. Dürrigl M, Kwokal A, Hafner A, Klarić MŠ, Dumičić A, Cetina-Čižmek B, et al. Spray dried microparticles for controlled delivery of mupirocin calcium: Process-tailored modulation of drug release. J Microencapsul. 2011;28(2):108-121.
36. Squillante E, Needham T, Zia H. Solubility and in vitro transdermal permeation of nifedipine. Int J Pharm. 1997;159(2):171-180.
37. Kolter K, Karl M, Gryczke A. Hot-melt extrusion with BASF Pharma polymers. 2 ed. Ludwigshafen, Germany: BASF SE; 2012.
38. Greenhalgh DJ, Williams AC, Timmins P, York P. Solubility parameters as predictors of miscibility in solid dispersions. J Pharm Sci. 1999;88(11):1182-1190.
39. Janssens S, Van Den Mooter G. Review: Physical chemistry of solid dispersions. J Pharm Pharmacol. 2009;61(12):1571-1586.
40. Israelachvili JN. Intermolecular and surface forces. 3th ed. Barbara S, editor. CA, USA: Academic Press; 2011.
41. Moskala EJ, Howe SE, Painter PC, Coleman MM. On the role of intermolecular hydrogen bonding in miscible polymer blends. Macromolecules. 1984;17:1671-1678.

42. Hooton J. The nanoscale characterization and interparticulate interactions of pharmaceutical materials [Doctoral thesis]: The University of Nottingham; 2003.
43. Paudel A, Meeus J, Van den Mooter G. Structural characterization of amorphous solid dispersions. In: Shah N, Sandhu H, Choi DS, Chokshi H, Malick AW, editors. Amorphous Solid Dispersions: Theory and practice. New York: Springer 2014. p. 421-485.
44. United States Pharmacopeial Convention. United States Pharmacopeia and National Formulary (USP 35-NF 30). Rockville: United States Pharmacopeial Convention; 2011.
45. Maheswaram MPK. Characterization of pharmaceutical materials by thermal and analytical methods [Doctoral thesis]: Cleveland State University; 2012.
46. Hancock BC, Zografi G. The relationship between the glass transition temperature and the water content of amorphous pharmaceutical solids. Pharm Res. 1994;11(4):471-477.
47. McCreery RL. Raman spectroscopy for chemical analysis. Winefordner JD, editor. Canada: John Wiley & Sons, Inc.; 2000.
48. Tang XLC, Pikal MJ, Taylor LS. A spectroscopic investigation of hydrogen bond patterns in crystalline and amorphous phases in dihydropyridine calcium channel blockers. Pharm Res. 2002;19(4):477-483.
49. West AR. Basic solid state chemistry. 2nd ed. English: John Wiley & Sons, Ltd.; 1999.
50. Paudel A, Geppi M, Van Den Mooter G. Structural and dynamic properties of amorphous solid dispersions: The role of solid-state nuclear magnetic resonance spectroscopy and relaxometry. J Pharm Sci. 2014;103:2635-2662.
51. Aina AT. In situ monitoring of pharmaceutical crystallisation [Doctoral thesis]: The University of Nottingham; 2012.
52. Wikström H, Lewis IR, Taylor LS. Comparison of sampling techniques for in-line monitoring using Raman spectroscopy. Appl Spectrosc. 2005;59(7):934-941.

53. Strachan CJ, Rades T, Gordon KC, Rantanen J. Raman spectroscopy for quantitative analysis of pharmaceutical solids. J Pharm Pharmacol. 2007;59(2):179-192.

54. Palermo RN, Anderson CA, Drennen III JK. Review: Use of thermal, diffraction, and vibrational analytical methods to determine mechanisms of solid dispersion stability. J Pharm Innov. 2012;7(1):2-12.

55. Chan KLA, Fleming OS, Kazarian SG, Vassou D, Chryssikos GD, Gionis V. Polymorphism and devitrification of nifedipine under controlled humidity: A combined FT-Raman, IR and Raman microscopic investigation. J Raman Spectrosc. 2004;35(5):353-359.

56. OriginLab Corporation. [cited 2014 April, 4]; Available from: http://www.originlab.com/doc/Origin-Help

57. Chapra SC, Canale RP. Numerical methods for engineers. 6th ed. Singapore: McGraw-Hill; 2010.

58. Yu H, Wilamowski BM. Levenberg-Marquardt training. Irwin JD, editor: CRC Press; 2011.

59. Hu Y, Liu J, Li W. Resolution of overlapping spectra by curve-fitting. Anal Chim Acta. 2005;538:383-389.

60. Küpper H, Spiller M, Küpper FC. Photometric method for the quantification of chlorophylls and their derivatives in complex mixtures: Fitting with Gauss-peak spectra. Anal Biochem. 2000;286:247-256.

61. Dong J, Ozaki Y, Nakashima K. Infrared, Raman, and near-infrared spectroscopic evidence for the coexistence of various hydrogen-bond forms in poly(acrylic acid). Macromolecules. 1997;30(4):1111-1117.

62. MIMS annual. 20 ed. Bangkok, Thailand: TIMS (Thailand) Ltd; 2008.

63. MIMS annual 26 ed. Bangkok, Thailand: TIMS (Thailand) Ltd; 2014.

64. The Merck Index. 15th ed. Cambridge: The Royal Society of Chemistry; 2013.

65. Gunn E, Guzei IA, Cai T, Yu L. Polymorphism of nifedipine: Crystal structure and reversible transition of the metastable β polymorph. Cryst Growth Des. 2012;12(4):2037-2043.

66. Grooff D, Liebenberg W, De Villiers MM. Preparation and transformation of true nifedipine polymorphs: Investigated with differential scanning calorimetry and X-ray diffraction pattern fitting methods. J Pharm Sci. 2011;100(5):1944-1957.

67. Keratichewanun S, Yoshihashi Y, Sutanthavibul N, Terada K, Chatchawalsaisin J. An investigation of nifedipine miscibility in solid dispersions using Raman spectroscopy. Pharm Res. 2015;32(7):2458-2473.

68. Lin CW, Cham TM. Effect of particle size on the available surface area of nifedipine from nifedipine-polyethylene glycol 6000 solid dispersions. Int J Pharm. 1996;127(2):261-272.

69. Kojima Y, Ohta T, Shiraki K, Takano R, Maeda H, Ogawa Y. Effects of spray drying process parameters on the solubility behavior and physical stability of solid dispersions prepared using a laboratory-scale spray dryer. Drug Dev Ind Pharm. 2013;39(9):1484-1493.

70. Chan KLA, Kazarian SG. FTIR spectroscopic imaging of dissolution of a solid dispersion of nifedipine in poly(ethylene glycol). Mol Pharmaceutics. 2004;1(4):331-335.

71. Sugimoto I, Sasaki K, Kuchiki A, Ishihara T, Nakagawa H. Stability and bioavailability of nifedipine in fine granules. Chem Pharm Bull. 1982;30(12):4479-4488.

72. Save T, Venkitachalam P. Studies on solid dispersions of nifedipine. Drug Dev Ind Pharm. 1992;18(15):1663-1679.

73. Chutimaworapan S, Ritthidej GC, Yonemochi E, Oguchi T, Yamamoto K. Effect of water-soluble carriers on dissolution characteristics of nifedipine solid dispersions. Drug Dev Ind Pharm. 2000;26(11):1141-1150.

74. Zajc N, Obreza A, Bele M, Srčič S. Physical properties and dissolution behaviour of nifedipine/mannitol solid dispersions prepared by hot melt method. Int J Pharm. 2005;291(1-2):51-58.

75. Iqbal WS, Chan KL. FTIR spectroscopic study of poly(ethylene glycol)-nifedipine dispersion stability in different relative humidities. J Pharm Sci. 2015;104(1):280-284.

76. Michael L. *In vitro* characterization of the novel solubility enhancing excipient Soluplus® [Doctoral thesis]: Saarland University; 2011.

77. Soluplus®. BASF SE Care Chemicals Division: BASF SE; 2010.

78. Lim H. Dissolution and solubility enhancement of the poorly water soluble drug by forming solid dispersion with a novel polymeric solubilizer (Soluplus®) [Dotoral thesis]. UM Digital Archive: University of Maryland Baltimore; 2012.

79. United States Pharmacopeial Convention. United States Pharmacopeia and National Formulary (USP 36-NF 31). Rockville: United States Pharmacopeial Convention; 2012.

80. Forster A, Hempenstall J, Tucker I, Rades T. The potential of small-scale fusion experiments and the Gordon-Taylor equation to predict the suitability of drug/polymer blends for melt extrusion. Drug Dev Ind Pharm. 2001;27(6):549-560.

81. Grooff D, De Villiers MM, Liebenberg W. Thermal methods for evaluating polymorphic transitions in nifedipine. Thermochim Acta. 2007;454(1):33-42.

82. Richardson MJ, Savill NG. Derivation of accurate glass transition temperatures by differential scanning calorimetry. Polymer. 1975;16(10):753-757.

83. Thakral NK, Ray AR, Bar-Shalom D, Eriksson AH, Majumdar DK. Soluplus-solubilized citrated camptothecin-A potential drug delivery strategy in colon cancer. AAPS PharmSciTech. 2012;13(1):59-66.

84. Aso Y, Yoshioka S. Molecular mobility of nifedipine–PVP and phenobarbital–PVP solid dispersions as measured by ^{13}C-NMR spin-lattice relaxation time. J Pharm Sci. 2006;95(2):318-325.

85. Apperley DC, Forster AH, Fournier R, Harris RK, Hodgkinson P, Lancaster RW, et al. Characterization of indomethacin and nifedipine using variable-temperature solid-state NMR. Magn Reson Chem. 2005;43:881-892.

86. Yoshie N, Azuma Y, Sakurai M, Inoue Y. Crystallization and compatibility of poly(vinyl alcohol)/poly(3-hydroxybutyrate) blends: Influence of blend composition and tacticity of poly(vinyl alcohol). J Appl Polym Sci. 1995;56(1):17-24.

87. Teraoka R, Otsuka M, Matsuda Y. Evaluation of photostability of solid-state dimethyl 1,4-dihydro-2,6-dimethyl-4-(2-nitro-phenyl)-3,5-pyridinedicarboxylate

by using Fourier-transformed reflection-absorption infrared spectroscopy. Int J Pharm. 1999;184(1):35-43.

88. Qian F, Huang J, Zhu Q, Haddadin R, Gawel J, Garmise R, et al. Is a distinctive single T_g a reliable indicator for the homogeneity of amorphous solid dispersion? Int J Pharm. 2010;395(1–2):232-235.
89. Newman A, Engers D, Bates S, Ivanisevic I, Kelly RC, Zografi G. Characterization of amorphous API:Polymer mixtures using X-ray powder diffraction. J Pharm Sci. 2008;97(11):4840-4856.
90. Ford JL, Timmins P. Pharmaceutical thermal analysis: Techniques and applications. Chichester: Ellis Horwood Limited; 1989.
91. Konieczka P, Namieśnik J. Quality assurance and quality control in the analytical chemical laboratory: A practical approach. Lochmüller CH, editor. Boca Raton, FL: CRC Press; 2009.
92. Bliesner DM. Validating chromatographic methods: A practical guide. Hoboken, NJ: John Wiley & Sons, Inc.; 2006.

APPENDIX

a) Dynamic vapor sorption (DVS)

The moisture sorption profiles of am-NIF and Soluplus® during humidity increase from 0 to 98% RH are shown in Figure 29. am-NIF and Soluplus® showed the mass changes, due to water uptake, of 0.6 and 41.3% w/w, respectively. The mass of Soluplus® was rocketed when water vapor was increased from 65 to 98% RH. This result pointed out that Soluplus® was very hygroscopic in nature compared to am-NIF.

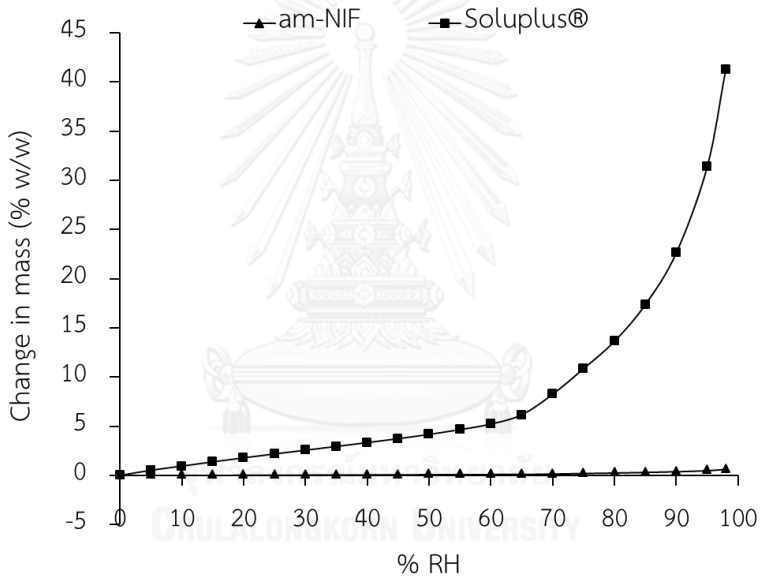

Figure 29 The moisture sorption profiles of am-NIF and Soluplus® during humidity increase from 0 to 98% RH.

b) Thermogravimetric analysis (TGA)

TGA was applied to monitor the residual solvents of prepared solid dispersions. The samples were heated to 120°C because the boiling points of methanol and tertiary-butyl alcohol are approximately 65 and 83°C, respectively. At the experimental temperature, it was postulated that the residual solvent was completely evaporated. The residual solvents of FD and SE samples after vacuum

dried over silica gel for at least 24 h are present in Table VIII. Most FD and SE samples consisted of less than 3.0% w/w of residual solvent.

Table VIII The residual solvents of FD and SE samples measured by % weight loss after heating the samples from room temperature (~25°C) to 120°C.

Sample (% w/w drug)	Residual solvent (% w/w)
FD 10%	1.36[a], 2.60[b]
FD 30%	1.10, 3.28
FD 50%	0.86, 1.01
FD 70%	1.15, 1.16
FD 90%	1.20, 1.33
SE 10%	1.71, 0.97
SE 30%	0.40, 0.90
SE 50%	0.56, 0.59
SE 70%	0.97, 0.25
SE 90%	0.85, 0.36

[a] Value of the first batch

[b] Value of the second batch

c) High performance liquid chromatography (HPLC)

Analytical method verification

Specificity

Soluplus® was not eluted by the proposed HPLC condition. Thus, the polymer did not interfere the analysis of nifedipine content.

Linearity and range

Nifedipine was eluted at about 24.0 min. Nitrosophenylpyridine analog, the related compound of nifedipine, was eluted at about 21.4 min. The retention time of nitrosophenylpyridine anolog was 0.9 relative to that of nifedipine which was

complied with USP 36. The representative chromatogram of nifedipine standard solution is shown in Figure 30.

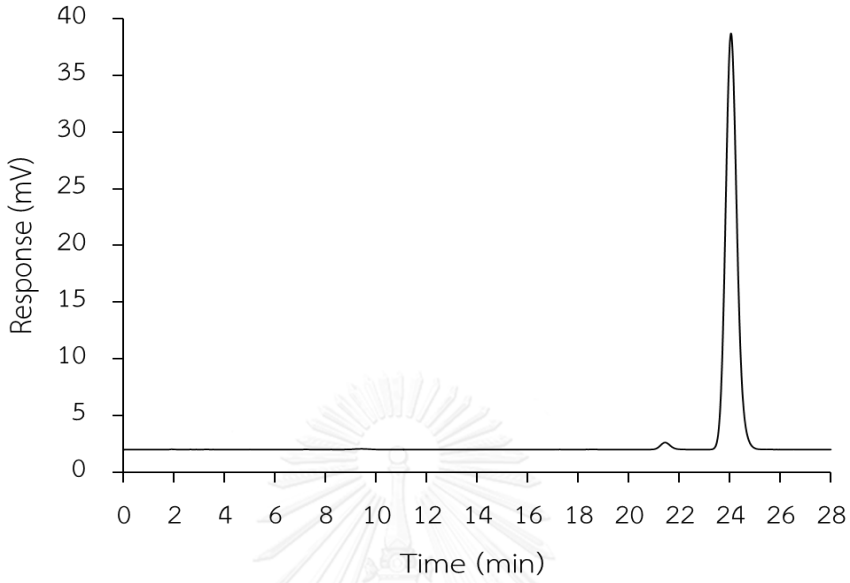

Figure 30 The chromatogram of nifedipine standard solution concentration of 0.1 mg/ml showing the elution of nitrosophenylpyridine analog peak and nifedipine peak, respectively.

The calibration parameters i.e. slope (a), intercept (b), correlation coefficient (R), coefficient of determination (R^2) derived from the plot of nifedipine concentrations over the range of 0 to 0.12 mg/ml versus responses are present in Table IX. The correlation coefficients obtained from the calibration curves were greater than 0.999 and the y-intercepts were less than 5% of the midrange concentration responses. The range of the analytical method was between 0 to 0.12 mg/ml.

Table IX Calibration parameters of the proposed method obtained from the plot of nifedipine concentrations over the range of 0 to 0.12 mg/ml versus responses.

Parameter / Day	a	b	R	R^2
1	11805563	-4153	0.9999	0.9998
2	11814026	-9903	0.9999	0.9997
3	11706609	-226	0.99997	0.9999

Accuracy

The plot of added nifedipine concentrations of 0.011, 0.055 and 0.110 mg/ml against the found concentrations is demonstrated in Figure 31. The slope and the y-intercept were approximately to 1 and 0, respectively; and the correlation coefficient was greater than 0.999. % Recovery was between 99.4 and 100.6%.

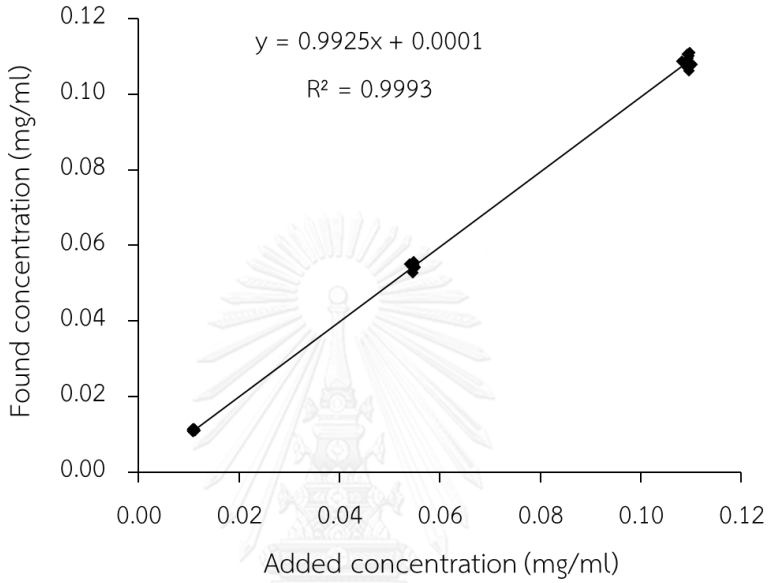

Figure 31 The plot of added versus found concentrations of nifedipine at 0.011, 0.055 and 0.110 mg/ml for verifying accuracy of the proposed method.

Precision

The RSD for repeatability precisions of day 1, 2 and 3 were 0.41, 0.36 and 0.76%, respectively. The RSD for intermediate precision was 0.52%. The overall RSD values were less than 2.0%.

The selectivity, linearity and range, accuracy and precision results indicated that the analytical method was acceptable for nifidpine assay (91, 92).

Assay

System suitability

The system suitability parameters obtained from six replicate injections of nifedipine concentration of 0.1 mg/ml were conformed to the acceptance criteria of USP 36 (79). The column efficiency was 13204 theoretical plates. The tailing factor was 1.1 and the RSD for replicate injections was 0.1%.

Sample assay

The chemical stability of nifedipine in am-NIF and solid dispersions were between 90.0-110.0% which was conformed to the acceptance criteria of USP 36 (79) as the results shown in Table X. The content of residual solvent obtained from TGA was accounted for the assay calculation.

Table X Chemical stability of prepared am-NIF and solid dispersion samples determined by a HPLC method according to USP 36.

Sample	% Assay
am-NIF	96.9 ± 0.6[a]
FD 10%	101.7 ± 0.8[b], 98.6 ± 1.0[c]
FD 30%	104.9 ± 1.1, 100.6 ± 1.7
FD 50%	98.7 ± 0.2, 97.3 ± 0.5
FD 70%	96.8 ± 0.6, 96.6 ± 0.2
FD 90%	100.2 ± 3.4, 100.4 ± 0.2
ME 10%	95.0 ± 0.1, 93.3 ± 0.3
ME 30%	98.0 ± 2.1, 93.3 ± 1.3
ME 50%	100.0 ± 0.3, 98.2 ± 0.7
ME 70%	99.1 ± 0.9, 99.1 ± 3.5
ME 90%	99.6 ± 3.5, 101.9 ± 0.4
SE 10%	105.6 ± 1.1, 103.9 ± 0.3
SE 30%	99.6 ± 1.6, 100.6 ± 0.9
SE 50%	104.1 ± 0.5, 101.7 ± 1.4
SE 70%	104.4 ± 2.2, 101.1 ± 0.3
SE 90%	102.7 ± 2.0, 106.3 ± 0.7

[a] Standard deviation (n=2)

[b] Value of the first batch

[c] Value of the second batch

VITA

Education

2010: Master of Herbal Medicines, the University of Sydney, Sydney, Australia

2006: Bachelor of Science in Pharmacy, Chulalongkorn University, Bangkok, Thailand

2001: High school, Hatyaiwittayalaisomboonkulkunya, Songkhla, Thailand

Publications

Keratichewanun S, Yoshihashi Y, Sutanthavibul N, Terada K, Chatchawalsaisin J. An investigation of nifedipine miscibility in solid dispersions using Raman spectroscopy. Pharm Res. 2015;32(7):2458-2473.

Research and Work Experiences

2013 - 2014: Research collaboration, Faculty of Pharmaceutical Sciences, Toho University, Chiba, Japan

2010 - 2013: Research Assistant, Faculty of Pharmaceutical Sciences, Chulalongkorn University, Bangkok, Thailand

2006 - 2008: Research and Development Pharmacist, M&H Manufacturing Co., Ltd., Samuthprakarn, Thailand

2006: Production Pharmacist, Utopian Co., Ltd., Samuthprakarn, Thailand

Instrumental methods of pharmaceutical analysis: Raman spectroscopy, differential scanning calorimetry (DSC), X-ray powder diffractometry (XRPD), infrared spectroscopy (IR), solid state-nuclear magnetic resonance spectroscopy (ss-NMR), high-performance liquid chromatography (HPLC), thermogravimetric analysis (TGA), dynamic vapor sorption (DVS), UV-visible spectroscopy, dissolution apparatus, Karl Fisher titration, hot-stage microscopy (HSM)

Memberships

International Society for Pharmaceutical Engineering (ISPE), Thai Industrial Pharmacist Association (TIPA) and Pharmacy Council of Thailand